H

$J = 0$

was H^0

In the following H refers to the signal that has been discovered in the Higgs searches. Whereas the observed signal is labeled as a spin 0 particle and is called a Higgs Boson, the detailed properties of H and its role in the context of electroweak symmetry breaking need to be further clarified. These issues are addressed by the measurements listed below.

Concerning mass limits and cross section limits that have been obtained in the searches for neutral and charged Higgs bosons, see the sections "Searches for Neutral Higgs Bosons" and "Searches for Charged Higgs Bosons ($H^{\pm}$ and $H^{\pm\pm}$)", respectively.

H MASS

VALUE (GeV)	*DOCUMENT ID*		*TECN*	*COMMENT*
125.13±0.11 OUR AVERAGE	Error includes scale factor of 1.5. See the ideogram below.			
125.04±0.12	[1] HAYRAPETY...25L		CMS	pp, 13 TeV, $ZZ^* \to 4\ell$
125.10±0.11	[2] AAD	23BP	ATLS	pp, 13 TeV, $\gamma\gamma$, $ZZ^* \to 4\ell$
125.78±0.26	[3] SIRUNYAN	20L	CMS	pp, 13 TeV, $\gamma\gamma$
125.09±0.21±0.11	[4,5] AAD	15B	LHC	pp, 7, 8 TeV
• • • We do not use the following data for averages, fits, limits, etc. • • •				
124.99±0.18±0.04	[6] AAD	23AU	ATLS	pp, 13 TeV, $ZZ^* \to 4\ell$
124.94±0.17±0.03	[7] AAD	23AU	ATLS	pp, 7, 8, 13 TeV, $ZZ^* \to 4\ell$
125.11±0.11	[8] AAD	23BP	ATLS	pp, 7, 8, 13 TeV, $\gamma\gamma$, $ZZ^* \to 4\ell$
125.17±0.11±0.09	[9] AAD	23BU	ATLS	pp, 13 TeV, $\gamma\gamma$
125.22±0.11±0.09	[10] AAD	23BU	ATLS	pp, 7, 8, 13 TeV, $\gamma\gamma$
125.46±0.16	[11] SIRUNYAN	20L	CMS	pp, 13 TeV, $\gamma\gamma$, $ZZ^* \to 4\ell$
125.38±0.14	[12] SIRUNYAN	20L	CMS	pp, 7, 8, 13 TeV, $\gamma\gamma$, $ZZ^* \to 4\ell$
124.79±0.37	[13] AABOUD	18BM	ATLS	pp, 13 TeV, $ZZ^* \to 4\ell$
124.93±0.40	[14] AABOUD	18BM	ATLS	pp, 13 TeV, $\gamma\gamma$
124.86±0.27	[4] AABOUD	18BM	ATLS	pp, 13 TeV, $\gamma\gamma$, $ZZ^* \to 4\ell$
124.97±0.24	[4,15] AABOUD	18BM	ATLS	pp, 7, 8, 13 TeV, $\gamma\gamma$, $ZZ^* \to 4\ell$
125.26±0.20±0.08	[16] SIRUNYAN	17AV	CMS	pp, 13 TeV, $ZZ^* \to 4\ell$
125.07±0.25±0.14	[5] AAD	15B	LHC	pp, 7, 8 TeV, $\gamma\gamma$
125.15±0.37±0.15	[5] AAD	15B	LHC	pp, 7, 8 TeV, $ZZ^* \to 4\ell$
126.02±0.43±0.27	AAD	15B	ATLS	pp, 7, 8 TeV, $\gamma\gamma$
124.51±0.52±0.04	AAD	15B	ATLS	pp, 7, 8 TeV, $ZZ^* \to 4\ell$
125.59±0.42±0.17	AAD	15B	CMS	pp, 7, 8 TeV, $ZZ^* \to 4\ell$
$125.02^{+0.26+0.14}_{-0.27-0.15}$	[17] KHACHATRY...15AM		CMS	pp, 7, 8 TeV
125.36±0.37±0.18	[4,18] AAD	14W	ATLS	pp, 7, 8 TeV
125.98±0.42±0.28	[18] AAD	14W	ATLS	pp, 7, 8 TeV, $\gamma\gamma$
124.51±0.52±0.06	[18] AAD	14W	ATLS	pp, 7, 8 TeV, $ZZ^* \to 4\ell$

125.6 ± 0.4 ± 0.2	[19] CHATRCHYAN	14AA	CMS	pp, 7, 8 TeV, $ZZ^* \to 4\ell$
122 ± 7	[20] CHATRCHYAN	14K	CMS	pp, 7, 8 TeV, $\tau\tau$
124.70 $\pm 0.31 \pm 0.15$	[21] KHACHATRY...	14P	CMS	pp, 7, 8 TeV, $\gamma\gamma$
125.5 ± 0.2 $^{+0.5}_{-0.6}$	[4,22] AAD	13AK	ATLS	pp, 7, 8 TeV
126.8 ± 0.2 ± 0.7	[22] AAD	13AK	ATLS	pp, 7, 8 TeV, $\gamma\gamma$
124.3 $^{+0.6}_{-0.5}$ $^{+0.5}_{-0.3}$	[22] AAD	13AK	ATLS	pp, 7, 8 TeV, $ZZ^* \to 4\ell$
125.8 ± 0.4 ± 0.4	[4,23] CHATRCHYAN	13J	CMS	pp, 7, 8 TeV
126.2 ± 0.6 ± 0.2	[23] CHATRCHYAN	13J	CMS	pp, 7, 8 TeV, $ZZ^* \to 4\ell$
126.0 ± 0.4 ± 0.4	[4,24] AAD	12AI	ATLS	pp, 7, 8 TeV
125.3 ± 0.4 ± 0.5	[4,25] CHATRCHYAN	12N	CMS	pp, 7, 8 TeV

[1] HAYRAPETYAN 25L use 138 fb^{-1} of pp collisions at $E_{cm} = 13$ TeV with $H \to ZZ^* \to 4\ell$ where $\ell = e,\ \mu$.

[2] AAD 23BP combine 13 TeV results of $H \to \gamma\gamma$ (AAD 23BU) and $H \to ZZ^* \to 4\ell$ where $\ell = e,\ \mu$ (AAD 23AU) using 140 fb^{-1} of pp collision data. The result is 125.10 $\pm$ 0.09(stat) $\pm$ 0.07(syst) GeV.

[3] SIRUNYAN 20L use 35.9 fb^{-1} of pp collisions at $E_{cm} = 13$ TeV with $H \to \gamma\gamma$.

[4] Combined value from $\gamma\gamma$ and $ZZ^* \to 4\ell$ final states.

[5] ATLAS and CMS data are fitted simultaneously.

[6] AAD 23AU use 139 fb^{-1} of pp collisions at $E_{cm} = 13$ TeV with $H \to ZZ^* \to 4\ell$ where $\ell = e,\ \mu$.

[7] AAD 23AU combine 13 TeV results with 7 and 8 TeV results (AAD 14W).

[8] AAD 23BP combine 13 TeV results with 7 and 8 TeV results. The result is 125.11 $\pm$ 0.09(stat) $\pm$ 0.06(syst) GeV.

[9] AAD 23BU use 140 fb^{-1} of pp collisions at $E_{cm} = 13$ TeV with $H \to \gamma\gamma$.

[10] AAD 23BU combine 13 TeV results with 7 and 8 TeV results (AAD 15B).

[11] SIRUNYAN 20L result of $H \to \gamma\gamma$ is combined with that of $H \to ZZ^* \to 4\ell$ where $\ell = e,\ \mu$ (SIRUNYAN 17AV).

[12] SIRUNYAN 20L combine 13 TeV results with 7 and 8 TeV results (KHACHATRYAN 15AM).

[13] AABOUD 18BM use 36.1 fb^{-1} of pp collisions at $E_{cm} = 13$ TeV with $H \to ZZ^* \to 4\ell$ where $\ell = e,\ \mu$.

[14] AABOUD 18BM use 36.1 fb^{-1} of pp collisions at $E_{cm} = 13$ TeV with $H \to \gamma\gamma$.

[15] AABOUD 18BM combine 13 TeV results with 7 and 8 TeV results. Other combined results are summarized in their Fig. 4.

[16] SIRUNYAN 17AV use 35.9 fb^{-1} of pp collisions at $E_{cm} = 13$ TeV with $H \to ZZ^* \to 4\ell$ where $\ell = e,\ \mu$.

[17] KHACHATRYAN 15AM use up to 5.1 fb^{-1} of pp collisions at $E_{cm} = 7$ TeV and up to 19.7 fb^{-1} at $E_{cm} = 8$ TeV.

[18] AAD 14W use 4.5 fb^{-1} of pp collisions at $E_{cm} = 7$ TeV and 20.3 fb^{-1} at 8 TeV.

[19] CHATRCHYAN 14AA use 5.1 fb^{-1} of pp collisions at $E_{cm} = 7$ TeV and 19.7 fb^{-1} at $E_{cm} = 8$ TeV.

[20] CHATRCHYAN 14K use 4.9 fb^{-1} of pp collisions at $E_{cm} = 7$ TeV and 19.7 fb^{-1} at $E_{cm} = 8$ TeV.

[21] KHACHATRYAN 14P use 5.1 fb^{-1} of pp collisions at $E_{cm} = 7$ TeV and 19.7 fb^{-1} at $E_{cm} = 8$ TeV.

[22] AAD 13AK use 4.7 fb^{-1} of pp collisions at E_{cm}=7 TeV and 20.7 fb^{-1} at E_{cm}=8 TeV. Superseded by AAD 14W.

[23] CHATRCHYAN 13J use 5.1 fb^{-1} of pp collisions at $E_{cm} = 7$ TeV and 12.2 fb^{-1} at $E_{cm} = 8$ TeV.

[24] AAD 12AI obtain results based on 4.6–4.8 fb^{-1} of pp collisions at $E_{cm} = 7$ TeV and 5.8–5.9 fb^{-1} at $E_{cm} = 8$ TeV. An excess of events over background with a local significance of 5.9 σ is observed at $m_H = 126$ GeV. See also AAD 12DA.

[25] CHATRCHYAN 12N obtain results based on 4.9–5.1 fb^{-1} of pp collisions at $E_{cm} = 7$ TeV and 5.1–5.3 fb^{-1} at $E_{cm} = 8$ TeV. An excess of events over background with a local significance of 5.0 σ is observed at about $m_H = 125$ GeV. See also CHATRCHYAN 12BY and CHATRCHYAN 13Y.

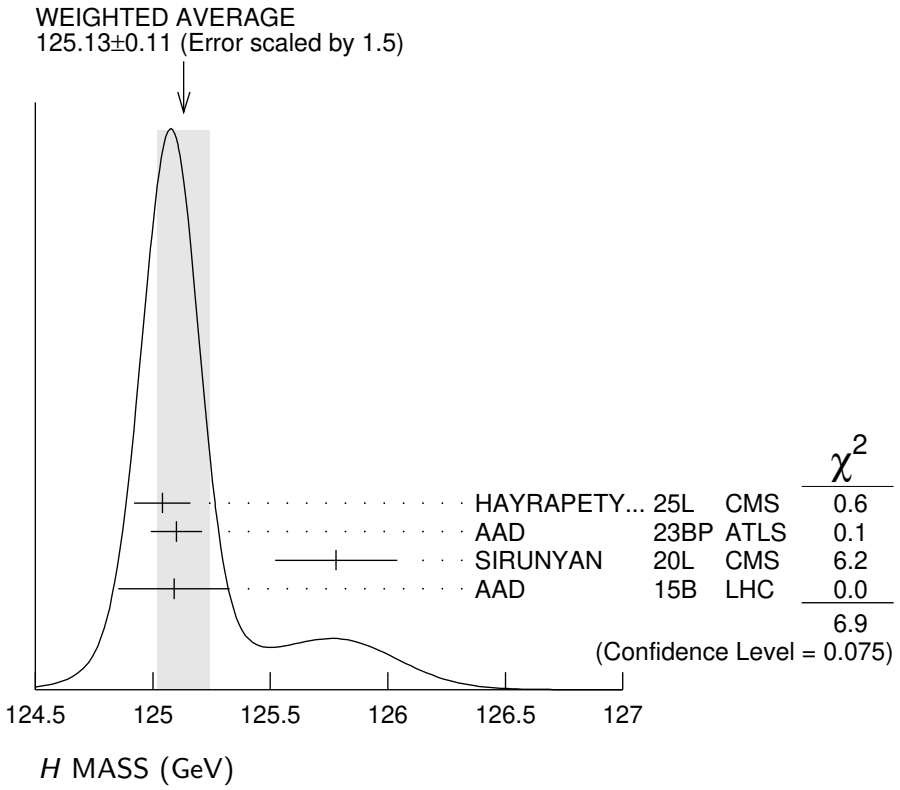

H SPIN AND *CP* PROPERTIES

The observation of the signal in the $\gamma\gamma$ final state rules out the possibility that the discovered particle has spin 1, as a consequence of the Landau-Yang theorem. This argument relies on the assumptions that the decaying particle is an on-shell resonance and that the decay products are indeed two photons rather than two pairs of boosted photons, which each could in principle be misidentified as a single photon.

Concerning distinguishing the spin 0 hypothesis from a spin 2 hypothesis, some care has to be taken in modelling the latter in order to ensure that the discriminating power is actually based on the spin properties rather than on unphysical behavior that may affect the model of the spin 2 state.

Under the assumption that the observed signal consists of a single state rather than an overlap of more than one resonance, it is sufficient to discriminate between distinct hypotheses in the spin analyses. On the other hand, the determination of the *CP* properties is in general much more difficult since in principle the observed state could consist of any admixture of *CP*-even and *CP*-odd components. As a first step, the compatibility of

the data with distinct hypotheses of pure *CP*-even and pure *CP*-odd states with different spin assignments has been investigated. In order to treat the case of a possible mixing of different *CP* states, certain cross section ratios are considered. Those cross section ratios need to be distinguished from the amount of mixing between a *CP*-even and a *CP*-odd state, as the cross section ratios depend in addition also on the coupling strengths of the *CP*-even and *CP*-odd components to the involved particles. A small relative coupling implies a small sensitivity of the corresponding cross section ratio to effects of *CP* mixing.

VALUE	*DOCUMENT ID*		*TECN*	*COMMENT*
• • • We do not use the following data for averages, fits, limits, etc. • • •				
	[1] AAD	25BC	ATLS	$H \to \tau\tau$, VBF, 13 TeV
	[2] AAD	25BK	ATLS	WW^* ($\to \ell\nu\ell\nu$), ggF+VBF, 13 TeV
	[3] HAYRAPETY...	25R	CMS	$t\bar{t}H$, tH, $H \to b\bar{b}$, 13 TeV
	[4] AAD	24AG	ATLS	$H \to ZZ^* \to 4\ell$, VBF, 13 TeV
	[5] AAD	24J	ATLS	$t\bar{t}H$, tH, $H \to b\bar{b}$, 13 TeV
	[6] AAD	23AK	ATLS	$H \to \tau\tau$, 13 TeV
	[7] AAD	23AN	ATLS	$H \to \gamma\gamma$, VBF, 13 TeV
	[8] TUMASYAN	23AJ	CMS	$H \to \tau\tau$, 13 TeV
	[9] TUMASYAN	23P	CMS	$t\bar{t}H$, $H \to WW^*$, $\tau\tau$, 13 TeV
	[10] AAD	22V	ATLS	WW^* ($\to e\nu\mu\nu$)+2j, 13 TeV
	[11] TUMASYAN	22Y	CMS	$H \to \tau\tau$, 13 TeV
	[12] AAD	20N	ATLS	$H \to \tau\tau$, VBF, 13 TeV
	[13] AAD	20Z	ATLS	$t\bar{t}H$, $H \to \gamma\gamma$, 13 TeV
	[14] SIRUNYAN	20AS	CMS	$t\bar{t}H$, $H \to \gamma\gamma$, 13 TeV
	[15] SIRUNYAN	19BL	CMS	pp, 7, 8, 13 TeV, $ZZ^*/ZZ \to 4\ell$
	[16] SIRUNYAN	19BZ	CMS	$pp \to H$+2jets (VBF, ggF, VH), $H \to \tau\tau$, 13 TeV
	[17] AABOUD	18AJ	ATLS	$H \to ZZ^* \to 4\ell$ ($\ell = e,\ \mu$), 13TeV
	[18] SIRUNYAN	17AM	CMS	$pp \to H+ \geq 2j$, $H \to 4\ell$ ($\ell = e,\ \mu$)
	[19] AAD	16	ATLS	$H \to \gamma\gamma$
	[20] AAD	16BL	ATLS	$pp \to Hjj X$ (VBF), $H \to \tau\tau$, 8 TeV
	[21] KHACHATRY...	16AB	CMS	$pp \to WH$, ZH, $H \to b\bar{b}$, 8 TeV
	[22] AAD	15AX	ATLS	$H \to WW^*$
	[23] AAD	15CI	ATLS	$H \to ZZ^*$, WW^*, $\gamma\gamma$
	[24] AALTONEN	15	TEVA	$p\bar{p} \to WH$, ZH, $H \to b\bar{b}$
	[25] AALTONEN	15B	CDF	$p\bar{p} \to WH$, ZH, $H \to b\bar{b}$
	[26] KHACHATRY...	15Y	CMS	$H \to 4\ell$, WW^*, $\gamma\gamma$
	[27] ABAZOV	14F	D0	$p\bar{p} \to WH$, ZH, $H \to b\bar{b}$
	[28] CHATRCHYAN	14AA	CMS	$H \to ZZ^*$
	[29] CHATRCHYAN	14G	CMS	$H \to WW^*$
	[30] KHACHATRY...	14P	CMS	$H \to \gamma\gamma$
	[31] AAD	13AJ	ATLS	$H \to \gamma\gamma$, $ZZ^* \to 4\ell$, $WW^* \to \ell\nu\ell\nu$
	[32] CHATRCHYAN	13J	CMS	$H \to ZZ^* \to 4\ell$

[1] AAD 25BC study *CP* properties in H production via VBF using $H \to \tau\tau$ decay channel with 140 fb^{-1} at $E_{\rm cm} = 13$ TeV. By using the Optimal Observable method, the data constrain a parameter $\tilde{d}$, which is for the strength of *CP* violation in an effective field theory using the HISZ basis, and Wilson coefficient $c_{H\widetilde{W}}$ (Warsaw basis with $\Lambda = 1$ TeV) to be $[-0.012, 0.044]$ and $[-0.24, 0.83]$ at 95% CL, respectively, in both cases considering the linear and quadratic terms in the reweighting procedure. See their Fig. 6 and Table 9.

[2] AAD 25BK measure the *CP* properties using $H \to WW^* \to \ell\nu\ell\nu$ ($\ell = e, \mu$) with data of 140 fb^{-1} pp collisions at $E_{\rm cm} = 13$ TeV. By adding the azimuthal angular difference between the forward and backward jets to the reduced stage-1.2 simplified template cross section framework (see their Fig. 4), the signal strengths are measured as shown in their Fig. 12, which is compatible with a *CP*-conserving scenario (p-value of 75%). EFT interpretations in *CP*-conserving and *CP*-violating scenarios are given as the five rotated-basis Wilson coefficients obtained from the 16 Warsaw-basis Wilson coefficients (see their Fig. 14) for the *CP*-conserving one and the 4 Warsaw-basis Wilson coefficients for the *CP*-violating one. The results are shown in their Figs. 15 and 16, respectively.

[3] HAYRAPETYAN 25R measure the $t\bar{t}H$ and tH productions with $H \to b\bar{b}$ decay channel using 138 fb^{-1} of data at $E_{\rm cm} = 13$ TeV. Two-dimensional likelihood scan of $(\kappa_t, \tilde{\kappa}_t)$ to measure the *CP* structure of the top Yukawa coupling is shown in their Fig. 16, where $\kappa_V = 1$. With other channels (SIRUNYAN 20AS, SIRUNYAN 21AE, TUMASYAN 23P), the *CP*-odd fraction f_{CP} and the *CP* mixing angle α are constrain to be $|f_{CP}| < 0.85$ and $\cos\alpha > 0.39$ at 95% CL.

[4] AAD 24AG search for *CP* violation in the decay kinematics and VBF production of the Higgs boson using $H \to ZZ^* \to 4\ell$ decay channel ($\ell = e, \mu$) with 139 fb^{-1} at $E_{\rm cm} = 13$ TeV. By using the optimal observables, the data constrain six *CP*-odd Wilson coefficients in two effective field theory bases: the Warsaw basis and the Higgs basis. The result is given in their Table 5 and Figs. 7–11. The differential fiducial cross sections for the four optimal observables are measured as shown in their Fig. 13. The VBF fiducial cross sections are given in their Table 6.

[5] AAD 24J measure the *CP* structure of the top Yukawa coupling using 139 fb^{-1} of data at $E_{\rm cm} = 13$ TeV. The *CP*-mixing angle α for top Yukawa coupling is measured to be $(11^{+52}_{-73})^\circ$ with the top Yukawa coupling strength modifier κ_t. See their Fig. 3. The data disfavour the pure *CP*-odd ($\alpha = 90^\circ$) at 1.2 σ.

[6] AAD 23AK measure the *CP* structure of the τ Yukawa coupling using 139 fb^{-1} of data at $E_{\rm cm} = 13$ TeV. The *CP*-mixing angle α for τ Yukawa coupling is measured to be $9 \pm 16^\circ$. The data disfavour the pure *CP*-odd ($\alpha = 90^\circ$) at 3.4 σ.

[7] AAD 23AN test *CP* invariance in H production via VBF using $H \to \gamma\gamma$ decay channel with 139 fb^{-1} at $E_{\rm cm} = 13$ TeV. By using the Optimal Observable method, the data constrain parameters describing the strength of the *CP*-odd component in the coupling between Higgs and W/Z in effective field theory bases: $\tilde{d}$ in the HISZ basis and $c_{H\widetilde{W}}$ in the Warsaw basis. The result is -0.010 $\leq \tilde{d} \leq$ 0.040 and -0.15 $\leq c_{H\widetilde{W}} \leq$ 0.67 at 68% CL. See their Table I, which shows the result combined with $H \to \tau\tau$ (AAD 20N): -0.012 $\leq \tilde{d} \leq$ 0.030 at 68% CL.

[8] TUMASYAN 23AJ constraint anomalous couplings of the Higgs to vector bosons and fermions using $pp \to H \to \tau\tau$ at $E_{\rm cm} = 13$ TeV with 138 fb^{-1} data. The *CP*-violating parameter in gluon-fusion production f_{a3}^{ggH} and the effective mixing angle α^{Hff} are given in their Table VII with $H \to \tau\tau$ and f_{a3}^{ggH} in their Table X with $H \to \tau\tau$ and $H \to 4\ell$. Using the VBF production analysis, the *CP*-violating parameter f_{a3} and the *CP*-conserving parameters f_{a2}, $f_{\Lambda1}$ and $f_{\Lambda1}^{Z\gamma}$ are given in their Table VIII with $H \to \tau\tau$ and Table IX with $H \to \tau\tau$ and $H \to 4\ell$. The *CP*-violating parameter f_{CP}^{Htt} is constrained to be $0.03^{+0.17}_{-0.03}$ using $H \to \tau\tau$, $H \to 4\ell$ and $H \to \gamma\gamma$.

[9] TUMASYAN 23P constrain $\widetilde{\kappa}_t$ from $t\overline{t}H$ and tH decaying $H \to WW^*$ and $H \to \tau\tau$ (multilepton decay mode) with 138 fb^{-1} pp collision data at $E_{\rm cm} = 13$ TeV. The $\widetilde{\kappa}_t$ is constrained to be $|\widetilde{\kappa}_t| \leq 1.4$ at 95% CL by fixing $\kappa_t = 1$ and other couplings (κ_V etc.) to the SM values, see their Table 6 (see their Fig. 9 for 2-dim contours). The fractional contribution of the *CP*-odd component $|f_{CP}^{Htt}|$ is constrained to (0.24, 0.81) at 68% CL with a best fit value of 0.59. The combination with other $t\overline{t}H$ decaying $H \to \gamma\gamma$ (SIRUNYAN 20AS) and $H \to 4\ell$ (SIRUNYAN 21AE) constraints to be $|\widetilde{\kappa}_t| \leq 1.07$ at 95% CL and $|f_{CP}^{Htt}| < 0.55$ at 68% CL with a best fit value of 0.28.

[10] AAD 22V measure the *CP* properties of the effective Higgs-gluon interaction using gluon fusion $H \to WW^* \to e\nu\mu\nu$ plus two jets with 36.1 fb^{-1} of data at $E_{\rm cm} = 13$ TeV. The measured tangent of the *CP*-mixing angle tanα is $0.0 \pm 0.4 \pm 0.3$ assuming the standard model HVV couplings. See their Fig. 6.

[11] TUMASYAN 22Y measure the *CP* structure of the τ Yukawa coupling using 137 fb^{-1} of data at $E_{\rm cm} = 13$ TeV. The *CP*-mixing angle α for τ Yukawa coupling is measured to be $-1 \pm 19^\circ$. The data disfavour the pure *CP*-odd ($\alpha = 90^\circ$) at 3.0 σ.

[12] AAD 20N test *CP* invariance in H production via VBF using $H \to \tau\tau$ decay channel with 36.1 fb^{-1} at $E_{\rm cm} = 13$ TeV. By using the Optimal Observable method, the data constrain a parameter $\widetilde{d}$, which is for the strength of *CP* violation in an effective field theory, to be $-0.090 \leq \widetilde{d} \leq 0.035$ at 68% CL (see their Fig. 6).

[13] AAD 20Z exclude a *CP*-mixing angle α, $|\alpha| > 43^\circ$ at 95% CL, where $\alpha = 0$ represents the Standard Model, in 139 fb^{-1} of data at $E_{\rm cm} = 13$ TeV. The pure *CP*-odd structure of the top Yukawa coupling ($\alpha = 90^\circ$) is excluded at 3.9 σ.

[14] SIRUNYAN 20AS exclude the pure *CP*-odd structure of the top Yukawa coupling at 3.2 σ using $t\overline{t}H$, $H \to \gamma\gamma$ in 137 fb^{-1} of data at $E_{\rm cm} = 13$ TeV. The fractional contribution of the *CP*-odd component $f_{CP}^{t\overline{t}H}$ is measured to be 0.00 ± 0.33.

[15] SIRUNYAN 19BL measure the anomalous HVV couplings from on-shell and off-shell production in the 4ℓ final state. Data of 80.2 fb^{-1} at 13 TeV, 19.7 fb^{-1} at 8 TeV, and 5.1 fb^{-1} at 7 TeV are used. See their Tables VI and VII for anomalous HVV couplings of *CP*-violating and *CP*-conserving parameters with on- and off-shells.

[16] SIRUNYAN 19BZ constrain anomalous HVV couplings of the Higgs boson with data of 35.9 fb^{-1} at $E_{\rm cm} = 13$ TeV using Higgs boson candidates with two jets produced in VBF, ggF, and VH that decay to $\tau\tau$. See their Table 2 and Fig. 10, which show 68% CL and 95% CL intervals. Combining those with the $H \to 4\ell$ (SIRUNYAN 19BL, on-shell scenario), results shown in their Tables 3, 4, and Fig. 11 are obtained. A *CP*-violating parameter is set to be $f_{a3}\cos(\phi_{a3}) = (0.00 \pm 0.27) \times 10^{-3}$ and *CP*-conserving parameters are $f_{a2}\cos(\phi_{a2}) = (0.08^{+1.04}_{-0.21}) \times 10^{-3}$, $f_{\Lambda1}\cos(\phi_{\Lambda1}) = (0.00^{+0.53}_{-0.09}) \times 10^{-3}$, and $f_{\Lambda1}^{Z\gamma}\cos(\phi_{\Lambda1}^{Z\gamma}) = (0.0^{+1.1}_{-1.3}) \times 10^{-3}$.

[17] AABOUD 18AJ study the tensor structure of the Higgs boson couplings using an effective Lagrangian using 36.1 fb^{-1} of pp collision data at $E_{\rm cm} = 13$ TeV. Constraints are set on the non-Standard-Model *CP*-even and *CP*-odd couplings to Z bosons and on the *CP*-odd coupling to gluons. See their Figs. 9 and 10, and Tables 10 and 11.

[18] SIRUNYAN 17AM constrain anomalous couplings of the Higgs boson with 5.1 fb^{-1} of pp collisions at $E_{\rm cm} = 7$ TeV, 19.7 fb^{-1} at $E_{\rm cm} = 8$ TeV, and 38.6 fb^{-1} at $E_{\rm cm} = 13$ TeV. See their Table 3 and Fig. 3, which show 68% CL and 95% CL intervals. A *CP* violation parameter f_{a3} is set to be $f_{a3}\cos(\phi_{a3}) = [-0.38, 0.46]$ at 95% CL ($\phi_{a3} = 0$ or π).

[19] AAD 16 study $H \to \gamma\gamma$ with an effective Lagrangian including *CP* even and odd terms in 20.3 fb^{-1} of pp collisions at $E_{\rm cm} = 8$ TeV. The data is consistent with the expectations for the Higgs boson of the Standard Model. Limits on anomalous couplings are also given.

[20] AAD 16BL study VBF $H \to \tau\tau$ with an effective Lagrangian including a *CP* odd term in 20.3 fb^{-1} of pp collisions at $E_{\rm cm} = 8$ TeV. The measurement is consistent with

the expectation of the Standard Model. The *CP*-mixing parameter $\widetilde{d}$ (a dimensionless coupling $\widetilde{d}$=$-(m_W^2/\Lambda^2)f_{\widetilde{W}W}$) is constrained to the interval of (-0.11, 0.05) at 68% CL under the assumption of $\widetilde{d} = \widetilde{d}_B$.

[21] KHACHATRYAN 16AB search for anomalous pseudoscalar couplings of the Higgs boson to W and Z with 18.9 fb^{-1} of pp collisions at E_{cm} = 8 TeV. See their Table 5 and Figs 5 and 6 for limits on possible anomalous pseudoscalar coupling parameters.

[22] AAD 15AX compare the J^{CP}= 0^+ Standard Model assignment with other J^{CP} hypotheses in 20.3 fb^{-1} of pp collisions at E_{cm} = 8 TeV, using the process $H \to WW^* \to e\nu\mu\nu$. 2^+ hypotheses are excluded at 84.5–99.4%CL, 0^- at 96.5%CL, 0^+ (field strength coupling) at 70.8%CL. See their Fig. 19 for limits on possible *CP* mixture parameters.

[23] AAD 15CI compare the J^{CP}= 0^+ Standard Model assignment with other J^{CP} hypotheses in 4.5 fb^{-1} of pp collisions at E_{cm} = 7 TeV and 20.3 fb^{-1} at E_{cm} = 8 TeV, using the processes $H \to ZZ^* \to 4\ell$. $H \to \gamma\gamma$ and combine with AAD 15AX data. 0^+ (field strength coupling), 0^- and several 2^+ hypotheses are excluded at more than 99.9% CL. See their Tables 7–9 for limits on possible *CP* mixture parameters.

[24] AALTONEN 15 combine AALTONEN 15B and ABAZOV 14F data. An upper limit of 0.36 of the Standard Model production rate at 95% CL is obtained both for a 0^- and a 2^+ state. Assuming the SM event rate, the $J^{CP} = 0^-$ (2^+) hypothesis is excluded at the 5.0σ (4.9σ) level.

[25] AALTONEN 15B compare the $J^{CP} = 0^+$ Standard Model assignment with other J^{CP} hypotheses in 9.45 fb^{-1} of $p\overline{p}$ collisions at E_{cm} = 1.96 TeV, using the processes $ZH \to \ell\ell b\overline{b}$, $WH \to \ell\nu b\overline{b}$, and $ZH \to \nu\nu b\overline{b}$. Bounds on the production rates of 0^- and 2^+ (graviton-like) states are set, see their tables II and III.

[26] KHACHATRYAN 15Y compare the $J^{CP} = 0^+$ Standard Model assignment with other J^{CP} hypotheses in up to 5.1 fb^{-1} of pp collisions at E_{cm} = 7 TeV and up to 19.7 fb^{-1} at E_{cm} = 8 TeV, using the processes $H \to 4\ell$, $H \to WW^*$, and $H \to \gamma\gamma$. 0^- is excluded at 99.98% CL, and several 2^+ hypotheses are excluded at more than 99% CL. Spin 1 models are excluded at more than 99.999% CL in ZZ^* and WW^* modes. Limits on anomalous couplings and several cross section fractions, treating the case of *CP*-mixed states, are also given.

[27] ABAZOV 14F compare the J^{CP}= 0^+ Standard Model assignment with J^{CP}= 0^- and 2^+ (graviton-like coupling) hypotheses in up to 9.7 fb^{-1} of $p\overline{p}$ collisions at E_{cm} = 1.96 TeV. They use kinematic correlations between the decay products of the vector boson and the Higgs boson in the final states $ZH \to \ell\ell b\overline{b}$, $WH \to \ell\nu b\overline{b}$, and $ZH \to \nu\nu b\overline{b}$. The 0^- (2^+) hypothesis is excluded at 97.6% CL (99.0% CL). In order to treat the case of a possible mixture of a 0^+ state with another J^{CP} state, the cross section fractions $f_X = \sigma_X/(\sigma_{0^+} + \sigma_X)$ are considered, where $X = 0^-$, 2^+. Values for f_{0^-} (f_{2^+}) above 0.80 (0.67) are excluded at 95% CL under the assumption that the total cross section is that of the SM Higgs boson.

[28] CHATRCHYAN 14AA compare the J^{CP}= 0^+ Standard Model assignment with various J^{CP} hypotheses in 5.1 fb^{-1} of pp collisions at E_{cm} = 7 TeV and 19.7 fb^{-1} at E_{cm} = 8 TeV. J^{CP}= 0^- and $1^\pm$ hypotheses are excluded at 99% CL, and several $J = 2$ hypotheses are excluded at 95% CL. In order to treat the case of a possible mixture of a 0^+ state with another J^{CP} state, the cross section fraction $f_{a3} = |a_3|^2\,\sigma_3$ / ($|a_1|^2\,\sigma_1 + |a_2|^2\,\sigma_2 + |a_3|^2\,\sigma_3$) is considered, where the case $a_3 = 1$, $a_1 = a_2 = 0$ corresponds to a pure *CP*-odd state. Assuming $a_2 = 0$, a value for f_{a3} above 0.51 is excluded at 95% CL.

[29] CHATRCHYAN 14G compare the J^{CP}= 0^+ Standard Model assignment with J^{CP}= 0^- and 2^+ (graviton-like coupling) hypotheses in 4.9 fb^{-1} of pp collisions at E_{cm} =

7 TeV and 19.4 fb^{-1} at $E_{cm} = 8$ TeV. Varying the fraction of the production of the 2^+ state via gg and $q\overline{q}$, 2^+ hypotheses are disfavored at CL between 83.7 and 99.8%. The 0^- hypothesis is disfavored against 0^+ at the 65.3% CL.

[30] KHACHATRYAN 14P compare the $J^{CP} = 0^+$ Standard Model assignment with a 2^+ (graviton-like coupling) hypothesis in 5.1 fb^{-1} of pp collisions at $E_{cm} = 7$ TeV and 19.7 fb^{-1} at $E_{cm} = 8$ TeV. Varying the fraction of the production of the 2^+ state via gg and $q\overline{q}$, 2^+ hypotheses are disfavored at CL between 71 and 94%.

[31] AAD 13AJ compare the spin 0, *CP*-even hypothesis with specific alternative hypotheses of spin 0, *CP*-odd, spin 1, *CP*-even and *CP*-odd, and spin 2, *CP*-even models using the Higgs boson decays $H \to \gamma\gamma$, $H \to ZZ^* \to 4\ell$ and $H \to WW^* \to \ell\nu\ell\nu$ and combinations thereof. The data are compatible with the spin 0, *CP*-even hypothesis, while all other tested hypotheses are excluded at confidence levels above 97.8%.

[32] CHATRCHYAN 13J study angular distributions of the lepton pairs in the ZZ^* channel where both Z bosons decay to e or μ pairs. Under the assumption that the observed particle has spin 0, the data are found to be consistent with the pure *CP*-even hypothesis, while the pure *CP*-odd hypothesis is disfavored.

H DECAY WIDTH

The total decay width for a light Higgs boson with a mass in the observed range is not expected to be directly observable at the LHC. For the case of the Standard Model the prediction for the total width is about 4 MeV, which is three orders of magnitude smaller than the experimental mass resolution. There is no indication from the results observed so far that the natural width is broadened by new physics effects to such an extent that it could be directly observable. Furthermore, as all LHC Higgs channels rely on the identification of Higgs decay products, the total Higgs width cannot be measured indirectly without additional assumptions. The different dependence of on-peak and off-peak contributions on the total width in Higgs decays to ZZ^* and interference effects between signal and background in Higgs decays to $\gamma\gamma$ can provide additional information in this context. Constraints on the total width from the combination of on-peak and off-peak contributions in Higgs decays to ZZ^* rely on the assumption of equal on- and off-shell effective couplings. Without an experimental determination of the total width or further theoretical assumptions, only ratios of couplings can be determined at the LHC rather than absolute values of couplings.

VALUE (MeV)	*CL%*	*DOCUMENT ID*		*TECN*	*COMMENT*
$3.0^{+1.5}_{-0.7}$ OUR AVERAGE					
$4.3^{+2.7}_{-1.9}$		[1] AAD	25AQ	ATLS	pp, 13 TeV, $ZZ^*/ZZ \to 4\ell$, $ZZ \to 2\ell 2\nu$
$0.9^{+3.4}_{-0.9}$		[2] AAD	25AV	ATLS	pp, 13 TeV, $WW^{(*)} \to 2\ell 2\nu$
$3.0^{+2.0}_{-1.5}$		[3] HAYRAPETY...	25L	CMS	pp, 13 TeV, $ZZ^*/ZZ \to 4\ell$, $ZZ \to 2\ell 2\nu$
• • • We do not use the following data for averages, fits, limits, etc. • • •					
< 160	95	[4] AAD	25E	ATLS	pp, 13 TeV, on-shell Higgs and $t\overline{t}t\overline{t}$

< 330	95	[5] HAYRAPETY...25L	CMS	pp, 13 TeV, $ZZ^* \to 4\ell$	
$2.9^{+2.3}_{-1.7}$		[6] HAYRAPETY...25L	CMS	pp, 13 TeV, $ZZ^* \to 4\ell$	
$4.4^{+3.0}_{-2.2}$		[7] AAD	23BR ATLS	pp, 13 TeV, $ZZ^*/ZZ \to 4\ell$, $ZZ \to 2\ell 2\nu$	
$3.2^{+2.4}_{-1.7}$		[8] TUMASYAN	22AM CMS	pp, 13 TeV, $ZZ^*/ZZ \to 4\ell$, $ZZ \to 2\ell 2\nu$	
$3.2^{+2.8}_{-2.2}$		[9] SIRUNYAN	19BL CMS	pp, 7, 8, 13 TeV, $ZZ^*/ZZ \to 4\ell$	
< 14.4	95	[10] AABOUD	18BP ATLS	pp, 13 TeV, $ZZ \to 4\ell$, $2\ell 2\nu$	
<1100	95	[11] SIRUNYAN	17AV CMS	pp, 13 TeV, $ZZ^* \to 4\ell$	
< 26	95	[12] KHACHATRY...16BA	CMS	pp, 7, 8 TeV, $WW^{(*)}$	
< 13	95	[13] KHACHATRY...16BA	CMS	pp, 7, 8 TeV, $ZZ^{(*)}, WW^{(*)}$	
< 22.7	95	[14] AAD	15BE ATLS	pp, 8 TeV, $ZZ^{(*)}$, $WW^{(*)}$	
<1700	95	[15] KHACHATRY...15AM	CMS	pp, 7, 8 TeV	
$> 3.5 \times 10^{-9}$	95	[16] KHACHATRY...15BA	CMS	pp, 7, 8 TeV, flight distance	
< 46	95	[17] KHACHATRY...15BA	CMS	pp, 7, 8 TeV, $ZZ^{(*)} \to 4\ell$	
<5000	95	[18] AAD	14W ATLS	pp, 7, 8 TeV, $\gamma\gamma$	
<2600	95	[18] AAD	14W ATLS	pp, 7, 8 TeV, $ZZ^* \to 4\ell$	
<3400	95	[19] CHATRCHYAN	14AA CMS	pp, 7, 8 TeV, $ZZ^* \to 4\ell$	
< 22	95	[20] KHACHATRY...14D	CMS	pp, 7, 8 TeV, $ZZ^{(*)}$	
<2400	95	[21] KHACHATRY...14P	CMS	pp, 7, 8 TeV, $\gamma\gamma$	

[1] AAD 25AQ use 140 fb^{-1} at $E_{\text{cm}} = 13$ TeV. The off-shell Higgs boson production in the $ZZ \to 4\ell$ ($\ell = e,\ \mu$) decay channel is combined with the on-shell production in the $ZZ^* \to 4\ell$ (AAD 20AQ) decay channel and the off-shell production in the $ZZ \to 2\ell 2\nu$ decay channel (AAD 23BR, AAD 25AP) to measure the total width assuming the same on-shell and off-shell coupling modifiers for gluon-fusion and for gauge-boson ($\kappa^2_{g,\text{on-shell}}\,\kappa^2_{V,\text{on-shell}} = \kappa^4_{V,\text{on-shell}} = \kappa^2_{g,\text{off-shell}}\,\kappa^2_{V,\text{off-shell}} = \kappa^4_{V,\text{off-shell}}$). $R_{gg} = \kappa^2_{g,\text{on-shell}}/\kappa^2_{g,\text{off-shell}}$ and $R_{VV} = \kappa^2_{V,\text{on-shell}}/\kappa^2_{V,\text{off-shell}}$ are measured to be $1.19^{+0.89}_{-0.66}$ and $0.95^{+0.44}_{-0.35}$, respectively. Using AAD 25AQ and AAD 23BR, $\kappa_{g,\text{off-shell}}$ and $\kappa_{V,\text{off-shell}}$ are measured to be $1.09^{+0.39}_{-0.35}$ and $0.99^{+0.16}_{-0.19}$, respectively. The quoted errors are values at 68%CL.

[2] AAD 25AV measure the total width Γ_H from off-shell $H^* \to WW \to 2\ell 2\nu$ and on-shell $H \to WW^* \to 2\ell 2\nu$ with data of 140 fb^{-1} pp collisions at $E_{\text{cm}} = 13$ TeV, assuming the off- and on-shell coupling modifiers are the same for both ggF and EW production modes. The quoted value corresponds to $\Gamma_H < 13.1$ MeV at 95% CL. The off-shell Higgs signal strength $\mu_{\text{off-shell}}$ is measured to be $0.3^{+0.9}_{-0.3}$ corresponding $\mu_{\text{off-shell}} < 3.4$ at 95% CL. The two off-shell signal strengths for ggF and EW production modes ($\mu^{\text{ggF}}_{\text{off-shell}}$, $\mu^{\text{EW}}_{\text{off-shell}}$) are measured to be $\mu^{\text{ggF}}_{\text{off-shell}} = 0.2^{+1.3}_{-0.2}$ and $\mu^{\text{EW}}_{\text{off-shell}} = 0.4^{+3.4}_{-0.4}$.

[3] HAYRAPETYAN 25L use 138 fb^{-1} at $E_{\text{cm}} = 13$ TeV. The on- and off-shell Higgs boson production in the $ZZ \to 4\ell$ ($\ell = e,\ \mu$) decay channel is combined with the off-shell Higgs boson production in the $ZZ \to 2\ell 2\nu$ (TUMASYAN 22AM) decay channel to measure the total width. The off-shell Higgs signal strength is measured to be $0.67^{+0.42}_{-0.32}$. The scenario of no off-shell contribution is excluded at 3.8 σ.

[4] AAD 25E constrain the total width using on-shell Higgs measurements and the four top quarks production with 13 TeV data. The tree-level Higgs-top Yukawa coupling is assumed to be the same for on-shell and off-shell Higgs boson production processes. Another assumption is that no BSM contributions affect the $t\bar{t}t\bar{t}$ production. The quoted value is obtained by assuming the loop-induced ggF, $H \to \gamma\gamma$, and $H \to Z\gamma$ rates can be modeled as a function of κ_t and other SM couplings. Otherwise, $\Gamma_H < 450$ MeV is obtained at 95% CL. Two-dimensional likelihood scan of ($\Gamma_H/\Gamma_H^{\mathrm{SM}}$, κ_t) is shown in their Fig. 3.

[5] HAYRAPETYAN 25L obtain an upper limit on the width from the on-shell $H \to ZZ^* \to 4\ell$ ($\ell = e,\ \mu$) decays. Data of 138 fb^{-1} pp collisions at $E_{\mathrm{cm}} = 13$ TeV is used.

[6] HAYRAPETYAN 25L use 138 fb^{-1} at $E_{\mathrm{cm}} = 13$ TeV. The on- and off-shell Higgs boson production in the $ZZ \to 4\ell$ ($\ell = e,\ \mu$) decay channel is used assuming that no new particles affect the gluon fusion production. The scenario of no off-shell contribution is excluded at 3.0 σ.

[7] AAD 23BR use 139 fb^{-1} at $E_{\mathrm{cm}} = 13$ TeV. The off-shell Higgs boson production in the $ZZ \to 4\ell$ and $ZZ \to 2\ell 2\nu$ decay channels and the on-shell production in the $ZZ^* \to 4\ell$ ($\ell = e,\ \mu$, AAD 20AQ) decay channels are used to measure the total width. The off-shell Higgs signal strength is measured to be $1.1^{+0.7}_{-0.6}$ assuming the same on-shell and off-shell coupling modifiers are used individually for gluon-fusion and for gauge-boson modes. The scenario of no off-shell contribution is excluded at 3.3 σ. Combining with the on-shell signal strength measurement, the total width normalized to its SM expectation Γ_H/Γ_H^{SM} is measured to be $1.1^{+0.7}_{-0.5}$ assuming the same on-shell and off-shell coupling modifiers are used individually for gluon-fusion and for gauge-boson modes. The observed upper limit on the total width is 10.1 MeV at 95% CL. See their Fig. 7. See corrected width values in their erratum AAD 25AP.

[8] TUMASYAN 22AM use up to 140 fb^{-1} at $E_{\mathrm{cm}} = 13$ TeV. The off-shell Higgs boson production in the $ZZ \to 4\ell$ and $ZZ \to 2\ell 2\nu$ decay channels and the on-shell production in the $ZZ^* \to 4\ell$ ($\ell = e,\ \mu$) decay channels are used to measure the total width. The off-shell Higgs signal strength is measured to be $0.62^{+0.68}_{-0.45}$ without the constraint on the ratio of the off-shell signal strengths for gluon-fusion and gauge-boson modes. The scenario of no off-shell contribution is excluded at 3.6 σ. The results are shown in their Table 1 with other constraint scenarios and the decay widths assuming the same coupling modifiers for on- and off-shell couplings (g_p and g_d in their notation). The measurement of anomalous HVV couplings is shown in their Extended Data Table 1 and Fig. 8.

[9] SIRUNYAN 19BL measure the width and anomalous HVV couplings from on-shell and off-shell production in the 4ℓ final state. Data of 80.2 fb^{-1} at 13 TeV, 19.7 fb^{-1} at 8 TeV, and 5.1 fb^{-1} at 7 TeV are used. The total width for the SM-like couplings is measured to be also [0.08, 9.16] MeV with 95% CL, assuming SM-like couplings for on- and off-shells (see their Table VIII). Constraints on the total width for anomalous HVV interaction cases are found in their Table IX. See their Table X for the Higgs boson signal strength in the off-shell region.

[10] AABOUD 18BP use 36.1 fb^{-1} at $E_{\mathrm{cm}} = 13$ TeV. An observed upper limit on the off-shell Higgs signal strength of 3.8 is obtained at 95% CL using off-shell Higgs boson production in the $ZZ \to 4\ell$ and $ZZ \to 2\ell 2\nu$ decay channels ($\ell = e,\ \mu$). Combining with the on-shell signal strength measurements, the quoted upper limit on the Higgs boson total width is obtained, assuming the ratios of the relevant Higgs-boson couplings to the SM predictions are constant with energy from on-shell production to the high-mass range.

[11] SIRUNYAN 17AV obtain an upper limit on the width from the $m_{4\ell}$ distribution in $ZZ^* \to 4\ell$ ($\ell = e,\ \mu$) decays. Data of 35.9 fb^{-1} pp collisions at $E_{\mathrm{cm}} = 13$ TeV is used. The expected limit is 1.60 GeV.

[12] KHACHATRYAN 16BA derive constraints on the total width from comparing $WW^{(*)}$ production via on-shell and off-shell H using 4.9 fb^{-1} of pp collisions at $E_{\mathrm{cm}} = 7$ TeV and 19.4 fb^{-1} at 8 TeV.

[13] KHACHATRYAN 16BA combine the $WW^{(*)}$ result with $ZZ^{(*)}$ results of KHACHATRYAN 15BA and KHACHATRYAN 14D.
[14] AAD 15BE derive constraints on the total width from comparing $ZZ^{(*)}$ and $WW^{(*)}$ production via on-shell and off-shell H using 20.3 fb^{-1} of pp collisions at $E_{cm} = 8$ TeV. The K factor for the background processes is assumed to be equal to that for the signal.
[15] KHACHATRYAN 15AM combine $\gamma\gamma$ and $ZZ^* \to 4\ell$ results. The expected limit is 2.3 GeV.
[16] KHACHATRYAN 15BA derive a lower limit on the total width from an upper limit on the decay flight distance $\tau < 1.9 \times 10^{-13}$ s. 5.1 fb^{-1} of pp collisions at $E_{cm} = 7$ TeV and 19.7 fb^{-1} at 8 TeV are used.
[17] KHACHATRYAN 15BA derive constraints on the total width from comparing $ZZ^{(*)}$ production via on-shell and off-shell H with an unconstrained anomalous coupling. 4ℓ final states in 5.1 fb^{-1} of pp collisions at $E_{cm} = 7$ TeV and 19.7 fb^{-1} at $E_{cm} = 8$ TeV are used.
[18] AAD 14W use 4.5 fb^{-1} of pp collisions at $E_{cm} = 7$ TeV and 20.3 fb^{-1} at 8 TeV. The expected limit is 6.2 GeV.
[19] CHATRCHYAN 14AA use 5.1 fb^{-1} of pp collisions at $E_{cm} = 7$ TeV and 19.7 fb^{-1} at $E_{cm} = 8$ TeV. The expected limit is 2.8 GeV.
[20] KHACHATRYAN 14D derive constraints on the total width from comparing $ZZ^{(*)}$ production via on-shell and off-shell H. 4ℓ and $\ell\ell\nu\nu$ final states in 5.1 fb^{-1} of pp collisions at $E_{cm} = 7$ TeV and 19.7 fb^{-1} at $E_{cm} = 8$ TeV are used.
[21] KHACHATRYAN 14P use 5.1 fb^{-1} of pp collisions at $E_{cm} = 7$ TeV and 19.7 fb^{-1} at $E_{cm} = 8$ TeV. The expected limit is 3.1 GeV.

H DECAY MODES

	Mode	Fraction (Γ_i/Γ)	Confidence level
Γ_1	WW^*	(25.7 $\pm$2.5) %	
Γ_2	ZZ^*	(2.80$\pm$0.30) %	
Γ_3	$\gamma\gamma$	(2.50$\pm$0.20) $\times 10^{-3}$	
Γ_4	$b\overline{b}$	(53 $\pm$8) %	
Γ_5	e^+e^-	$<$ 3.0 $\times 10^{-4}$	95%
Γ_6	$\mu^+\mu^-$	(3.0 $\pm$0.9) $\times 10^{-4}$	
Γ_7	$\tau^+\tau^-$	(6.0 $^{+0.8}_{-0.7}$) %	
Γ_8	$Z\gamma$	(3.4 $\pm$1.1) $\times 10^{-3}$	
Γ_9	$Z\rho(770)$	$<$ 1.21 %	95%
Γ_{10}	$Z\phi(1020)$	$<$ 3.6 $\times 10^{-3}$	95%
Γ_{11}	$Z\eta_c$		
Γ_{12}	ZJ/ψ	$<$ 1.9 $\times 10^{-3}$	95%
Γ_{13}	$Z\psi(2S)$	$<$ 6.6 $\times 10^{-3}$	95%
Γ_{14}	$J/\psi\gamma$	$<$ 2.0 $\times 10^{-4}$	95%
Γ_{15}	$J/\psi J/\psi$	$<$ 3.8 $\times 10^{-4}$	95%
Γ_{16}	$\psi(2S)\gamma$	$<$ 9.9 $\times 10^{-4}$	95%
Γ_{17}	$\psi(2S)J/\psi$	$<$ 2.1 $\times 10^{-3}$	95%
Γ_{18}	$\psi(2S)\psi(2S)$	$<$ 3.0 $\times 10^{-3}$	95%
Γ_{19}	$\Upsilon(1S)\gamma$	$<$ 2.5 $\times 10^{-4}$	95%
Γ_{20}	$\Upsilon(1S)\Upsilon(1S)$	$<$ 1.7 $\times 10^{-3}$	95%

Γ_{21}	$\Upsilon(2S)\gamma$		< 4.2	$\times 10^{-4}$	95%
Γ_{22}	$\Upsilon(3S)\gamma$		< 3.4	$\times 10^{-4}$	95%
Γ_{23}	$\Upsilon(\text{nS})\,\Upsilon(\text{mS})$		< 3.5	$\times 10^{-4}$	95%
Γ_{24}	$D^*\gamma$		< 1.0	$\times 10^{-3}$	95%
Γ_{25}	$\rho(770)\gamma$		< 3.7	$\times 10^{-4}$	95%
Γ_{26}	$\omega(782)\gamma$		< 5.5	$\times 10^{-4}$	95%
Γ_{27}	$K^*(892)\gamma$		< 2.2	$\times 10^{-4}$	95%
Γ_{28}	$\phi(1020)\gamma$		< 3.0	$\times 10^{-4}$	95%
Γ_{29}	$e\mu$	*LF*	< 4.4	$\times 10^{-5}$	95%
Γ_{30}	$e\tau$	*LF*	< 2.0	$\times 10^{-3}$	95%
Γ_{31}	$\mu\tau$	*LF*	< 1.5	$\times 10^{-3}$	95%
Γ_{32}	invisible		< 10.7	%	95%
Γ_{33}	γ invisible		< 1.3	%	95%

H BRANCHING RATIOS

$\Gamma(WW^*)/\Gamma_{\text{total}}$ Γ_1/Γ

VALUE	*DOCUMENT ID*		*TECN*	*COMMENT*
$\mathbf{0.257^{+0.026}_{-0.024}}$	[1] ATLAS	22	ATLS	pp, 13 TeV

[1] ATLAS 22 report combined results (see their Extended Data Table 1) using up to 139 fb^{-1} of data at $E_{\text{cm}} = 13$ TeV, assuming $m_H = 125.09$ GeV. SM values for the production cross-sections are assumed. See their Fig. 2b.

$\Gamma(ZZ^*)/\Gamma_{\text{total}}$ Γ_2/Γ

VALUE	*DOCUMENT ID*		*TECN*	*COMMENT*
$\mathbf{0.028 \pm 0.003}$	[1] ATLAS	22	ATLS	pp, 13 TeV

[1] ATLAS 22 report combined results (see their Extended Data Table 1) using up to 139 fb^{-1} of data at $E_{\text{cm}} = 13$ TeV, assuming $m_H = 125.09$ GeV. SM values for the production cross-sections are assumed. See their Fig. 2b.

$\Gamma(\gamma\gamma)/\Gamma_{\text{total}}$ Γ_3/Γ

VALUE	*DOCUMENT ID*		*TECN*	*COMMENT*
$\mathbf{0.0025 \pm 0.0002}$	[1] ATLAS	22	ATLS	pp, 13 TeV

[1] ATLAS 22 report combined results (see their Extended Data Table 1) using up to 139 fb^{-1} of data at $E_{\text{cm}} = 13$ TeV, assuming $m_H = 125.09$ GeV. SM values for the production cross-sections are assumed. See their Fig. 2b.

$\Gamma(b\bar{b})/\Gamma_{\text{total}}$ Γ_4/Γ

VALUE	*DOCUMENT ID*		*TECN*	*COMMENT*
$\mathbf{0.53 \pm 0.08}$	[1] ATLAS	22	ATLS	pp, 13 TeV

[1] ATLAS 22 report combined results (see their Extended Data Table 1) using up to 139 fb^{-1} of data at $E_{\text{cm}} = 13$ TeV, assuming $m_H = 125.09$ GeV. SM values for the production cross-sections are assumed. See their Fig. 2b.

$\Gamma(e^+e^-)/\Gamma_{\text{total}}$ Γ_5/Γ

VALUE	*CL%*	*DOCUMENT ID*		*TECN*	*COMMENT*
$\mathbf{< 3.0 \times 10^{-4}}$	95	[1] TUMASYAN	23AU	CMS	pp, 13 TeV

• • • We do not use the following data for averages, fits, limits, etc. • • •

$<3.6\times10^{-4}$	95	[2] AAD	20F	ATLS	pp, 13 TeV
$<1.9\times10^{-3}$	95	[3] KHACHATRY...	15H	CMS	pp, 7, 8 TeV

[1] TUMASYAN 23AU use 138 fb^{-1} of pp collisions at E_{cm} = 13 TeV.

[2] AAD 20F use 139 fb^{-1} of pp collisions at E_{cm} = 13 TeV. The best-fit value of the $H \to e e$ branching fraction is $(0.0 \pm 1.7 \pm 0.6)\times10^{-4}$ for m_H = 125 GeV.

[3] KHACHATRYAN 15H use 5.0 fb^{-1} of pp collisions at E_{cm} = 7 TeV and 19.7 fb^{-1} at 8 TeV.

$\Gamma(\mu^+\mu^-)/\Gamma_{total}$ Γ_6/Γ

VALUE (units 10^{-4})	*DOCUMENT ID*		*TECN*	*COMMENT*
3.0±0.9	[1] AAD	25AR	ATLS	pp, 13, 13.6 TeV

• • • We do not use the following data for averages, fits, limits, etc. • • •

2.6±1.3	[2] ATLAS	22	ATLS	pp, 13 TeV

[1] AAD 25AR report results using 140 fb^{-1} of data at E_{cm} = 13 TeV and 165 fb^{-1} of data at E_{cm} = 13.6 TeV assuming m_H = 125.09 GeV and SM values for the Higgs-boson production cross sections.

[2] ATLAS 22 report combined results (see their Extended Data Table 1) using up to 139 fb^{-1} of data at E_{cm} = 13 TeV, assuming m_H = 125.09 GeV. SM values for the production cross-sections are assumed. See their Fig. 2b.

$\Gamma(\tau^+\tau^-)/\Gamma_{total}$ Γ_7/Γ

VALUE	*DOCUMENT ID*		*TECN*	*COMMENT*
$\mathbf{0.060^{+0.008}_{-0.007}}$	[1] ATLAS	22	ATLS	pp, 13 TeV

[1] ATLAS 22 report combined results (see their Extended Data Table 1) using up to 139 fb^{-1} of data at E_{cm} = 13 TeV, assuming m_H = 125.09 GeV. SM values for the production cross-sections are assumed. See their Fig. 2b.

$\Gamma(Z\gamma)/\Gamma_{total}$ Γ_8/Γ

VALUE (units 10^{-3})	*DOCUMENT ID*		*TECN*	*COMMENT*
3.4±1.1	[1] AAD	24D	LHC	pp, 13 TeV

• • • We do not use the following data for averages, fits, limits, etc. • • •

3.2±1.5	[2] ATLAS	22	ATLS	pp, 13 TeV

[1] AAD 24D report combined results of ATLAS (AAD 20AG) and CMS (TUMASYAN 23F). SM values for the production cross-sections are assumed.

[2] ATLAS 22 report combined results (see their Extended Data Table 1) using up to 139 fb^{-1} of data at E_{cm} = 13 TeV, assuming m_H = 125.09 GeV. SM values for the production cross-sections are assumed. See their Fig. 2b.

$\Gamma(Z\rho(770))/\Gamma_{total}$ Γ_9/Γ

VALUE	*CL%*	*DOCUMENT ID*		*TECN*	*COMMENT*
$\mathbf{<1.21\times10^{-2}}$	95	[1] SIRUNYAN	20BK	CMS	pp, 13 TeV

[1] SIRUNYAN 20BK search for $H \to Z\rho$, $Z \to e^+e^-/\mu^+\mu^-$, $\rho \to \pi^+\pi^-$ with 137 fb^{-1} of pp collision data at E_{cm} = 13 TeV. The quoted branching fraction is for the unpolarized decay. See their Table 3 for different polarizations.

$\Gamma(Z\phi(1020))/\Gamma_{total}$ Γ_{10}/Γ

VALUE	*CL%*	*DOCUMENT ID*		*TECN*	*COMMENT*
$\mathbf{<3.6\times10^{-3}}$	95	[1] SIRUNYAN	20BK	CMS	pp, 13 TeV

[1] SIRUNYAN 20BK search for $H \to Z\phi$, $Z \to e^+e^-/\mu^+\mu^-$, $\phi \to K^+K^-$ with 137 fb^{-1} of pp collision data at $E_{cm} = 13$ TeV. The quoted branching fraction is for the unpolarized decay. See their Table 4 for different polarizations.

$\Gamma(Z\eta_c)/\Gamma_{total}$ Γ_{11}/Γ

VALUE	DOCUMENT ID		TECN	COMMENT
• • • We do not use the following data for averages, fits, limits, etc. • • •				
	[1] AAD	25AT	ATLS	pp, 13 TeV
	[2] AAD	20AE	ATLS	pp, 13 TeV

[1] AAD 25AT search for $H \to Z\eta_c$ with two-leptons ($e^+e^-/\mu^+\mu^-$) plus jet events using 140 fb^{-1} of pp collision data at $E_{cm} = 13$ TeV. The branching fraction B($H \to Z\eta_c$) > 1.2 is excluded at 95% CL.

[2] AAD 20AE search for $H \to Z\eta_c$ with two-leptons ($e^+e^-/\mu^+\mu^-$) plus jet events using 139 fb^{-1} of pp collision data at $E_{cm} = 13$ TeV. The upper limit of $\sigma(pp \to H)\cdot$B($H \to Z\eta_c$) is 110 pb at 95% CL.

$\Gamma(ZJ/\psi)/\Gamma_{total}$ Γ_{12}/Γ

VALUE	CL%	DOCUMENT ID		TECN	COMMENT
$<1.9 \times 10^{-3}$	95	[1] TUMASYAN	23C	CMS	pp, 13 TeV
• • • We do not use the following data for averages, fits, limits, etc. • • •					
		[2] AAD	25AT	ATLS	pp, 13 TeV
		[3] AAD	20AE	ATLS	pp, 13 TeV

[1] TUMASYAN 23C search for $H \to ZJ/\psi$, $Z \to e^+e^-$ or $\mu^+\mu^-$, $J/\psi \to \mu^+\mu^-$ with 138 fb^{-1} of pp collision data at $E_{cm} = 13$ TeV. The quoted value is for the Higgs decays for longitudinally polarized mesons. See their Table 1 for other cases.

[2] AAD 25AT search for $H \to ZJ/\psi$ with two-leptons ($e^+e^-/\mu^+\mu^-$) plus jet events using 140 fb^{-1} of pp collision data at $E_{cm} = 13$ TeV. The branching fraction B($H \to ZJ/\psi$) > 1.4 is excluded at 95% CL.

[3] AAD 20AE search for $H \to ZJ/\psi$ with two-leptons ($e^+e^-/\mu^+\mu^-$) plus jet events using 139 fb^{-1} of pp collision data at $E_{cm} = 13$ TeV. The upper limit of $\sigma(pp \to H)\cdot$B($H \to ZJ/\psi$) is 100 pb at 95% CL.

$\Gamma(Z\psi(2S))/\Gamma_{total}$ Γ_{13}/Γ

VALUE	CL%	DOCUMENT ID		TECN	COMMENT
$<6.6 \times 10^{-3}$	95	[1] TUMASYAN	23C	CMS	pp, 13 TeV

[1] TUMASYAN 23C search for $H \to Z\psi(2S)$, $Z \to e^+e^-$ or $\mu^+\mu^-$, $\psi(2S) \to \mu^+\mu^-$ with 138 fb^{-1} of pp collision data at $E_{cm} = 13$ TeV. The quoted value is for the Higgs decays for longitudinally polarized mesons. See their Table 1 for other cases.

$\Gamma(J/\psi\gamma)/\Gamma_{total}$ Γ_{14}/Γ

VALUE	CL%	DOCUMENT ID		TECN	COMMENT
$<2.0 \times 10^{-4}$	95	[1] AAD	23CD	ATLS	13 TeV, 138 fb^{-1}
• • • We do not use the following data for averages, fits, limits, etc. • • •					
$<2.6 \times 10^{-4}$	95	[2] HAYRAPETY...25H		CMS	13 TeV, 123 fb^{-1}
$<7.6 \times 10^{-4}$	95	[3] SIRUNYAN	19AJ	CMS	13 TeV, 35.9 fb^{-1}
$<3.5 \times 10^{-4}$	95	[4] AABOUD	18BL	ATLS	13 TeV, 36.1 fb^{-1}
$<1.5 \times 10^{-3}$	95	[5] KHACHATRY...16B		CMS	8 TeV
$<1.5 \times 10^{-3}$	95	[6] AAD	15I	ATLS	8 TeV

[1] AAD 23CD search for $H \to J/\psi\gamma$, $J/\psi \to \mu^+\mu^-$ with 138 fb^{-1} of pp collision data at $E_{cm} = 13$ TeV. SM values for the production cross-sections are assumed.

[2] HAYRAPETYAN 25H search for $H \to J/\psi\gamma$, $J/\psi \to \mu^+\mu^-$ with 123 fb^{-1} of pp collision data at $E_{cm} = 13$ TeV. SM values for the production cross-sections are assumed. See their Table 4 and Fig. 5.

[3] SIRUNYAN 19AJ search for $H \to J/\psi\gamma$, $J/\psi \to \mu^+\mu^-$ with 35.9 fb^{-1} of pp collision data at $E_{cm} = 13$ TeV. The upper limit corresponds to 260 times the SM prediction and by combining the KHACHATRYAN 16B, it is 220 times the SM prediction.

[4] AABOUD 18BL search for $H \to J/\psi\gamma$, $J/\psi \to \mu^+\mu^-$ with 36.1 fb^{-1} of pp collision data at $E_{cm} = 13$ TeV.

[5] KHACHATRYAN 16B use 19.7 fb^{-1} of pp collision data at 8 TeV.

[6] AAD 15I use 19.7 fb^{-1} of pp collision data at 8 TeV.

$\Gamma(J/\psi J/\psi)/\Gamma_{total}$ Γ_{15}/Γ

VALUE	CL%	DOCUMENT ID		TECN	COMMENT
$<3.8 \times 10^{-4}$	95	[1] TUMASYAN	23C	CMS	pp, 13 TeV
• • • We do not use the following data for averages, fits, limits, etc. • • •					
$<1.8 \times 10^{-3}$	95	[2] SIRUNYAN	19BR	CMS	pp at 13 TeV

[1] TUMASYAN 23C search for $H \to J/\psi J/\psi$, $J/\psi \to \mu^+\mu^-$ with 138 fb^{-1} of pp collision data at $E_{cm} = 13$ TeV. The quoted value is for the Higgs decays for longitudinally polarized mesons. See their Table 1 for other cases.

[2] SIRUNYAN 19BR search for $H \to J/\psi J/\psi$, $J/\psi \to \mu^+\mu^-$ with 37.5 fb^{-1} of pp collision data at $E_{cm} = 13$ TeV. J/ψs from the Higgs decay are assumed to be unpolarized. For fully longitudinal (transverse) polarized J/ψs, limits change by -22% ($+10\%$).

$\Gamma(\psi(2S)\gamma)/\Gamma_{total}$ Γ_{16}/Γ

VALUE	CL%	DOCUMENT ID		TECN	COMMENT
$<9.9 \times 10^{-4}$	95	[1] HAYRAPETY...25H		CMS	13 TeV, 123 fb^{-1}
• • • We do not use the following data for averages, fits, limits, etc. • • •					
$<1.05 \times 10^{-3}$	95	[2] AAD	23CD	ATLS	13 TeV, 138 fb^{-1}
$<2.0 \times 10^{-3}$	95	[3] AABOUD	18BL	ATLS	13 TeV, 36.1 fb^{-1}

[1] HAYRAPETYAN 25H search for $H \to \psi(2S)\gamma$, $\psi(2S) \to \mu^+\mu^-$ with 123 fb^{-1} of pp collision data at $E_{cm} = 13$ TeV. SM values for the production cross-sections are assumed. See their Table 4 and Fig. 5.

[2] AAD 23CD search for $H \to \psi(2S)\gamma$, $\psi(2S) \to \mu^+\mu^-$ with 138 fb^{-1} of pp collision data at $E_{cm} = 13$ TeV. SM values for the production cross-sections are assumed.

[3] AABOUD 18BL search for $H \to \psi(2S)\gamma$, $\psi(2S) \to \mu^+\mu^-$ with 36.1 fb^{-1} of pp collision data at $E_{cm} = 13$ TeV.

$\Gamma(\psi(2S)J/\psi)/\Gamma_{total}$ Γ_{17}/Γ

VALUE	CL%	DOCUMENT ID		TECN	COMMENT
$<2.1 \times 10^{-3}$	95	[1] TUMASYAN	23C	CMS	pp, 13 TeV

[1] TUMASYAN 23C search for $H \to \psi(2S)J/\psi$, $\psi(2S) \to \mu^+\mu^-$, $J/\psi \to \mu^+\mu^-$ with 138 fb^{-1} of pp collision data at $E_{cm} = 13$ TeV. The quoted value is for the Higgs decays for longitudinally polarized mesons. See their Table 1 for other cases.

$\Gamma(\psi(2S)\psi(2S))/\Gamma_{total}$ Γ_{18}/Γ

VALUE	CL%	DOCUMENT ID		TECN	COMMENT
$<3.0 \times 10^{-3}$	95	[1] TUMASYAN	23C	CMS	pp, 13 TeV

[1] TUMASYAN 23C search for $H \to \psi(2S)\psi(2S)$, $\psi(2S) \to \mu^+\mu^-$ with 138 fb^{-1} of pp collision data at $E_{cm} = 13$ TeV. The quoted value is for the Higgs decays for longitudinally polarized mesons. See their Table 1 for other cases.

$\Gamma(\Upsilon(1S)\gamma)/\Gamma_{\text{total}}$ Γ_{19}/Γ

VALUE	CL%	DOCUMENT ID		TECN	COMMENT
$<2.5\times10^{-4}$	95	[1] AAD	23CD	ATLS	13 TeV, 138 fb^{-1}
• • • We do not use the following data for averages, fits, limits, etc. • • •					
$<4.9\times10^{-4}$	95	[2] AABOUD	18BL	ATLS	13 TeV, 36.1 fb^{-1}
$<1.3\times10^{-3}$	95	[3] AAD	15I	ATLS	8 TeV

[1] AAD 23CD search for $H\to\ \Upsilon(1S)\gamma$, $\Upsilon(1S)\to\ \mu^+\mu^-$ with 138 fb^{-1} of pp collision data at $E_{\text{cm}}=13$ TeV. SM values for the production cross-sections are assumed.

[2] AABOUD 18BL search for $H\to\ \Upsilon(1S)\gamma$, $\Upsilon(1S)\to\ \mu^+\mu^-$ with 36.1 fb^{-1} of pp collision data at $E_{\text{cm}}=13$ TeV.

[3] AAD 15I use 19.7 fb^{-1} of pp collision data at 8 TeV.

$\Gamma(\Upsilon(1S)\,\Upsilon(1S))/\Gamma_{\text{total}}$ Γ_{20}/Γ

VALUE	CL%	DOCUMENT ID		TECN	COMMENT
$<1.7\times10^{-3}$	95	[1] TUMASYAN	23C	CMS	pp, 13 TeV

[1] TUMASYAN 23C search for $H\to\ \Upsilon(1S)\,\Upsilon(1S)$, $\Upsilon(1S)\to\ \mu^+\mu^-$ with 138 fb^{-1} of pp collision data at $E_{\text{cm}}=13$ TeV. The quoted value is for the Higgs decays for longitudinally polarized mesons. See their Table 1 for other cases.

$\Gamma(\Upsilon(2S)\gamma)/\Gamma_{\text{total}}$ Γ_{21}/Γ

VALUE	CL%	DOCUMENT ID		TECN	COMMENT
$<4.2\times10^{-4}$	95	[1] AAD	23CD	ATLS	13 TeV, 138 fb^{-1}
• • • We do not use the following data for averages, fits, limits, etc. • • •					
$<5.9\times10^{-4}$	95	[2] AABOUD	18BL	ATLS	13 TeV, 36.1 fb^{-1}
$<1.9\times10^{-3}$	95	[3] AAD	15I	ATLS	8 TeV

[1] AAD 23CD search for $H\to\ \Upsilon(2S)\gamma$, $\Upsilon(2S)\to\ \mu^+\mu^-$ with 138 fb^{-1} of pp collision data at $E_{\text{cm}}=13$ TeV. SM values for the production cross-sections are assumed.

[2] AABOUD 18BL search for $H\to\ \Upsilon(2S)\gamma$, $\Upsilon(2S)\to\ \mu^+\mu^-$ with 36.1 fb^{-1} of pp collision data at $E_{\text{cm}}=13$ TeV.

[3] AAD 15I use 19.7 fb^{-1} of pp collision data at 8 TeV.

$\Gamma(\Upsilon(3S)\gamma)/\Gamma_{\text{total}}$ Γ_{22}/Γ

VALUE	CL%	DOCUMENT ID		TECN	COMMENT
$<3.4\times10^{-4}$	95	[1] AAD	23CD	ATLS	13 TeV, 138 fb^{-1}
• • • We do not use the following data for averages, fits, limits, etc. • • •					
$<5.7\times10^{-4}$	95	[2] AABOUD	18BL	ATLS	13 TeV, 36.1 fb^{-1}
$<1.3\times10^{-3}$	95	[3] AAD	15I	ATLS	8 TeV

[1] AAD 23CD search for $H\to\ \Upsilon(3S)\gamma$, $\Upsilon(3S)\to\ \mu^+\mu^-$ with 138 fb^{-1} of pp collision data at $E_{\text{cm}}=13$ TeV. SM values for the production cross-sections are assumed.

[2] AABOUD 18BL search for $H\to\ \Upsilon(3S)\gamma$, $\Upsilon(3S)\to\ \mu^+\mu^-$ with 36.1 fb^{-1} of pp collision data at $E_{\text{cm}}=13$ TeV.

[3] AAD 15I use 19.7 fb^{-1} of pp collision data at 8 TeV.

$\Gamma(\Upsilon(nS)\,\Upsilon(mS))/\Gamma_{\text{total}}$ Γ_{23}/Γ

VALUE	CL%	DOCUMENT ID		TECN	COMMENT
$<3.5\times10^{-4}$	95	[1] TUMASYAN	23C	CMS	pp, 13 TeV
• • • We do not use the following data for averages, fits, limits, etc. • • •					
$<1.4\times10^{-3}$	95	[2] SIRUNYAN	19BR	CMS	pp, 13 TeV

[1] TUMASYAN 23C search for $H \to \Upsilon(nS)\,\Upsilon(mS)$ with $\Upsilon(nS)$, $\Upsilon(mS) \to \mu^+\mu^-$ (n, m = 1, 2, 3) with 138 fb^{-1} of pp collision data at E_{cm} = 13 TeV. The quoted value is for the Higgs decays for longitudinally polarized mesons. See their Table 1 for other cases.

[2] SIRUNYAN 19BR search for $H \to \Upsilon(nS)\,\Upsilon(mS)$ with $\Upsilon(nS), \Upsilon(mS) \to \mu^+\mu^-$ (n, m = 1, 2, 3) for 37.5 fb^{-1} of pp collision data at E_{cm} = 13 TeV. Υs from the Higgs decay are assumed to be unpolarized. For fully longitudinal (transverse) polarized Υs, limits change by −22% (+10%). The three Υ states selected in a mass range of 8.5–11 GeV are not distinguished.

$\Gamma(D^*\gamma)/\Gamma_{total}$ Γ_{24}/Γ

VALUE	CL%	DOCUMENT ID		TECN	COMMENT
<1.0 × 10^{-3}	95	[1] AAD	24R	ATLS	pp, 13 TeV

[1] AAD 24R use 136.3 fb^{-1} of pp collision data at 13 TeV. The 95% CL upper limit on the cross section times the branching ratio is 58 fb. The SM Higgs production cross section of m_H = 125.09 GeV is assumed. See their Table 3.

$\Gamma(\rho(770)\gamma)/\Gamma_{total}$ Γ_{25}/Γ

VALUE	CL%	DOCUMENT ID		TECN	COMMENT
< 3.7 × 10^{-4}	95	[1] HAYRAPETY...25G		CMS	pp, 13 TeV
• • • We do not use the following data for averages, fits, limits, etc. • • •					
<10.4 × 10^{-4}	95	[2] AABOUD	18AU	ATLS	pp, 13 TeV

[1] HAYRAPETYAN 25G search for $H \to \rho^0\gamma$, $\rho^0 \to \pi^+\pi^-$ with up to 138 fb^{-1} of pp collision data at E_{cm} = 13 TeV.

[2] AABOUD 18AU use 35.6 fb^{-1} of pp collision data at 13 TeV. See their erratum AABOUD 23A.

$\Gamma(\omega(782)\gamma)/\Gamma_{total}$ Γ_{26}/Γ

VALUE	CL%	DOCUMENT ID		TECN	COMMENT
<5.5 × 10^{-4}	95	[1] AAD	23BS	ATLS	pp, 13 TeV

[1] AAD 23BS use 89.5 fb^{-1} of pp collision data at 13 TeV.

$\Gamma(K^*(892)\gamma)/\Gamma_{total}$ Γ_{27}/Γ

VALUE	CL%	DOCUMENT ID		TECN	COMMENT
<2.2 × 10^{-4}	95	[1] AAD	23BS	ATLS	pp, 13 TeV
• • • We do not use the following data for averages, fits, limits, etc. • • •					
<3.0 × 10^{-4}	95	[2] HAYRAPETY...25G		CMS	pp, 13 TeV

[1] AAD 23BS use 134 fb^{-1} of pp collision data at 13 TeV.

[2] HAYRAPETYAN 25G search for $H \to K^{*0}\gamma$, $K^{*0} \to K^\pm\pi^\mp$ with up to 138 fb^{-1} of pp collision data at E_{cm} = 13 TeV.

$\Gamma(\phi(1020)\gamma)/\Gamma_{total}$ Γ_{28}/Γ

VALUE	CL%	DOCUMENT ID		TECN	COMMENT
<3.0 × 10^{-4}	95	[1] HAYRAPETY...25G		CMS	pp, 13 TeV
• • • We do not use the following data for averages, fits, limits, etc. • • •					
<5.0 × 10^{-4}	95	[2] AABOUD	18AU	ATLS	pp, 13 TeV
<1.4 × 10^{-3}	95	[3] AABOUD	16K	ATLS	pp, 13 TeV

[1] HAYRAPETYAN 25G search for $H \to \phi\gamma$, $\phi \to K^+K^-$ with up to 138 fb^{-1} of pp collision data at E_{cm} = 13 TeV.

[2] AABOUD 18AU use 35.6 fb^{-1} of pp collision data at 13 TeV. See their erratum AABOUD 23A.

[3] AABOUD 16K use 2.7 fb^{-1} of pp collision data at 13 TeV.

$\Gamma(e\mu)/\Gamma_{\text{total}}$ Γ_{29}/Γ

VALUE	CL%	DOCUMENT ID		TECN	COMMENT
$<4.4\times10^{-5}$	95	[1] HAYRAPETY...23C		CMS	pp, 13 TeV
• • • We do not use the following data for averages, fits, limits, etc. • • •					
$<6.1\times10^{-5}$	95	[2] AAD	20F	ATLS	pp, 13 TeV
$<3.5\times10^{-4}$	95	[3] KHACHATRY...16CD		CMS	pp, 8 TeV

[1] HAYRAPETYAN 23C use 138 fb^{-1} of pp collisions at $E_{\text{cm}} = 13$ TeV. The limit constrains the $Y_{e\mu}$ Yukawa coupling to $\sqrt{|Y_{e\mu}|^2+|Y_{\mu e}|^2} < 1.9\times10^{-4}$ at 95% CL (see their Fig. 6).

[2] AAD 20F use 139 fb^{-1} of pp collisions at $E_{\text{cm}} = 13$ TeV. The best-fit value of the $H\to e\mu$ branching fraction is $(0.4\pm2.9\pm0.3)\times10^{-5}$ for $m_H = 125$ GeV.

[3] KHACHATRYAN 16CD search for $H\to e\mu$ in 19.7 fb^{-1} of pp collisions at $E_{\text{cm}} = 8$ TeV. The limit constrains the $Y_{e\mu}$ Yukawa coupling to $\sqrt{|Y_{e\mu}|^2+|Y_{\mu e}|^2} < 5.4\times10^{-4}$ at 95% CL (see their Fig. 6).

$\Gamma(e\tau)/\Gamma_{\text{total}}$ Γ_{30}/Γ

VALUE	CL%	DOCUMENT ID		TECN	COMMENT
$<2.0\times10^{-3}$	95	[1] AAD	23Q	ATLS	pp, 13 TeV
• • • We do not use the following data for averages, fits, limits, etc. • • •					
$<2.3\times10^{-3}$	95	[2] AAD	23Q	ATLS	pp, 13 TeV
$<2.2\times10^{-3}$	95	[3] SIRUNYAN	21Z	CMS	pp, 13 TeV
$<4.7\times10^{-3}$	95	[4] AAD	20A	ATLS	pp, 13 TeV
$<6.1\times10^{-3}$	95	[5] SIRUNYAN	18BH	CMS	pp, 13 TeV
$<10.4\times10^{-3}$	95	[6] AAD	17	ATLS	pp, 8 TeV
$<6.9\times10^{-3}$	95	[7] KHACHATRY...16CD		CMS	pp, 8 TeV

[1] AAD 23Q search for $H\to e\tau$ in 138 fb^{-1} of pp collisions at $E_{\text{cm}} = 13$ TeV. The result is obtained from a simultaneous fit of possible $H\to e\tau$ and $H\to\mu\tau$ signals (see their Figs. 13 and 14). The limit constrains the $Y_{e\tau}$ Yukawa coupling to $\sqrt{|Y_{e\tau}|^2+|Y_{\tau e}|^2} < 1.3\times10^{-3}$ at 95% CL (see their Fig. 15).

[2] AAD 23Q search for $H\to e\tau$ in 138 fb^{-1} of pp collisions at $E_{\text{cm}} = 13$ TeV. The limit constrains the $Y_{e\tau}$ Yukawa coupling to $\sqrt{|Y_{e\tau}|^2+|Y_{\tau e}|^2} < 1.4\times10^{-3}$ at 95% CL (see their Fig. 12).

[3] SIRUNYAN 21Z search for $H\to e\tau$ in 137 fb^{-1} of pp collisions at $E_{\text{cm}} = 13$ TeV. The limit constrains the $Y_{e\tau}$ Yukawa coupling to $\sqrt{|Y_{e\tau}|^2+|Y_{\tau e}|^2} < 1.35\times10^{-3}$ at 95% CL (see their Fig. 8).

[4] AAD 20A search for $H\to e\tau$ in 36.1 fb^{-1} of pp collisions at $E_{\text{cm}} = 13$ TeV. The limit constrains the $Y_{e\tau}$ Yukawa coupling to $\sqrt{|Y_{e\tau}|^2+|Y_{\tau e}|^2} < 2.0\times10^{-3}$ at 95% CL (see their Fig. 5).

[5] SIRUNYAN 18BH search for $H\to e\tau$ in 35.9 fb^{-1} of pp collisions at $E_{\text{cm}} = 13$ TeV. The limit constrains the $Y_{e\tau}$ Yukawa coupling to $\sqrt{|Y_{e\tau}|^2+|Y_{\tau e}|^2} < 2.26\times10^{-3}$ at 95% CL (see their Fig. 10).

[6] AAD 17 search for $H\to e\tau$ in 20.3 fb^{-1} of pp collisions at $E_{\text{cm}} = 8$ TeV.

[7] KHACHATRYAN 16CD search for $H\to e\tau$ in 19.7 fb^{-1} of pp collisions at $E_{\text{cm}} = 8$ TeV. The limit constrains the $Y_{e\tau}$ Yukawa coupling to $\sqrt{|Y_{e\tau}|^2+|Y_{\tau e}|^2} < 2.4\times10^{-3}$ at 95% CL (see their Fig. 6).

$\Gamma(\mu\tau)/\Gamma_{\text{total}}$ Γ_{31}/Γ

VALUE	CL%	DOCUMENT ID		TECN	COMMENT
$< 1.5 \times 10^{-3}$	95	[1] SIRUNYAN	21Z	CMS	pp, 13 TeV
• • • We do not use the following data for averages, fits, limits, etc. • • •					
$< 1.8 \times 10^{-3}$	95	[2] AAD	23Q	ATLS	pp, 13 TeV
$< 1.7 \times 10^{-3}$	95	[3] AAD	23Q	ATLS	pp, 13 TeV
$< 2.8 \times 10^{-3}$	95	[4] AAD	20A	ATLS	pp, 13 TeV
$<26 \times 10^{-2}$	95	[5] AAIJ	18AM	LHCB	pp, 8 TeV
$< 2.5 \times 10^{-3}$	95	[6] SIRUNYAN	18BH	CMS	pp, 13 TeV
$< 1.43 \times 10^{-2}$	95	[7] AAD	17	ATLS	pp, 8 TeV
$< 1.51 \times 10^{-2}$	95	[8] KHACHATRY...	15Q	CMS	pp, 8 TeV

[1] SIRUNYAN 21Z search for $H \to \mu\tau$ in 137 fb^{-1} of pp collisions at $E_{\text{cm}} = 13$ TeV. The limit constrains the $Y_{\mu\tau}$ Yukawa coupling to $\sqrt{|Y_{\mu\tau}|^2 + |Y_{\tau\mu}|^2} < 1.11 \times 10^{-3}$ at 95% CL (see their Fig. 8).

[2] AAD 23Q search for $H \to \mu\tau$ in 138 fb^{-1} of pp collisions at $E_{\text{cm}} = 13$ TeV. The result is obtained from a simultaneous fit of possible $H \to e\tau$ and $H \to \mu\tau$ signals (see their Figs. 13 and 14). The limit constrains the $Y_{\mu\tau}$ Yukawa coupling to $\sqrt{|Y_{\mu\tau}|^2 + |Y_{\tau\mu}|^2} < 1.2 \times 10^{-3}$ at 95% CL (see their Fig. 15).

[3] AAD 23Q search for $H \to \mu\tau$ in 138 fb^{-1} of pp collisions at $E_{\text{cm}} = 13$ TeV. The limit constrains the $Y_{\mu\tau}$ Yukawa coupling to $\sqrt{|Y_{\mu\tau}|^2 + |Y_{\tau\mu}|^2} < 1.2 \times 10^{-3}$ at 95% CL (see their Fig. 12).

[4] AAD 20A search for $H \to \mu\tau$ in 36.1 fb^{-1} of pp collisions at $E_{\text{cm}} = 13$ TeV. The limit constrains the $Y_{\mu\tau}$ Yukawa coupling to $\sqrt{|Y_{\mu\tau}|^2 + |Y_{\tau\mu}|^2} < 1.5 \times 10^{-3}$ at 95% CL (see their Fig. 5).

[5] AAIJ 18AM search for $H \to \mu\tau$ in 2.0 fb^{-1} of pp collisions at $E_{\text{cm}} = 8$ TeV. The limit constrains the $Y_{\mu\tau}$ Yukawa coupling to $\sqrt{|Y_{\mu\tau}|^2 + |Y_{\tau\mu}|^2} < 1.7 \times 10^{-2}$ at 95% CL assuming SM production cross sections.

[6] SIRUNYAN 18BH search for $H \to \mu\tau$ in 35.9 fb^{-1} of pp collisions at $E_{\text{cm}} = 13$ TeV. The limit constrains the $Y_{\mu\tau}$ Yukawa coupling to $\sqrt{|Y_{\mu\tau}|^2 + |Y_{\tau\mu}|^2} < 1.43 \times 10^{-3}$ at 95% CL (see their Fig. 10).

[7] AAD 17 search for $H \to \mu\tau$ in 20.3 fb^{-1} of pp collisions at $E_{\text{cm}} = 8$ TeV.

[8] KHACHATRYAN 15Q search for $H \to \mu\tau$ with τ decaying electronically or hadronically in 19.7 fb^{-1} of pp collisions at $E_{\text{cm}} = 8$ TeV. The fit gives $\text{B}(H \to \mu\tau) = (0.84^{+0.39}_{-0.37})\%$ with a significance of 2.4 σ.

$\Gamma(\text{invisible})/\Gamma_{\text{total}}$ Γ_{32}/Γ

Invisible final states.

VALUE	CL%	DOCUMENT ID		TECN	COMMENT
<0.107	95	[1] AAD	23A	ATLS	pp, 7, 8, 13 TeV
• • • We do not use the following data for averages, fits, limits, etc. • • •					
<0.113	95	[2] AAD	23A	ATLS	pp, 13 TeV
<0.38	95	[3] AAD	23AF	ATLS	$pp \to t\bar{t}H$, 13 TeV
<0.54	95	[4] TUMASYAN	23BA	CMS	$pp \to t\bar{t}H$, $V(\to q\bar{q})H$, 13 TeV
<0.15	95	[5] TUMASYAN	23BA	CMS	pp, 7, 8, 13 TeV
<0.19	95	[6] AAD	22D	ATLS	$pp \to ZH$, 13 TeV
<0.145	95	[7] AAD	22P	ATLS	$pp \to qqH$, 13 TeV
<0.37	95	[8] AAD	22S	ATLS	$pp \to qqH\gamma$, 13 TeV

<0.13	95	[9] ATLAS	22	ATLS	pp, 13 TeV
<0.16	95	[10] CMS	22	CMS	pp, 13 TeV
<0.18	95	[11] TUMASYAN	22G	CMS	$pp \to qqH$, 8, 13 TeV
<0.18	95	[12] TUMASYAN	22G	CMS	$pp \to qqH$, 13 TeV
<0.34	95	[13] AAD	21F	ATLS	pp, 13 TeV
<0.29	95	[14] SIRUNYAN	21A	CMS	$pp \to ZH$, 13 TeV
<0.278	95	[15] TUMASYAN	21D	CMS	pp, 13 TeV, jet or $V(\to q\overline{q})$
<0.37	95	[16] AABOUD	19AI	ATLS	$pp \to qqH$, 13 TeV
<0.38	95	[17] AABOUD	19AL	ATLS	pp, 13 TeV
<0.26	95	[18] AABOUD	19AL	ATLS	pp, 7, 8, 13 TeV
<0.22	95	[19] SIRUNYAN	19AT	CMS	pp, 13 TeV
<0.33	95	[20] SIRUNYAN	19BO	CMS	$pp \to qqH$, 13 TeV
<0.26	95	[21] SIRUNYAN	19BO	CMS	pp, 13 TeV
<0.19	95	[22] SIRUNYAN	19BO	CMS	pp, 7, 8, 13 TeV
<0.67	95	[23] AABOUD	18	ATLS	$pp \to ZH$, 13 TeV
<0.83	95	[24] AABOUD	18CA	ATLS	$pp \to WH/ZH$, $W/Z \to jj$, 13 TeV
<0.40	95	[25] SIRUNYAN	18BV	CMS	$pp \to ZH$, 13 TeV
<0.53	95	[26] SIRUNYAN	18S	CMS	pp, 13 TeV, jet or $V(\to q\overline{q})$
<0.46	95	[27] AABOUD	17BD	ATLS	$pp \to Hj$, qqH, 13 TeV
<0.24	95	[28] KHACHATRY...	17F	CMS	pp, 7, 8, 13 TeV
<0.28	95	[29] AAD	16AF	ATLS	$pp \to qqH$, 8 TeV
<0.34	95	[30] AAD	16AN	LHC	pp, 7, 8 TeV
<0.78	95	[31] AAD	15BD	ATLS	$pp \to WH/ZH$, 8 TeV
<0.25	95	[32] AAD	15CX	ATLS	pp, 7, 8 TeV
<0.75	95	[33] AAD	14O	ATLS	$pp \to ZH$, 7, 8 TeV
<0.58	95	[34] CHATRCHYAN	14B	CMS	$pp \to ZH$, qqH
<0.81	95	[35] CHATRCHYAN	14B	CMS	$pp \to ZH$, 7, 8 TeV
<0.65	95	[36] CHATRCHYAN	14B	CMS	$pp \to qqH$, 8 TeV

[1] AAD 23A report the combined results of 7, 8 (AAD 15CX) and 13 TeV assuming the Standard Model cross section ($m_H = 125$ GeV). See their Table 1 and Fig. 3.

[2] AAD 23A report the combined results using 139 fb^{-1} of data at $E_{\text{cm}} = 13$ TeV, where H decaying to invisible final states in VBF (AAD 22P), ZH, $Z \to ee$, $\mu\mu$ (AAD 22D), $pp \to t\overline{t}H$ (AAD 23AF), VBF+γ (AAD 22S) and gluon-fusion production with an energetic jet (AAD 21F) assuming the Standard Model cross section ($m_H = 125$ GeV). See their Table 1 and Fig. 3.

[3] AAD 23AF search for $pp \to t\overline{t}H$ with H decaying to invisible final states using 139 fb^{-1} of data. The quoted limit on the branching ratio is given for $m_H = 125$ GeV and assumes the Standard Model cross section. See their Table 3 for different decay topologies.

[4] TUMASYAN 23BA search for H decaying to invisible final states produced in association with a $t\overline{t}$ or a V, which decay to a fully hadronic final state. 138 fb^{-1} of data is used. The quoted limit on the branching ratio is given for $m_H = 125$ GeV and assumes the Standard Model cross section. See their Fig. 6 for the results of individual topologies.

[5] TUMASYAN 23BA report the combined results of 7, 8, and 13 TeV assuming the Standard Model cross section ($m_H = 125$ GeV). They combine results from TUMASYAN 22G, SIRUNYAN 21A, SIRUNYAN 21B, TUMASYAN 21D, SIRUNYAN 20AH, KHACHATRYAN 17F, CHATRCHYAN 14B as shown in their Table 8. See their Fig. 7 and Table 9 for the results of individual topologies.

[6] AAD 22D search for H decaying to invisible final states associated with a Z decaying $ee/\mu\mu$ using 139 fb^{-1} at 13 TeV. The limit is obtained for $m_H = 125$ GeV and

assuming the SM ZH production cross section. The branching ratio is obtained to be $(0.3 \pm 9.0)\%$.

[7] AAD 22P search for $pp \to qqHX$ (VBF) with H decaying to invisible final states using 139 fb^{-1} of data. The quoted limit on the branching ratio is given for $m_H = 125$ GeV and assumes the Standard Model cross section.

[8] AAD 22S observe electroweak $Z(\to \nu\nu)\gamma$+2jets production process with 139 fb^{-1} of data. This result is applicable to search for $pp \to qqH\gamma X$ (VBF+γ) with H decaying to invisible final states. The quoted limit on the branching ratio is given for $m_H = 125$ GeV and assumes the Standard Model cross section.

[9] ATLAS 22 report the combined results using 139 fb^{-1} of data at $E_{\text{cm}} = 13$ TeV, where H decaying to invisible final states in VBF (AAD 22P), and ZH, $Z \to ee$, $\mu\mu$ (AAD 22D), assuming $\kappa_V \leq 1$ and $B_{undetected} \geq 0$.

[10] CMS 22 report the combined results using (a part of) 138 fb^{-1} of data at $E_{\text{cm}} = 13$ TeV, where H decaying to invisible final states in VBF (SIRUNYAN 19BO), associated with an energetic jet or a $V(\to q\overline{q})$ (TUMASYAN 21D), and ZH, $Z \to ee$, $\mu\mu$ (SIRUNYAN 21A) and assuming $\kappa_V \leq 1$ and $B_{undetected} \geq 0$.

[11] TUMASYAN 22G combine 13 TeV 101 fb^{-1} results with 8 TeV (KHACHATRYAN 17F) and other 13 TeV (KHACHATRYAN 17F for 2015 and SIRUNYAN 19BO for 2016) for H decaying to invisible final states with VBF topology. The quoted limit on the branching ratio is given for $m_H = 125.38$ GeV and assumes the Standard Model production rates. The branching ratio is obtained to be $0.086^{+0.054}_{-0.052}$. See their Figs. 11 and 12.

[12] TUMASYAN 22G search for $pp \to qqHX$ (VBF) with H decaying to invisible final states using 101 fb^{-1} of data (2017 and 2018). The quoted limit on the branching ratio is given for $m_H = 125.38$ GeV and assumes the Standard Model cross section. See their Figs. 11 and 12.

[13] AAD 21F search for an invisibly decaying Higgs boson with an energetic jet ($p_T > 150$ GeV) and missing transverse momentum (> 200 GeV) in 139 fb^{-1} at $E_{\text{cm}} = 13$ TeV. The quoted limit on the branching ratio is given for $m_H = 125$ GeV.

[14] SIRUNYAN 21A search for H decaying to invisible final states associated with a Z decaying $ee/\mu\mu$ using 137 fb^{-1} at 13 TeV. The limit is obtained for $m_H = 125$ GeV and assuming the SM ZH production cross section.

[15] TUMASYAN 21D search for H decaying to invisible final states associated with an energetic jet or a V, $V \to q\overline{q}$ using 101 fb^{-1} at 13 TeV and the result is combined with SIRUNYAN 18S.

[16] AABOUD 19AI search for $pp \to qqHX$ (VBF) with H decaying to invisible final states using 36.1 fb^{-1} of data. The quoted limit on the branching ratio is given for $m_H = 125$ GeV and assumes the Standard Model rates for VBF and gluon-fusion production.

[17] AABOUD 19AL combine results of H decaying to invisible final states with VBF(AABOUD 19AI), ZH, and WH productions (AABOUD 18, AABOUD 18CA), which use 36.1 fb^{-1} of data at 13 TeV. The quoted limit is given for $m_H = 125$ GeV and assumes the Standard Model rates for gluon fusion, VBF, ZH, and WH productions.

[18] AABOUD 19AL combine results of 7, 8 (AAD 15CX), and 13 TeV for H decaying to invisible final states.

[19] SIRUNYAN 19AT perform a combined fit with visible decay using 35.9 fb^{-1} of data at 13 TeV.

[20] SIRUNYAN 19BO search for $pp \to qqHX$ (VBF) with H decaying to invisible final states using 35.9 fb^{-1} of data. The quoted limit on the branching ratio is given for $m_H = 125.09$ GeV and assumes the Standard Model production rates.

[21] SIRUNYAN 19BO combine the VBF channel with results of other 13 TeV analyses: SIRUNYAN 18BV and SIRUNYAN 18S. The quoted limit on the branching ratio is given for $m_H = 125.09$ GeV and assumes the Standard Model production rates.

[22] SIRUNYAN 19BO combine 13 TeV 35.9 fb^{-1} results with 7, 8, 13 TeV (KHACHATRYAN 17F) for H decaying to invisible final states. The quoted limit on the branching

ratio is given for $m_H = 125.09$ GeV and assumes the Standard Model production rates. The branching ratio is obtained to be 0.05 $\pm$ 0.03 (stat) $\pm$0.07(syst).

[23] AABOUD 18 search for $pp \to HZX$, $Z \to ee$, $\mu\mu$ with H decaying to invisible final states in 36.1 fb^{-1} at $E_{\rm cm} = 13$ TeV. The quoted limit on the branching ratio is given for $m_H = 125$ GeV and assumes the Standard Model rate for HZ production.

[24] AABOUD 18CA search for H decaying to invisible final states using WH, and ZH productions, where W and Z hadronically decay. The data of 36.1 fb^{-1} at $E_{\rm cm} = 13$ TeV is used. The quoted limit assumes SM production cross sections with combining the contributions from WH, ZH, ggF and VBF production modes.

[25] SIRUNYAN 18BV search for H decaying to invisible final states associated with a Z, $Z \to \ell\ell$ using 35.9 fb^{-1} at 13 TeV.The limit is obtained for $m_H = 125$ GeV and assuming the SM ZH production cross section.

[26] SIRUNYAN 18S search for H decaying to invisible final states associated with an energetic jet or a V, $V \to q\overline{q}$ using 35.9 fb^{-1} at 13 TeV.

[27] AABOUD 17BD search for H decaying to invisible final states with ≥ 1 jet and VBF events using 3.2 fb^{-1} of pp collisions at $E_{\rm cm} = 13$ TeV. A cross-section ratio $R^{\rm miss}$ is used in the measurement. The quoted limit is given for $m_H = 125$ GeV.

[28] KHACHATRYAN 17F search for H decaying to invisible final states with gluon fusion, VBF, ZH, and WH productions using 2.3 fb^{-1} of pp collisions at $E_{\rm cm} = 13$ TeV, 19.7 fb^{-1} at 8 TeV, and 5.1 fb^{-1} at 7 TeV. The quoted limit is given for $m_H = 125$ GeV and assumes the Standard Model rates for gluon fusion, VBF, ZH, and WH productions.

[29] AAD 16AF search for $pp \to qqHX$ (VBF) with H decaying to invisible final states in 20.3 fb^{-1} at $E_{\rm cm} = 8$ TeV. The quoted limit on the branching ratio is given for $m_H =$ 125 GeV and assumes the Standard Model rates for VBF and gluon-fusion production.

[30] AAD 16AN perform fits to the ATLAS and CMS data at $E_{\rm cm} = 7$ and 8 TeV. The branching fraction of decays into BSM particles that are invisible or into undetected decay modes is measured for $m_0 = 125.09$ GeV.

[31] AAD 15BD search for $pp \to HWX$ and $pp \to HZX$ with W or Z decaying hadronically and H decaying to invisible final states using data at $E_{\rm cm} = 8$ TeV. The quoted limit is given for $m_H = 125$ GeV, assumes the Standard Model rates for the production processes and is based on a combination of the contributions from HW, HZ and the gluon-fusion process.

[32] AAD 15CX search for H decaying to invisible final states with VBF, ZH, and WH productions using 20.3 fb^{-1} at 8 TeV, and 4.7 fb^{-1} at 7 TeV. The quoted limit is given for $m_H = 125.36$ GeV and assumes the Standard Model rates for gluon fusion, VBF, ZH, and WH productions. The upper limit is improved to 0.23 by adding the measured visible decay rates.

[33] AAD 14O search for $pp \to HZX$, $Z \to \ell\ell$, with H decaying to invisible final states in 4.5 fb^{-1} at $E_{\rm cm} = 7$ TeV and 20.3 fb^{-1} at $E_{\rm cm} = 8$ TeV. The quoted limit on the branching ratio is given for $m_H = 125.5$ GeV and assumes the Standard Model rate for HZ production.

[34] CHATRCHYAN 14B search for $pp \to HZX$, $Z \to \ell\ell$ and $Z \to b\overline{b}$, and also $pp \to qqHX$ with H decaying to invisible final states using data at $E_{\rm cm} = 7$ and 8 TeV. The quoted limit on the branching ratio is obtained from a combination of the limits from HZ and qqH. It is given for $m_H = 125$ GeV and assumes the Standard Model rates for the two production processes.

[35] CHATRCHYAN 14B search for $pp \to HZX$ with H decaying to invisible final states and $Z \to \ell\ell$ in 4.9 fb^{-1} at $E_{\rm cm} = 7$ TeV and 19.7 fb^{-1} at $E_{\rm cm} = 8$ TeV, and also with $Z \to b\overline{b}$ in 18.9 fb^{-1} at $E_{\rm cm} = 8$ TeV. The quoted limit on the branching ratio is given for $m_H = 125$ GeV and assumes the Standard Model rate for HZ production.

[36] CHATRCHYAN 14B search for $pp \to qqHX$ (vector boson fusion) with H decaying to invisible final states in 19.5 fb^{-1} at $E_{\rm cm} = 8$ TeV. The quoted limit on the branching ratio is given for $m_H = 125$ GeV and assumes the Standard Model rate for qqH production.

$\Gamma(\gamma\,\text{invisible})/\Gamma_{\text{total}}$ Γ_{33}/Γ

VALUE	CL%	DOCUMENT ID		TECN	COMMENT
<0.013	95	[1] AAD	24BH	ATLS	VBF, HZ, $H \to \gamma +$ invisible, 13 TeV
• • • We do not use the following data for averages, fits, limits, etc. • • •					
<0.035	95	[2] SIRUNYAN	21L	CMS	VBF, $H \to \gamma+$ invisible, 13 TeV
<0.029	95	[2,3] SIRUNYAN	21L	CMS	VBF, HZ, $H \to \gamma +$ invisible, 13 TeV
<0.046	95	[4] SIRUNYAN	19CG	CMS	$pp \to HZ$, $H \to \gamma+$ invisible, $Z \to \ell\ell$, 13 TeV

[1] AAD 24BH search for H decaying to an invisible final state plus a γ in the VBF and HZ production using 139 fb^{-1} data at $E_{\text{cm}} = 13$ TeV. The invisible state is called a dark photon. The quoted limit on the branching ratio is given for $m_H = 125$ GeV assuming the Standard Model rates. The 95% CL upper limits on the branching ratio for the VBF and HZ production are 1.8% and 2.3%, respectively. See their Fig. 3(a).

[2] SIRUNYAN 21L search for H decaying to an invisible final state plus a γ in the VBF production using 130 fb^{-1} data at $E_{\text{cm}} = 13$ TeV. The invisible state is called a dark photon. The quoted limit on the branching ratio is given for $m_H = 125$ GeV assuming the Standard Model rates.

[3] The result of the VBF production is combined with the $pp \to HZ$ result (SIRUNYAN 19CG).

[4] SIRUNYAN 19CG search for $pp \to HZ$, $Z \to ee$, $\mu\mu$ with H decaying to invisible final states plus a γ in 137 fb^{-1} at $E_{\text{cm}} = 13$ TeV. The quoted limit on the branching ratio is given for $m_H = 125$ GeV assuming the Standard Model rate for HZ production and is obtained in the context of a theoretical model, where the undetected (invisible) particle is massless.

H SIGNAL STRENGTHS IN DIFFERENT CHANNELS

The H signal strength in a particular final state xx is given by the cross section times branching ratio in this channel normalized to the Standard Model (SM) value, $\sigma \cdot \text{B}(H \to xx) \,/\, (\sigma \cdot \text{B}(H \to xx))_{\text{SM}}$, for the specified mass value of H. For the SM predictions, see DITTMAIER 11, DITTMAIER 12, and HEINEMEYER 13A. Results for fiducial and differential cross sections are also listed below.

Combined final state

VALUE	DOCUMENT ID		TECN	COMMENT
1.03 ±0.04 OUR AVERAGE				
1.05 ±0.06	[1] ATLAS	22	ATLS	pp, 13 TeV
1.002±0.057	[2] CMS	22	CMS	pp, 13 TeV
$1.09 \pm 0.07 \pm 0.04^{+0.08}_{-0.07}$	[3,4] AAD	16AN	LHC	pp, 7, 8 TeV
$1.44^{+0.59}_{-0.56}$	[5] AALTONEN	13M	TEVA	$p\overline{p} \to HX$, 1.96 TeV
• • • We do not use the following data for averages, fits, limits, etc. • • •				
$1.11^{+0.09}_{-0.08}$	[6] AAD	20	ATLS	pp, 13 TeV
1.17 ±0.10	[7] SIRUNYAN	19AT	CMS	pp, 13 TeV
	[8] SIRUNYAN	19BA	CMS	pp, 13 TeV, diiferential cross sections
$1.20 \pm 0.10 \pm 0.06^{+0.09}_{-0.08}$	[4] AAD	16AN	ATLS	pp, 7, 8 TeV
$0.97 \pm 0.09 \pm 0.05^{+0.08}_{-0.07}$	[4] AAD	16AN	CMS	pp, 7, 8 TeV

$1.18\ \pm0.10\ \pm0.07^{+0.08}_{-0.07}$		[9] AAD	16K	ATLS	pp, 7, 8 TeV
$0.75\ ^{+0.28}_{-0.26}\ ^{+0.13+0.08}_{-0.11-0.05}$		[9] AAD	16K	ATLS	pp, 7 TeV
$1.28\ \pm0.11\ ^{+0.08+0.10}_{-0.07-0.08}$		[9] AAD	16K	ATLS	pp, 8 TeV
		[10] AAD	15P	ATLS	pp, 8 TeV, cross section
$1.00\ \pm0.09\ \pm0.07^{+0.08}_{-0.07}$		[11] KHACHATRY...	15AM	CMS	pp, 7, 8 TeV
$1.33\ ^{+0.14}_{-0.10}\ \pm0.15$		[12] AAD	13AK	ATLS	pp, 7 and 8 TeV
$1.54\ ^{+0.77}_{-0.73}$		[13] AALTONEN	13L	CDF	$p\overline{p} \to HX$, 1.96 TeV
$1.40\ ^{+0.92}_{-0.88}$		[14] ABAZOV	13L	D0	$p\overline{p} \to HX$, 1.96 TeV
$1.4\ \pm0.3$		[15] AAD	12AI	ATLS	$pp \to HX$, 7, 8 TeV
$1.2\ \pm0.4$		[15] AAD	12AI	ATLS	$pp \to HX$, 7 TeV
$1.5\ \pm0.4$		[15] AAD	12AI	ATLS	$pp \to HX$, 8 TeV
$0.87\ \pm0.23$		[16] CHATRCHYAN	12N	CMS	$pp \to HX$, 7, 8 TeV

[1] ATLAS 22 report combined results (see their Extended Data Table 1) using up to 139 fb^{-1} of data at $E_{\rm cm} = 13$ TeV, assuming $m_H = 125.09$ GeV. The Higgs production cross-sections, branching fractions and several ratios are found in their Figs. 2 and 3.

[2] CMS 22 report combined results (see their Extended Data Table 2) using 138 fb^{-1} of data at $E_{\rm cm} = 13$ TeV, assuming $m_H = 125.38$ GeV. Signal strengths for production modes and decay channels are found in their Fig. 2.

[3] AAD 16AN perform fits to the ATLAS and CMS data at $E_{\rm cm} = 7$ and 8 TeV. The signal strengths for individual production processes are $1.03^{+0.16}_{-0.14}$ for gluon fusion, $1.18^{+0.25}_{-0.23}$ for vector boson fusion, $0.89^{+0.40}_{-0.38}$ for WH production, $0.79^{+0.38}_{-0.36}$ for ZH production, and $2.3^{+0.7}_{-0.6}$ for $t\overline{t}H$ production.

[4] AAD 16AN: The uncertainties represent statistics, experimental systematics, and added in quadrature theory systematics on the background and on the signal. The quoted signal strengths are given for $m_H = 125.09$ GeV. In the fit, relative branching ratios and relative production cross sections are fixed to those in the Standard Model.

[5] AALTONEN 13M combine all Tevatron data from the CDF and D0 Collaborations with up to 10.0 fb^{-1} and 9.7 fb^{-1}, respectively, of $p\overline{p}$ collisions at $E_{\rm cm} = 1.96$ TeV. The quoted signal strength is given for $m_H = 125$ GeV.

[6] AAD 20 combine results of up to 79.8 fb^{-1} of data at $E_{\rm cm} = 13$ TeV, assuming $m_H = 125.09$ GeV: $\gamma\gamma$, ZZ^*, WW^*, $\tau\tau$, $b\overline{b}$, $\mu\mu$, invisible, and off-shell analyses (see their Table I). The signal strengths for individual production processes are 1.04 ± 0.09 for gluon fusion, $1.21^{+0.24}_{-0.22}$ for vector boson fusion, $1.30^{+0.40}_{-0.38}$ for WH production, $1.05^{+0.31}_{-0.29}$ for ZH production, and $1.21^{+0.26}_{-0.24}$ for $t\overline{t}H+tH$ production (see their Fig. 2 and Table IV). Several results with the simplified template cross section and κ-frameworks are presented: see their Figs. 9–11, Figs 20, 21 and Table VIII for stage-1 simplified template cross sections, their Figs. 12–17 and Tables X–XII for the κ-framework.

[7] SIRUNYAN 19AT combine results of 35.9 fb^{-1} of data at $E_{\rm cm} = 13$ TeV, assuming $m_H = 125.09$ GeV. The signal strengths for individual production processes are $1.22^{+0.14}_{-0.12}$ for gluon fusion, $0.73^{+0.30}_{-0.27}$ for vector boson fusion, $2.18^{+0.58}_{-0.55}$ for WH production, $0.87^{+0.44}_{-0.42}$ for ZH production, and $1.18^{+0.30}_{-0.27}$ for $t\overline{t}H$ production. Several results with the simplified template cross section and κ-frameworks are presented: see their Fig. 8 and Table 5 for stage-0 simplified template cross sections, their Figs. 9–18 and Tables 7–11 for the κ-framework.

[8] SIRUNYAN 19BA measure differential cross sections for the Higgs boson transverse momentum, the number of jets, the rapidity of the Higgs boson and the transverse momentum of the leading jet using 35.9 fb^{-1} of data at $E_{cm} = 13$ TeV with $H \to \gamma\gamma$, $H \to ZZ^*$, and $H \to b\overline{b}$. The total cross section for Higgs boson production is measured to be $61.1 \pm 6.0 \pm 3.7$ pb using $H \to \gamma\gamma$ and $H \to ZZ^*$ channels. Several coupling measurements in the κ-framework are performed.

[9] AAD 16K use up to 4.7 fb^{-1} of pp collisions at $E_{cm} = 7$ TeV and up to 20.3 fb^{-1} at $E_{cm} = 8$ TeV. The third uncertainty in the measurement is theory systematics. The signal strengths for individual production modes are $1.23 \pm 0.14^{+0.09}_{-0.08}{}^{+0.16}_{-0.12}$ for gluon fusion, $1.23^{+0.28}_{-0.27}{}^{+0.13}_{-0.12}{}^{+0.11}_{-0.09}$ for vector boson fusion, $0.80^{+0.31}_{-0.30} \pm 0.17^{+0.10}_{-0.05}$ for W/ZH production, and $1.81^{+0.52}_{-0.50}{}^{+0.58}_{-0.55}{}^{+0.31}_{-0.12}$ for $t\overline{t}H$ production. The quoted signal strengths are given for $m_H = 125.36$ GeV.

[10] AAD 15P measure total and differential cross sections of the process $pp \to HX$ at $E_{cm} = 8$ TeV with 20.3 fb^{-1}. $\gamma\gamma$ and 4ℓ final states are used. $\sigma(pp \to HX) = 33.0 \pm 5.3 \pm 1.6$ pb is given. See their Figs. 2 and 3 for data on differential cross sections.

[11] KHACHATRYAN 15AM use up to 5.1 fb^{-1} of pp collisions at $E_{cm} = 7$ TeV and up to 19.7 fb^{-1} at $E_{cm} = 8$ TeV. The third uncertainty in the measurement is theory systematics. Fits to each production mode give the value of $0.85^{+0.19}_{-0.16}$ for gluon fusion, $1.16^{+0.37}_{-0.34}$ for vector boson fusion, $0.92^{+0.38}_{-0.36}$ for WH, ZH production, and $2.90^{+1.08}_{-0.94}$ for $t\overline{t}H$ production.

[12] AAD 13AK use 4.7 fb^{-1} of pp collisions at $E_{cm} = 7$ TeV and 20.7 fb^{-1} at $E_{cm} = 8$ TeV. The combined signal strength is based on the $\gamma\gamma$, $ZZ^* \to 4\ell$, and $WW^* \to \ell\nu\ell\nu$ channels. The quoted signal strength is given for $m_H = 125.5$ GeV. Reported statistical error value modified following private communication with the experiment.

[13] AALTONEN 13L combine all CDF results with 9.45–10.0 fb^{-1} of $p\overline{p}$ collisions at $E_{cm} = 1.96$ TeV. The quoted signal strength is given for $m_H = 125$ GeV.

[14] ABAZOV 13L combine all D0 results with up to 9.7 fb^{-1} of $p\overline{p}$ collisions at $E_{cm} = 1.96$ TeV. The quoted signal strength is given for $m_H = 125$ GeV.

[15] AAD 12AI obtain results based on 4.6–4.8 fb^{-1} of pp collisions at $E_{cm} = 7$ TeV and 5.8–5.9 fb^{-1} at $E_{cm} = 8$ TeV. An excess of events over background with a local significance of 5.9 σ is observed at $m_H = 126$ GeV. The quoted signal strengths are given for $m_H = 126$ GeV. See also AAD 12DA.

[16] CHATRCHYAN 12N obtain results based on 4.9–5.1 fb^{-1} of pp collisions at $E_{cm} = 7$ TeV and 5.1–5.3 fb^{-1} at $E_{cm} = 8$ TeV. An excess of events over background with a local significance of $5.0\,\sigma$ is observed at about $m_H = 125$ GeV. The combined signal strength is based on the $\gamma\gamma$, ZZ^*, WW^*, $\tau^+\tau^-$, and $b\overline{b}$ channels. The quoted signal strength is given for $m_H = 125.5$ GeV. See also CHATRCHYAN 13Y.

WW^* final state

VALUE	DOCUMENT ID		TECN	COMMENT
1.00±0.08 OUR AVERAGE				
0.97 ± 0.09	[1] CMS	22	CMS	pp, 13 TeV
$1.09^{+0.18}_{-0.16}$	[2,3] AAD	16AN	LHC	pp, 7, 8 TeV
$0.94^{+0.85}_{-0.83}$	[4] AALTONEN	13M	TEVA	$p\overline{p} \to HX$, 1.96 TeV
• • • We do not use the following data for averages, fits, limits, etc. • • •				
$0.92^{+0.21}_{-0.20}{}^{+0.13}_{-0.12} \pm 0.02$	[5] AAD	25AG	CMS	$pp \to WH/ZH$, 13 TeV
	[6] AAD	25BK	ATLS	pp, 13 TeV, cross sections

$1.20 \pm 0.50 \pm 0.11$	[7] HAYRAPETY...25AC	CMS	$pp \to ZH$, 13 TeV
	[8] HAYRAPETY...24AG	CMS	pp, $H \to WW^*$ ($\to e\nu\mu\nu$), 13 TeV
	[9] AAD	23AP ATLS	pp, 13 TeV, cross sections
	[10] AAD	23BV ATLS	pp, 13 TeV, cross sections
$0.95^{+0.10}_{-0.09}$	[11,12] TUMASYAN	23W CMS	pp, 13 TeV
$0.92^{+0.11}_{-0.10}$	[11,13,14] TUMASYAN	23W CMS	pp, 13 TeV
$0.71^{+0.28}_{-0.25}$	[11,13,15] TUMASYAN	23W CMS	pp, 13 TeV
2.2 ± 0.6	[11,13,16] TUMASYAN	23W CMS	pp, 13 TeV
2.0 ± 0.7	[11,13,17] TUMASYAN	23W CMS	pp, 13 TeV
	[11,18] TUMASYAN	23W CMS	pp, 13 TeV
$0.5 \pm 0.4\ ^{+0.7}_{-0.6}$	[19] AAD	22V ATLS	pp, WW^* ($\to e\nu\mu\nu$) $+2j$, 13 TeV
	[20] AAD	22V ATLS	pp, WW^* ($\to e\nu\mu\nu$) $+2j$, 13 TeV
	[21] AABOUD	19F ATLS	pp, 13 TeV, cross sections
$2.5\ ^{+0.9}_{-0.8}$	[22] AAD	19A ATLS	$pp \to HW/HZ$, $H \to WW^*$, 13 TeV
$1.28^{+0.17}_{-0.16}$	[23] SIRUNYAN	19AT CMS	pp, 13 TeV
$1.28^{+0.18}_{-0.17}$	[24] SIRUNYAN	19AX CMS	pp, 13 TeV
$1.22^{+0.23}_{-0.21}$	[3] AAD	16AN ATLS	pp, 7, 8 TeV
$0.90^{+0.23}_{-0.21}$	[3] AAD	16AN CMS	pp, 7, 8 TeV
	[25] AAD	16AO ATLS	pp, 8 TeV, cross sections
$1.18 \pm 0.16^{+0.17}_{-0.14}$	[26] AAD	16K ATLS	pp, 7, 8 TeV
$1.09^{+0.16}_{-0.15}{}^{+0.17}_{-0.14}$	[27] AAD	15AA ATLS	pp, 7, 8 TeV
$3.0\ ^{+1.3}_{-1.1}\ ^{+1.0}_{-0.7}$	[28] AAD	15AQ ATLS	$pp \to HW/ZX$, 7, 8 TeV
$1.16^{+0.16}_{-0.15}{}^{+0.18}_{-0.15}$	[29] AAD	15AQ ATLS	pp, 7, 8 TeV
$0.72 \pm 0.12 \pm 0.10^{+0.12}_{-0.10}$	[30] CHATRCHYAN	14G CMS	pp, 7, 8 TeV
$0.99^{+0.31}_{-0.28}$	[31] AAD	13AK ATLS	pp, 7 and 8 TeV
$0.00^{+1.78}_{-0.00}$	[32] AALTONEN	13L CDF	$p\overline{p} \to HX$, 1.96 TeV
$1.90^{+1.63}_{-1.52}$	[33] ABAZOV	13L D0	$p\overline{p} \to HX$, 1.96 TeV
1.3 ± 0.5	[34] AAD	12AI ATLS	$pp \to HX$, 7, 8 TeV
0.5 ± 0.6	[34] AAD	12AI ATLS	$pp \to HX$, 7 TeV
1.9 ± 0.7	[34] AAD	12AI ATLS	$pp \to HX$, 8 TeV
$0.60^{+0.42}_{-0.37}$	[35] CHATRCHYAN	12N CMS	$pp \to HX$, 7, 8 TeV

[1] CMS 22 report combined results (see their Extended Data Table 2) using up to 138 fb^{-1} of data at $E_{cm} = 13$ TeV, assuming $m_H = 125.38$ GeV. See their Fig. 2 right.

[2] AAD 16AN perform fits to the ATLAS and CMS data at $E_{cm} = 7$ and 8 TeV. The signal strengths for individual production processes are 0.84 ± 0.17 for gluon fusion, 1.2 ± 0.4

for vector boson fusion, $1.6^{+1.2}_{-1.0}$ for WH production, $5.9^{+2.6}_{-2.2}$ for ZH production, and $5.0^{+1.8}_{-1.7}$ for $t\bar{t}H$ production.

[3] AAD 16AN: In the fit, relative production cross sections are fixed to those in the Standard Model. The quoted signal strength is given for $m_H = 125.09$ GeV.

[4] AALTONEN 13M combine all Tevatron data from the CDF and D0 Collaborations with up to 10.0 fb^{-1} and 9.7 fb^{-1}, respectively, of $p\overline{p}$ collisions at $E_{cm} = 1.96$ TeV. The quoted signal strength is given for $m_H = 125$ GeV.

[5] AAD 25AG measure the signal strengths using $H \to WW^* \to \ell\nu\ell\nu$ and $H \to WW^* \to \ell\nu jj$ ($\ell = e,\ \mu$) with 140 fb^{-1} data at $E_{cm} = 13$ TeV. The last measurement uncertainty is due to the normalizing SM value. The signal strengths are summarized in their Table 9 and Fig. 12. The sum of WH and ZH cross sections times the $H \to WW^*$ branching ratio is measured to be $0.44^{+0.10}_{-0.09}{}^{+0.06}_{-0.05}$ pb and these two-dimensional likelihood scans are shown in their Fig. 14. Cross sections times the $H \to WW^*$ branching ratio and ratios to the SM values are given in their Tables 12, 13, 14 and Figs. 15 and 16, which are based on the simplified template cross section framework (reduced stage-1.2).

[6] AAD 25BK measure cross-sections times the $H \to WW^*$ branching fraction using $WW^* \to \ell\nu\ell\nu$ ($\ell = e,\ \mu$) with data of 140 fb^{-1} pp collisions at $E_{cm} = 13$ TeV: $\sigma_{ggF}\times$B($H \to WW^*$) $= 12.4^{+1.3}_{-1.2}$ pb and $\sigma_{VBF}\times$B($H \to WW^*$) $= 0.79^{+0.18}_{-0.16}$ pb. See their Fig. 11 for 2-dim contours. Measured cross sections and ratios to the SM predictions in the reduced stage-1.2 simplified template cross section framework (see their Fig. 2) are shown in their Fig. 10. The results are given for $m_H = 125.09$ GeV.

[7] HAYRAPETYAN 25AC measure the ZH production cross section to the SM prediction using $H \to WW^*$ decay channel with 138 fb^{-1} and 62 fb^{-1} of pp collision data at $E_{cm} = 13$ TeV and 13.6 TeV, respectively. Events with 4ℓ ($\ell = e,\ \mu$) are used. The cross section times the $H \to WW^*$ branching fraction and the signal strength for each center of mass energy are shown in their Table I. The corresponding significances are given in their Table II.

[8] HAYRAPETYAN 24AG search for the anomalous couplings of the Higgs boson to vector bosons, including CP violation effects using $H \to WW^* \to e\nu\mu\nu$ decay channel ($\ell = e,\ \mu$) with 138 fb^{-1} at $E_{cm} = 13$ TeV. The anomalous HVV and Hgg coupling parameters are given in their Table 7. The data constrain the SMEFT Higgs and Warsaw bases coupling parameters as shown in their Tables 8, 9 and Fig. 12.

[9] AAD 23AP measure cross-sections times the $H \to WW^*$ branching fraction in the $H \to WW^* \to e\nu\mu\nu$ channel using 139 fb^{-1} of pp collisions at $E_{cm} = 13$ TeV: $\sigma_{ggF}\times$B($H \to WW^*$) $= 12.0 \pm 1.4$ pb, $\sigma_{VBF}\times$B($H \to WW^*$) $= 0.75^{+0.19}_{-0.16}$ pb, and $\sigma_{ggF+VBF}\times$B($H \to WW^*$) $= 12.3 \pm 1.3$ pb. The results are given for $m_H = 125.09$ GeV. Measured cross sections and ratios to the SM predictions in the reduced stage-1.2 (see their Fig. 5) simplified template cross section framework are shown in their Table VII and Fig. 15.

[10] AAD 23BV measure fiducial total and differential cross sections of VBF process at $E_{cm} = 13$ TeV with 139 fb^{-1} using $H \to WW^* \to e\nu\mu\nu$. The measured total fiducial cross section is $1.68 \pm 0.33(\text{stat}) \pm 0.23(\text{syst})$ fb in their fiducial region (Table II and Section V). See their Fig. 9 for the comparison with theory predictions. The fiducial differential cross sections are shown in their Figs. 11, 12, and 13. Wilson coefficients in the Warsaw basis at 95% confidence interval are measured; see their Table V and Fig. 16.

[11] TUMASYAN 23W measure Higgs production rates with $H \to WW^*$ at $E_{cm} = 13$ TeV with 138 fb^{-1} data. The quoted results are given for $m_H = 125.38$ GeV.

[12] The quoted global signal strength is obtained assuming the relative ratios of different Higgs production modes fixed to the SM values.

[13] The 4 signal strengths for gluon-fusion (ggF), VBF, WH and ZH modes are fit assuming $t\bar{t}H$ and $b\bar{b}H$ fixed to the SM values.

[14] The quoted result is for ggF production mode.

[15] The quoted result is for VBF production mode.

[16] The quoted result is for WH production mode.

[17] The quoted result is for ZH production mode.

[18] Measured cross sections and ratios to the SM predictions in the reduced stage-1.2 (see their Fig. 17) simplified template cross section framework (6 ggF, 4 VBF, and 4 VH) are shown in their Table 18 and Fig. 26.

[19] AAD 22V measure the signal strength for ggF+2jets with 36.1 fb^{-1} data at 13 TeV.

[20] AAD 22V probe the Higgs couplings to longitudinally and transversely polarized W and Z using VBF ($H \to WW^* \to e\nu\mu\nu$ plus two jets) with 36.1 fb^{-1} of data at $E_{\rm cm} = 13$ TeV. The ratios of the polarization-dependent couplings $g_{HV_LV_L}$ and $g_{HV_TV_T}$ to the Higgs-V coupling predicted by the SM, $a_L = g_{HV_LV_L}/g^{\rm SM}_{HVV}$ and $a_T = g_{HV_TV_T}/g^{\rm SM}_{HVV}$ are measured to be $0.91^{+0.10+0.09}_{-0.18-0.17}$ and $1.2 \pm 0.4^{+0.2}_{-0.3}$, respectively, assuming the standard Hgg coupling. These measurements are translated into pseudo-observables of κ_{VV} and ϵ_{VV}: $\kappa_{VV} = 0.91^{+0.10+0.09}_{-0.18-0.17}$ and $\epsilon_{VV} = 0.13^{+0.28+0.08}_{-0.20-0.10}$, where $\kappa_{VV} = 1$ and $\epsilon_{VV} = 0$ for the SM. See their Tables 9 and 10.

[21] AABOUD 19F measure cross-sections times the $H \to WW^*$ branching fraction in the $H \to WW^* \to e\nu\mu\nu$ channel using 36.1 fb^{-1} of pp collisions at $E_{\rm cm} = 13$ TeV: $\sigma_{ggF}\times$B($H \to WW^*$) $= 11.4^{+1.2+1.8}_{-1.1-1.7}$ pb and $\sigma_{VBF}\times$B($H \to WW^*$) $= 0.50^{+0.24}_{-0.22} \pm 0.17$ pb.

[22] AAD 19A use 36.1 fb^{-1} data at 13 TeV. The cross section times branching fraction values are measured to be $0.67^{+0.31+0.18}_{-0.27-0.14}$ pb for WH, $H \to WW^*$ and $0.54^{+0.31+0.15}_{-0.24-0.07}$ pb for ZH, $H \to WW^*$.

[23] SIRUNYAN 19AT perform a combine fit to 35.9 fb^{-1} of data at $E_{\rm cm} = 13$ TeV.

[24] SIRUNYAN 19AX measure the signal strengths, cross sections and so on using gluon fusion, VBF and VH production processes with 35.9 fb^{-1} of data. The quoted signal strength is given for $m_H = 125.09$ GeV. Signal strengths for each production process is found in their Fig. 9. Measured cross sections and ratios to the SM predictions in the stage-0 simplified template cross section framework are shown in their Fig. 10. $\kappa_F = 1.52^{+0.48}_{-0.41}$ and $\kappa_V = 1.10 \pm 0.08$ are obtained (see their Fig. 11 (right)).

[25] AAD 16AO measure fiducial total and differential cross sections of gluon fusion process at $E_{\rm cm} = 8$ TeV with 20.3 fb^{-1} using $H \to WW^* \to e\nu\mu\nu$. The measured fiducial total cross section is 36.0 ± 9.7 fb in their fiducial region (Table 7). See their Fig. 6 for fiducial differential cross sections. The results are given for $m_H = 125$ GeV.

[26] AAD 16K use up to 4.7 fb^{-1} of pp collisions at $E_{\rm cm} = 7$ TeV and up to 20.3 fb^{-1} at $E_{\rm cm} = 8$ TeV. The quoted signal strength is given for $m_H = 125.36$ GeV.

[27] AAD 15AA use 4.5 fb^{-1} of pp collisions at $E_{\rm cm} = 7$ TeV and 20.3 fb^{-1} at $E_{\rm cm} = 8$ TeV. The signal strength for the gluon fusion and vector boson fusion mode is $1.02 \pm 0.19^{+0.22}_{-0.18}$ and $1.27^{+0.44+0.30}_{-0.40-0.21}$, respectively. The quoted signal strengths are given for $m_H = 125.36$ GeV.

[28] AAD 15AQ use 4.5 fb^{-1} of pp collisions at $E_{\rm cm} = 7$ TeV and 20.3 fb^{-1} at $E_{\rm cm} = 8$ TeV. The quoted signal strength is given for $m_H = 125.36$ GeV.

[29] AAD 15AQ combine their result on W/ZH production with the results of AAD 15AA (gluon fusion and vector boson fusion, slightly updated). The quoted signal strength is given for $m_H = 125.36$ GeV.

[30] CHATRCHYAN 14G use 4.9 fb^{-1} of pp collisions at E_{cm} = 7 TeV and 19.4 fb^{-1} at E_{cm} = 8 TeV. The last uncertainty in the measurement is theory systematics. The quoted signal strength is given for m_H = 125.6 GeV.

[31] AAD 13AK use 4.7 fb^{-1} of pp collisions at E_{cm} = 7 TeV and 20.7 fb^{-1} at E_{cm} = 8 TeV. The quoted signal strength is given for m_H = 125.5 GeV. Superseded by AAD 15AA.

[32] AALTONEN 13L combine all CDF results with 9.45–10.0 fb^{-1} of $p\overline{p}$ collisions at E_{cm} = 1.96 TeV. The quoted signal strength is given for m_H = 125 GeV.

[33] ABAZOV 13L combine all D0 results with up to 9.7 fb^{-1} of $p\overline{p}$ collisions at E_{cm} = 1.96 TeV. The quoted signal strength is given for m_H = 125 GeV.

[34] AAD 12AI obtain results based on 4.7 fb^{-1} of pp collisions at E_{cm} = 7 TeV and 5.8 fb^{-1} at E_{cm} = 8 TeV. The quoted signal strengths are given for m_H = 126 GeV. See also AAD 12DA.

[35] CHATRCHYAN 12N obtain results based on 4.9 fb^{-1} of pp collisions at E_{cm} = 7 TeV and 5.1 fb^{-1} at E_{cm} = 8 TeV. The quoted signal strength is given for m_H = 125.5 GeV. See also CHATRCHYAN 13Y.

ZZ^* final state

VALUE	CL%	DOCUMENT ID		TECN	COMMENT
1.02±0.08 OUR AVERAGE					
$0.97^{+0.12}_{-0.11}$		[1] CMS	22	CMS	pp, 13 TeV
1.01±0.11		[2,3] AAD	20AQ	ATLS	pp, 13 TeV
$1.29^{+0.26}_{-0.23}$		[4,5] AAD	16AN	LHC	pp, 7, 8 TeV
• • • We do not use the following data for averages, fits, limits, etc. • • •					
$1.06^{+0.61}_{-0.45}$		[6] AAD	25AQ	ATLS	pp, 13 TeV, off-shell
		[7] CHEKHOVSKY	25B	CMS	pp, 13.6 TeV, cross sections
		[8] AAD	24AQ	ATLS	pp, 13.6 TeV, cross sections
		[9] HAYRAPETY...	23	CMS	pp, 13 TeV cross sections
		[10] SIRUNYAN	21AE	CMS	pp, 13 TeV, couplings
$0.94\pm0.07^{+0.09}_{-0.08}$		[11] SIRUNYAN	21S	CMS	pp, 13 TeV
		[2,12] AAD	20AQ	ATLS	pp, 13 TeV
		[13] AAD	20BA	ATLS	pp, 13 TeV cross sections
<6.5	95	[14] AABOUD	19N	ATLS	pp, 13 TeV, off-shell
$1.06^{+0.19}_{-0.17}$		[15] SIRUNYAN	19AT	CMS	pp, 13 TeV
$1.28^{+0.21}_{-0.19}$		[16] AABOUD	18AJ	ATLS	pp, 13 TeV
<3.8	95	[17] AABOUD	18BP	ATLS	pp, 13 TeV, off-shell
$1.05^{+0.15+0.11}_{-0.14-0.09}$		[18] SIRUNYAN	17AV	CMS	pp, 13 TeV
$1.52^{+0.40}_{-0.34}$		[5] AAD	16AN	ATLS	pp, 7, 8 TeV
$1.04^{+0.32}_{-0.26}$		[5] AAD	16AN	CMS	pp, 7, 8 TeV
$1.46^{+0.35+0.19}_{-0.31-0.13}$		[19] AAD	16K	ATLS	pp, 7, 8 TeV
		[20] KHACHATRY...	16AR	CMS	pp, 7, 8 TeV cross sections
$1.44^{+0.34+0.21}_{-0.31-0.11}$		[21] AAD	15F	ATLS	$pp \to HX$, 7, 8 TeV

	[22] AAD	14AR	ATLS	pp, 8 TeV, cross sections
$0.93^{+0.26+0.13}_{-0.23-0.09}$	[23] CHATRCHYAN	14AA	CMS	pp, 7, 8 TeV
$1.43^{+0.40}_{-0.35}$	[24] AAD	13AK	ATLS	pp, 7 and 8 TeV
$0.80^{+0.35}_{-0.28}$	[25] CHATRCHYAN	13J	CMS	$pp \to HX$, 7, 8 TeV
1.2 ± 0.6	[26] AAD	12AI	ATLS	$pp \to HX$, 7, 8 TeV
1.4 ± 1.1	[26] AAD	12AI	ATLS	$pp \to HX$, 7 TeV
1.1 ± 0.8	[26] AAD	12AI	ATLS	$pp \to HX$, 8 TeV
$0.73^{+0.45}_{-0.33}$	[27] CHATRCHYAN	12N	CMS	$pp \to HX$, 7, 8 TeV

[1] CMS 22 report combined results (see their Extended Data Table 2) using up to 138 fb^{-1} of data at $E_{\rm cm} = 13$ TeV, assuming $m_H = 125.38$ GeV. See their Fig. 2 right.

[2] AAD 20AQ perform analyses using $H \to ZZ^* \to 4\ell$ ($\ell = e,\ \mu$) with data of 139 fb^{-1} at $E_{\rm cm} = 13$ TeV. Results are given for $m_H = 125$ GeV.

[3] AAD 20AQ measured the inclusive cross section times branching ratio for $H \to ZZ^*$ decay ($|y(H)| < 2.5$) to be 1.34 ± 0.12 pb (with 1.33 ± 0.08 pb expected in the SM).

[4] AAD 16AN perform fits to the ATLAS and CMS data at $E_{\rm cm} = 7$ and 8 TeV. The signal strengths for individual production processes are $1.13^{+0.34}_{-0.31}$ for gluon fusion and $0.1^{+1.1}_{-0.6}$ for vector boson fusion.

[5] AAD 16AN: In the fit, relative production cross sections are fixed to those in the Standard Model. The quoted signal strength is given for $m_H = 125.09$ GeV.

[6] AAD 25AQ measure the off-shell Higgs signal strength to be $0.87^{+0.75}_{-0.54}$ using $H^* \to ZZ \to 4\ell$ ($\ell = e,\ \mu$) with data of 140 fb^{-1} at $E_{\rm cm} = 13$ TeV. This result is combined with $ZZ \to 2\ell 2\nu$ decay channel (AAD 23BR), which corresponds to a significance of 3.7 σ. The quoted errors are values at 68%CL.

[7] CHEKHOVSKY 25B measure the fiducial cross section using $H \to ZZ^* \to 4\ell$ ($\ell = e,\ \mu$) with data of 34.7 fb^{-1} at $E_{\rm cm} = 13.6$ TeV. The inclusive fiducial cross section is $2.89^{+0.53+0.29}_{-0.49-0.21}$ fb with their defined fiducial region (see their Table 1), where $3.09^{+0.27}_{-0.24}$ fb is expected in the SM. Differential fiducial cross sections are shown in their Fig. 5. The quoted results are given for $m_H = 125.38$ GeV.

[8] AAD 24AQ measure fiducial and total cross sections at $E_{\rm cm} = 13.6$ TeV with 29.0 fb^{-1} data. The quoted results are given for $m_H = 125.09$ GeV. The inclusive fiducial cross section is 2.80 ± 0.74 fb with their defined fiducial region (see their Table 5), where 3.67 ± 0.19 fb is expected in the SM. Assuming SM values for the acceptance and the branching fraction, the total cross section is 46 ± 12 pb, where 59.9 ± 2.6 pb is expected in the SM.

[9] HAYRAPETYAN 23 measure the cross sections for $pp \to H \to ZZ^* \to 4\ell$ ($\ell = e$, μ) using 138 fb^{-1} at $E_{\rm cm} = 13$ TeV. They give $\sigma = 2.73 \pm 0.22$(stat) ± 0.15(syst) fb in their fiducial region (see their Section5 and Table 2), where 2.86 ± 0.15 fb is expected in the Standard Model for $m_H = 125.38$ GeV. 26 differential and 6 double-differential cross sections are given; see their Figs. 6-23 and 24-25.

[10] SIRUNYAN 21AE obtains constraints on anomalous couplings to vector bosons (W, Z, and gluon) and top quark using $H \to ZZ^* \to 4\ell$ ($\ell = e,\ \mu$) with data of 137 fb^{-1} at $E_{\rm cm} = 13$ TeV. Their Table 5 and Figs 14–17 show (effective) couplings to gluon and top with combining gluon fusion, $t\bar{t}H$ and tH production channels and the result of $t\bar{t}H$, $H \to \gamma\gamma$ (SIRUNYAN 20AS). Their Tables 6–9 and Figs 18–22 show couplings to W and Z for different assumptions and bases (Higgs and Warsaw).

[11] SIRUNYAN 21S measure cross sections with the $H \to ZZ^* \to 4\ell$ ($\ell = e,\ \mu$) channel using 137 fb^{-1} data at $E_{\rm cm} = 13$ TeV. Results are given for $m_H = 125.38$ GeV. The

signal strengths for individual production processes in their Table 4. Cross sections are given in their Table 6 and Fig. 14, which are based on the simplified template cross section framework (reduced stage-1.2).

[12] AAD 20AQ present several results for the channel $H \to ZZ^* \to 4\ell$ ($\ell = e,\ \mu$) with the simplified template cross section with κ-frameworks and the effective field theory (EFT) approach; see their Table 8 and Fig. 10 for simplified template cross sections. $\kappa_V = 1.02 \pm 0.06$ and $\kappa_F = 0.88 \pm 0.16$ are obtained, see their Fig. 12 for the κ-framework. See their Tables 9 and 10 and Figs. 16–18 for the EFT-framework.

[13] AAD 20BA measure the cross section for $pp \to H \to ZZ^* \to 4\ell$ ($\ell = e,\ \mu$) using 139 fb^{-1} at $E_{\rm cm} = 13$ TeV. They give $\sigma \cdot B = 3.28 \pm 0.30 \pm 0.11$ fb in their fiducial region, where 3.41 $\pm$ 0.18 fb is expected in the Standard Model for $m_H = 125$ GeV. Various differential cross sections are also given; see their Figs. 19-39. Constraints on Yukawa couplings for bottom and charm quarks are given in their Table 9 and Fig. 41.

[14] AABOUD 19N measure the spectrum of the four-lepton invariant mass $m_{4\ell}$ ($\ell = e$ or μ) using 36.1 fb^{-1} of data at $E_{\rm cm} = 13$ TeV. The quoted signal strength upper limit is obtained from 180 GeV $< m_{4\ell} <$ 1200 GeV.

[15] SIRUNYAN 19AT perform a combine fit to 35.9 fb^{-1} of data at $E_{\rm cm} = 13$ TeV.

[16] AABOUD 18AJ perform analyses using $H \to ZZ^* \to 4\ell$ ($\ell = e,\ \mu$) with data of 36.1 fb^{-1} at $E_{\rm cm} = 13$ TeV. Results are given for $m_H = 125.09$ GeV. The inclusive cross section times branching ratio for $H \to ZZ^*$ decay ($|\eta(H)| < 2.5$) is measured to be $1.73^{+0.26}_{-0.24}$ pb (with $1.34^{+0.09}_{-0.09}$ pb expected in the SM).

[17] AABOUD 18BP measure an off-shell Higgs boson production using $ZZ \to 4\ell$ and $ZZ \to 2\ell 2\nu$ ($\ell = e,\ \mu$) decay channels with 36.1 fb^{-1} of data at $E_{\rm cm} = 13$ TeV. The quoted signal strength upper limit is obtained from a combination of these two channels, where 220 GeV $< m_{4\ell} <$ 2000 GeV for $ZZ \to 4\ell$ and 250 GeV $< m_T^{ZZ} <$ 2000 GeV for $ZZ \to 2\ell 2\nu$ (m_T^{ZZ} is defined in their Section 5). See their Table 2 for each measurement.

[18] SIRUNYAN 17AV use 35.9 fb^{-1} of pp collisions at $E_{\rm cm} = 13$ TeV. The quoted signal strength, obtained from the analysis of $H \to ZZ^* \to 4\ell$ ($\ell = e,\ \mu$) decays, is given for $m_H = 125.09$ GeV. The signal strengths for different production modes are given in their Table 3. The fiducial and differential cross sections are shown in their Fig. 10.

[19] AAD 16K use up to 4.7 fb^{-1} of pp collisions at $E_{\rm cm} = 7$ TeV and up to 20.3 fb^{-1} at $E_{\rm cm} = 8$ TeV. The quoted signal strength is given for $m_H = 125.36$ GeV.

[20] KHACHATRYAN 16AR use data of 5.1 fb^{-1} at $E_{\rm cm} = 7$ TeV and 19.7 fb^{-1} at 8 TeV. The fiducial cross sections for the production of 4 leptons via $H \to 4\ell$ decays are measured to be $0.56^{+0.67}_{-0.44}{}^{+0.21}_{-0.06}$ fb at 7 TeV and $1.11^{+0.41}_{-0.35}{}^{+0.14}_{-0.10}$ fb at 8 TeV in their fiducial region (Table 2). The differential cross sections at $E_{\rm cm} = 8$ TeV are also shown in Figs. 4 and 5. The results are given for $m_H = 125$ GeV.

[21] AAD 15F use 4.5 fb^{-1} of pp collisions at $E_{\rm cm} = 7$ TeV and 20.3 fb^{-1} at $E_{\rm cm} = 8$ TeV. The quoted signal strength is given for $m_H = 125.36$ GeV. The signal strength for the gluon fusion production mode is $1.66^{+0.45}_{-0.41}{}^{+0.25}_{-0.15}$, while the signal strength for the vector boson fusion production mode is $0.26^{+1.60}_{-0.91}{}^{+0.36}_{-0.23}$.

[22] AAD 14AR measure the cross section for $pp \to H \to ZZ^* \to 4\ell$ ($\ell = e,\ \mu$) using 20.3fb^{-1} at $E_{\rm cm} = 8$ TeV. They give $\sigma \cdot B = 2.11^{+0.53}_{-0.47} \pm 0.08$ fbin their fiducial region, where 1.30 $\pm$ 0.13 fb is expected in the Standard Model for m_H= 125.4 GeV. Various differential cross sections are also given; see their Fig. 2.

[23] CHATRCHYAN 14AA use 5.1 fb^{-1} of pp collisions at $E_{\rm cm} = 7$ TeV and 19.7 fb^{-1} at $E_{\rm cm} = 8$ TeV. The quoted signal strength is given for $m_H = 125.6$ GeV. The signal strength for the gluon fusion and $t\bar{t}H$ production mode is $0.80^{+0.46}_{-0.36}$, while the signal strength for the vector boson fusion and WH, ZH production mode is $1.7^{+2.2}_{-2.1}$.

[24] AAD 13AK use 4.7 fb^{-1} of pp collisions at $E_{cm} = 7$ TeV and 20.7 fb^{-1} at $E_{cm} = 8$ TeV. The quoted signal strength is given for $m_H = 125.5$ GeV.

[25] CHATRCHYAN 13J obtain results based on $ZZ \to 4\ell$ final states in 5.1 fb^{-1} of pp collisions at $E_{cm} = 7$ TeV and 12.2 fb^{-1} at $E_{cm} = 8$ TeV. The quoted signal strength is given for $m_H = 125.8$ GeV. Superseded by CHATRCHYAN 14AA.

[26] AAD 12AI obtain results based on 4.7–4.8 fb^{-1} of pp collisions at $E_{cm} = 7$ TeV and 5.8 fb^{-1} at $E_{cm} = 8$ TeV. The quoted signal strengths are given for $m_H = 126$ GeV. See also AAD 12DA.

[27] CHATRCHYAN 12N obtain results based on 4.9–5.1 fb^{-1} of pp collisions at $E_{cm} = 7$ TeV and 5.1–5.3 fb^{-1} at $E_{cm} = 8$ TeV. An excess of events over background with a local significance of 5.0 σ is observed at about $m_H = 125$ GeV. The quoted signal strengths are given for $m_H = 125.5$ GeV. See also CHATRCHYAN 12BY and CHATRCHYAN 13Y.

$\gamma\gamma$ final state

VALUE	DOCUMENT ID		TECN	COMMENT
1.10±0.06 OUR AVERAGE				
$1.04^{+0.10}_{-0.09}$	[1] AAD	23Y	ATLS	pp, 13 TeV
1.13±0.09	[2] CMS	22	CMS	pp, 13 TeV
$1.14^{+0.19}_{-0.18}$	[3,4] AAD	16AN	LHC	pp, 7, 8 TeV
$5.97^{+3.39}_{-3.12}$	[5] AALTONEN	13M	TEVA	$p\overline{p} \to HX$, 1.96 TeV
• • • We do not use the following data for averages, fits, limits, etc. • • •				
	[6] HAYRAPETY...25AL		CMS	pp, 13.6 TeV, diff. x-section
	[7] AAD	24AQ	ATLS	pp, 13.6 TeV, cross sections
	[8] TUMASYAN	23Q	CMS	pp, 13 TeV, cross sections
	[9] AAD	22N	ATLS	pp, 13 TeV, diff. x-sections
1.12±0.09	[10] SIRUNYAN	21O	CMS	pp, 13 TeV
$1.20^{+0.18}_{-0.14}$	[11] SIRUNYAN	19AT	CMS	pp, 13 TeV
	[12] SIRUNYAN	19L	CMS	pp, 13 TeV, diff. x-section
$0.99^{+0.15}_{-0.14}$	[13] AABOUD	18BO	ATLS	pp, 13 TeV
$1.18^{+0.17}_{-0.14}$	[14] SIRUNYAN	18DS	CMS	pp, $H \to \gamma\gamma$, 13 TeV, floated m_H
$1.14^{+0.27}_{-0.25}$	[4] AAD	16AN	ATLS	pp, 7, 8 TeV
$1.11^{+0.25}_{-0.23}$	[4] AAD	16AN	CMS	pp, 7, 8 TeV
	[15] KHACHATRY...16G		CMS	pp, 8 TeV, diff. x-section
$1.17\pm0.23^{+0.10+0.12}_{-0.08-0.08}$	[16] AAD	14BC	ATLS	$pp \to HX$, 7, 8 TeV
	[17] AAD	14BJ	ATLS	pp, 8 TeV, diff. x-section
$1.14\pm0.21^{+0.09+0.13}_{-0.05-0.09}$	[18] KHACHATRY...14P		CMS	pp, 7, 8 TeV
$1.55^{+0.33}_{-0.28}$	[19] AAD	13AK	ATLS	pp, 7 and 8 TeV
$7.81^{+4.61}_{-4.42}$	[20] AALTONEN	13L	CDF	$p\overline{p} \to HX$, 1.96 TeV
$4.20^{+4.60}_{-4.20}$	[21] ABAZOV	13L	D0	$p\overline{p} \to HX$, 1.96 TeV
1.8 ±0.5	[22] AAD	12AI	ATLS	$pp \to HX$, 7, 8 TeV
2.2 ±0.7	[22] AAD	12AI	ATLS	$pp \to HX$, 7 TeV
1.5 ±0.6	[22] AAD	12AI	ATLS	$pp \to HX$, 8 TeV

$1.54^{+0.46}_{-0.42}$ [23] CHATRCHYAN 12N CMS $pp \to HX$, 7, 8 TeV

[1] AAD 23Y use 139 fb^{-1} of pp collisions at $E_{cm} = 13$ TeV. The quoted results are given for $m_H = 125.09$ GeV and $\Gamma_H = 4.07$ MeV. Measured $\sigma \cdot B$ and ratios to the SM predictions for the different production modes are shown in their Table 9 and Fig. 9. Measured cross sections and ratios to the SM predictions in the reduced stage-1.2 (see their Fig. 11) simplified template cross section framework are shown in their Table 10 and Fig. 12. Wilson coefficients in the Warsaw basis (see their Table 11) at 95% CL are measured; see their Table 16 and Fig. 17.

[2] CMS 22 report combined results (see their Extended Data Table 2) using up to 138 fb^{-1} of data at $E_{cm} = 13$ TeV, assuming $m_H = 125.38$ GeV. See their Fig. 2 right.

[3] AAD 16AN perform fits to the ATLAS and CMS data at $E_{cm} = 7$ and 8 TeV. The signal strengths for individual production processes are $1.10^{+0.23}_{-0.22}$ for gluon fusion, 1.3 ± 0.5 for vector boson fusion, $0.5^{+1.3}_{-1.2}$ for WH production, $0.5^{+3.0}_{-2.5}$ for ZH production, and $2.2^{+1.6}_{-1.3}$ for $t\bar{t}H$ production.

[4] AAD 16AN: In the fit, relative production cross sections are fixed to those in the Standard Model. The quoted signal strength is given for $m_H = 125.09$ GeV.

[5] AALTONEN 13M combine all Tevatron data from the CDF and D0 Collaborations with up to 10.0 fb^{-1} and 9.7 fb^{-1}, respectively, of $p\bar{p}$ collisions at $E_{cm} = 1.96$ TeV. The quoted signal strength is given for $m_H = 125$ GeV.

[6] HAYRAPETYAN 25AL measure fiducial and differential cross sections of $pp \to H \to \gamma\gamma$ at $E_{cm} = 13.6$ TeV with 34.7 fb^{-1} data. The quoted results are given for $m_H = 125.38$ GeV. The inclusive fiducial cross section is $74 \pm 11^{+5}_{-4}$ fb with the fiducial region defined in their Section 6. Differential fiducial cross sections as a function of Higgs boson p_T, rapidity, the number of jets, leading jet p_T are shown in their Figs. 7–10.

[7] AAD 24AQ measure fiducial and total cross sections at $E_{cm} = 13.6$ TeV with 31.4 fb^{-1} data. The quoted results are given for $m_H = 125.09$ GeV. The inclusive fiducial cross section is 76^{+14}_{-13} fb with their defined fiducial region (see their Table 2), where 67.6 ± 3.7 fb is expected in the SM. Assuming SM values for the acceptance and the branching fraction, the total cross section is 67^{+12}_{-11} pb, where 59.9 ± 2.6 pb is expected in the SM.

[8] TUMASYAN 23Q measure fiducial and differential cross sections at $E_{cm} = 13$ TeV with 137 fb^{-1} data. The quoted results are given for $m_H = 125.38$ GeV. The inclusive fiducial $\sigma \cdot B$ is $73.4^{+5.4}_{-5.3}(\text{stat})^{+2.4}_{-2.2}(\text{syst})$ fb with their defined fiducial region (see their Section 7 and Table 2), where 75.4 ± 4.1 fb is expected in the Standard Model. See their Fig. 8 including other fiducial $\sigma \cdot B$ defined in their Table 3. Differential $\sigma \cdot B$ are shown in their Figs. 10–15. Double-differential $\sigma \cdot B$ are in their Figs. 16 and 17.

[9] AAD 22N measure fiducial and differential cross sections of $pp \to H \to \gamma\gamma$ at $E_{cm} = 13$ TeV with 139 fb^{-1} data. The quoted results are given for $m_H = 125.09$ GeV. The inclusive fiducial $\sigma \cdot B$ is $67 \pm 5 \pm 4$ fb with their defined fiducial region. Other fiducial $\sigma \cdot B$ are in their Table 3. Differential $\sigma \cdot B$ are shown in their Figs. 8–13, 15, 25–32, 35, 36. Double-differential $\sigma \cdot B$ are in their Figs. 14, 33, 34. Modifications of the b- and c-quark Yukawa couplings to H, κ_b and κ_c at 95% CL are in their Table 6 and Fig. 18. Wilson coefficients at 95% CL are in their Table 7 and Fig. 21.

[10] SIRUNYAN 21O measures cross sections and couplings with the $H \to \gamma\gamma$ channel using 137 fb^{-1} data at $E_{cm} = 13$ TeV. Results are given for $m_H = 125.38$ GeV. The signal strengths for individual production processes are given in their Fig. 16. Cross sections are given in their Tables 12 and 13 and Figs. 18 and 20, which are based on the simplified template cross section framework (reduced stage-1.2). Results in the κ-framework are given in their Fig. 22.

[11] SIRUNYAN 19AT perform a combine fit to 35.9 fb^{-1} of data at $E_{cm} = 13$ TeV.

[12] SIRUNYAN 19L measure fiducial and differential cross sections of the process $pp \to H \to \gamma\gamma$ at $E_{cm} = 13$ TeV with 35.9 fb^{-1}. See their Figs. 4–11.

[13] AABOUD 18BO use 36.1 fb^{-1} of pp collisions at $E_{cm} = 13$ TeV. The signal strengths for the individual production modes are: $0.81^{+0.19}_{-0.18}$ for gluon fusion, $2.0^{+0.6}_{-0.5}$ for vector boson fusion, $0.7^{+0.9}_{-0.8}$ for VH production ($V = W$, Z), and 0.5 ± 0.6 for $t\bar{t}H$ and tH production. Other measurements of cross sections and couplings are summarized in their Section 10. The quoted values are given for $m_H = 125.09$ GeV.

[14] SIRUNYAN 18DS use 35.9 fb^{-1} of $pp \to H$ collisions with $H \to \gamma\gamma$ at $E_{cm} = 13$ TeV. The Higgs mass is floated in the measurement of a signal strength. The result is $1.18^{+0.12}_{-0.11}(\text{stat.})^{+0.09}_{-0.07}(\text{syst.})^{+0.07}_{-0.06}(\text{theory})$, which is largely insensitive to the Higgs mass around 125 GeV.

[15] KHACHATRYAN 16G measure fiducial and differential cross sections of the process $pp \to HX$, $H \to \gamma\gamma$ at $E_{cm} = 8$ TeV with 19.7 fb^{-1}. See their Figs. 4–6 and Table 1 for data.

[16] AAD 14BC use 4.5 fb^{-1} of pp collisions at $E_{cm} = 7$ TeV and 20.3 fb^{-1} at $E_{cm} = 8$ TeV. The last uncertainty in the measurement is theory systematics. The quoted signal strength is given for $m_H = 125.4$ GeV. The signal strengths for the individual production modes are: 1.32 ± 0.38 for gluon fusion, 0.8 ± 0.7 for vector boson fusion, 1.0 ± 1.6 for WH production, $0.1^{+3.7}_{-0.1}$ for ZH production, and $1.6^{+2.7}_{-1.8}$ for $t\bar{t}H$ production.

[17] AAD 14BJ measure fiducial and differential cross sections of the process $pp \to HX$, $H \to \gamma\gamma$ at $E_{cm} = 8$ TeV with 20.3 fb^{-1}. See their Table 3 and Figs. 3–12 for data.

[18] KHACHATRYAN 14P use 5.1 fb^{-1} of pp collisions at $E_{cm} = 7$ TeV and 19.7 fb^{-1} at $E_{cm} = 8$ TeV. The last uncertainty in the measurement is theory systematics. The quoted signal strength is given for $m_H = 124.7$ GeV. The signal strength for the gluon fusion and $t\bar{t}H$ production mode is $1.13^{+0.37}_{-0.31}$, while the signal strength for the vector boson fusion and WH, ZH production mode is $1.16^{+0.63}_{-0.58}$.

[19] AAD 13AK use 4.7 fb^{-1} of pp collisions at $E_{cm} = 7$ TeV and 20.7 fb^{-1} at $E_{cm} = 8$ TeV. The quoted signal strength is given for $m_H = 125.5$ GeV.

[20] AALTONEN 13L combine all CDF results with 9.45–10.0 fb^{-1} of $p\bar{p}$ collisions at $E_{cm} = 1.96$ TeV. The quoted signal strength is given for $m_H = 125$ GeV.

[21] ABAZOV 13L combine all D0 results with up to 9.7 fb^{-1} of $p\bar{p}$ collisions at $E_{cm} = 1.96$ TeV. The quoted signal strength is given for $m_H = 125$ GeV.

[22] AAD 12AI obtain results based on 4.8 fb^{-1} of pp collisions at $E_{cm} = 7$ TeV and 5.9 fb^{-1} at $E_{cm} = 8$ TeV. The quoted signal strengths are given for $m_H = 126$ GeV. See also AAD 12DA.

[23] CHATRCHYAN 12N obtain results based on 5.1 fb^{-1} of pp collisions at E_{cm}=7 TeV and 5.3 fb^{-1} at E_{cm}=8 TeV. The quoted signal strength is given for m_H=125.5 GeV. See also CHATRCHYAN 13Y.

$c\bar{c}$ final state

VALUE	CL%	DOCUMENT ID		TECN	COMMENT
– 0.5± 3.4 OUR AVERAGE					
– 1.6 ± 4.5		[1] HAYRAPETY...26		CMS	pp, $t\bar{t}H$, 13 TeV
$1.0^{+5.4}_{-5.2}$		[2] AAD	25Y	ATLS	$pp \to WH/ZH$, 13 TeV
• • • We do not use the following data for averages, fits, limits, etc. • • •					
< 7.8	95	[1] HAYRAPETY...26		CMS	pp, $t\bar{t}H$, 13 TeV
< 11.5	95	[2] AAD	25Y	ATLS	$pp \to WH/ZH$, 13 TeV
$9.4^{+20.3}_{-19.9}$		[3] TUMASYAN	23AD	CMS	$pp \to WH/ZH$ (boosted), 13 TeV

$<$	47			95	[3] TUMASYAN	23AD	CMS	$pp \to WH/ZH$ (boosted), 13 TeV
$<$	14			95	[4] TUMASYAN	23AH	CMS	$pp \to WH/ZH$, 13 TeV
$-$	9	± 10	± 11		[5,6] AAD	22W	ATLS	$pp \to WH/ZH$, 13 TeV
$-$	9	± 10	± 12		[5,7] AAD	22W	ATLS	$pp \to WH/ZH$, 13 TeV
$<$	26			95	[5] AAD	22W	ATLS	$pp \to WH/ZH$, 13 TeV
	37	± 17	$^{+11}_{-9}$		[8] SIRUNYAN	20AE	CMS	pp, 13 TeV
$<$	110			95	[9] AABOUD	18M	ATLS	pp, 13 TeV

[1] HAYRAPETYAN 26 search for $t\bar{t}H$, $H \to c\bar{c}$ together with the $t\bar{t}H$, $H \to b\bar{b}$ measurement using 138 fb^{-1} of pp collision data at $E_{\text{cm}} = 13$ TeV. The quoted limit corresponds to $\sigma_{t\bar{t}H} \cdot \text{B}(H \to c\bar{c}) < 0.11$ pb at 95% CL.

[2] AAD 25Y present measurements of VH, $H \to b\bar{b}$ and $H \to c\bar{c}$ ($V = W, Z$) using 140 fb^{-1} of pp collision data at $E_{\text{cm}} = 13$ TeV. Two-dimensional likelihood scan of $(\mu_{VH}^{bb}, \mu_{VH}^{cc})$ is shown in their Fig. 11.

[3] TUMASYAN 23AD search for Higgs produced with transverse momenta greater than 450 GeV and decaying to $c\bar{c}$ using 138 fb^{-1} of pp collision data at $E_{\text{cm}} = 13$ TeV.

[4] TUMASYAN 23AH search for VH, $H \to c\bar{c}$ ($V = W, Z$) using 138 fb^{-1} of pp collision data at $E_{\text{cm}} = 13$ TeV. The upper limit on $\sigma(pp \to VH)\cdot\text{B}(H \to c\bar{c})$ is 0.94 pb at 95% CL. See their Fig. 4. The quoted values are given for $m_H = 125.38$ GeV.

[5] AAD 22W search for VH, $H \to c\bar{c}$ ($V = W, Z$) using 139 fb^{-1} of pp collision data at $E_{\text{cm}} = 13$ TeV. The results are given for $m_H = 125$ GeV.

[6] The analysis of VH, $H \to c\bar{c}$ is combined with VH, $H \to b\bar{b}$ (AAD 21AB). The ratio $|\kappa_c/\kappa_b|$ is constrained to be less than 4.5 at 95% CL. See their Fig. 7.

[7] The constraint on the charm Yukawa coupling modifier κ_c is measured to be $|\kappa_c| < 8.5$ at 95% CL. See their Fig. 4.

[8] SIRUNYAN 20AE use 35.9 fb^{-1} at of pp collisions at $E_{\text{cm}} = 13$ TeV. The measured best fit value of $\sigma(pp \to VH)\cdot\text{B}(H \to c\bar{c})$ is $2.40^{+1.12}_{-1.11}{}^{+0.65}_{-0.61}$ pb (equivalent to $<$ 4.5 pb at 95% CL upper limit, i.e. 70 times the standard model), where V is $W \to \ell\nu$, $Z \to \ell\ell$, or $Z \to \nu\nu$ ($\ell = e, \mu$). The quoted values are given for $m_H = 125$ GeV.

[9] AABOUD 18M use 36.1 fb^{-1} at of pp collisions at $E_{\text{cm}} = 13$ TeV. The upper limit on $\sigma(pp \to ZH)\cdot\text{B}(H \to c\bar{c})$ is 2.7 pb at 95% CL. This corresponds to 110 times the standard model. The quoted values are given for $m_H = 125$ GeV.

$b\bar{b}$ final state

VALUE	DOCUMENT ID		TECN	COMMENT
0.94 ± 0.11 OUR AVERAGE				
$0.92^{+0.16}_{-0.15}$	[1] AAD	25Y	ATLS	$pp \to VH$, $H \to b\bar{b}$, 13 TeV
$1.05^{+0.22}_{-0.21}$	[2] CMS	22	CMS	pp, 13 TeV
$0.95 \pm 0.32^{+0.20}_{-0.17}$	[3] AAD	21AJ	ATLS	VBF, $H \to b\bar{b}$, pp, 13 TeV, 126 fb^{-1}
$0.70^{+0.29}_{-0.27}$	[4,5] AAD	16AN	LHC	pp, 7, 8 TeV
$1.59^{+0.69}_{-0.72}$	[6] AALTONEN	13M	TEVA	$p\bar{p} \to HX$, 1.96 TeV
• • • We do not use the following data for averages, fits, limits, etc. • • •				
$0.91^{+0.26}_{-0.22}$	[7] HAYRAPETY...26		CMS	pp, $t\bar{t}H$, 13 TeV
	[8] CHEKHOVSKY 25A		CMS	VH, $H \to b\bar{b}$, pp, 13 TeV
$1.4\ ^{+1.0}_{-0.9}$	[9] AAD	24F	ATLS	VH, boosted $H \to b\bar{b}$, pp, 13 TeV

$2.2\ ^{+0.9}_{-0.8}$		[10] HAYRAPETY...24AM		CMS	$pp \to ZH$, $Z/H \to b\overline{b}$, 13 TeV
$4.9\ ^{+1.9}_{-1.6}$		[11] HAYRAPETY...24AY		CMS	ggF, VBF, boosted $H \to b\overline{b}$, pp, 13 TeV
$1.6\ ^{+1.7}_{-1.5}$		[12] HAYRAPETY...24AY		CMS	ggF, VBF, boosted $H \to b\overline{b}$, pp, 13 TeV
$1.01^{+0.55}_{-0.46}$		[13] HAYRAPETY...24U		CMS	VBF, $H \to b\overline{b}$, pp, 13 TeV, 90.8 fb^{-1}
$0.99^{+0.48}_{-0.41}$		[14] HAYRAPETY...24U		CMS	ggF, VBF, $H \to b\overline{b}$, pp, 13 TeV, 90.8 fb^{-1}
$-2.7\ ^{+5.6}_{-2.1}$	± 3.5	[15] HAYRAPETY...24U		CMS	ggF, $H \to b\overline{b}$, pp, 13 TeV, 90.8 fb^{-1}
$1.59^{+0.63}_{-0.72}$	± 0.54	[15] HAYRAPETY...24U		CMS	VBF, $H \to b\overline{b}$, pp, 13 TeV, 90.8 fb^{-1}
$1.15^{+0.22}_{-0.20}$		[16] TUMASYAN	24	CMS	$pp \to WH/ZH$, $H \to b\overline{b}$, 13 TeV, 138 fb^{-1}
$0.8\ \pm 3.2$		[17] AAD	22X	ATLS	boosted $H \to b\overline{b}$, pp, 13 TeV
$1.02^{+0.12}_{-0.11}{}^{+0.14}_{-0.13}$		[18] AAD	21AB	ATLS	$pp \to VH$, $H \to b\overline{b}$, 13 TeV
$0.95 \pm 0.18^{+0.19}_{-0.18}$		[18] AAD	21AB	ATLS	$pp \to HW$, $H \to b\overline{b}$, 13 TeV, 139 fb^{-1}
$1.08 \pm 0.17^{+0.18}_{-0.15}$		[18] AAD	21AB	ATLS	$pp \to HZ$, $H \to b\overline{b}$, 13 TeV, 139 fb^{-1}
$0.72^{+0.29}_{-0.28}{}^{+0.26}_{-0.22}$		[19] AAD	21H	ATLS	$pp \to HW/HZ$, $H \to b\overline{b}$, boosted W/Z, 13 TeV, 139 fb^{-1}
$1.3\ \pm 1.0$		[20] AAD	21M	ATLS	VBF+γ, $H \to b\overline{b}$, pp, 13 TeV, 132 fb^{-1}
$3.7\ \pm 1.2\ ^{+0.11}_{-0.9}$		[21] SIRUNYAN	20BL	CMS	boosted $H \to b\overline{b}$, pp, 13 TeV
		[22] AABOUD	19U	ATLS	$pp \to VH$, $H \to b\overline{b}$, 13 TeV, cross sections
1.12 ± 0.29		[23] SIRUNYAN	19AT	CMS	pp, 13 TeV
$1.16^{+0.27}_{-0.25}$		[24] AABOUD	18BN	ATLS	$pp \to HW/HZ$, $H \to b\overline{b}$, 13 TeV, 79.8 fb^{-1}
$0.98^{+0.22}_{-0.21}$		[25] AABOUD	18BN	ATLS	$pp \to HW/HZ$, $H \to b\overline{b}$, 7, 8, 13 TeV
1.01 ± 0.20		[26] AABOUD	18BN	ATLS	$pp \to HX$, ggF, VBF, VH, $t\overline{t}H$ 7, 8, 13 TeV
$2.5\ ^{+1.4}_{-1.3}$		[27,28] AABOUD	18BQ	ATLS	$pp \to HX$, VBF, ggF, VH, $t\overline{t}H$, 13 TeV
$3.0\ ^{+1.7}_{-1.6}$		[27,29] AABOUD	18BQ	ATLS	$pp \to HX$, VBF, 13 TeV
		[30] AALTONEN	18C	CDF	$p\overline{p} \to HX$, 1.96 TeV
$1.19^{+0.40}_{-0.38}$		[31] SIRUNYAN	18AE	CMS	$pp \to HW/HZ$, $H \to b\overline{b}$, 13 TeV
$1.06^{+0.31}_{-0.29}$		[32] SIRUNYAN	18AE	CMS	$pp \to HW/HZ$, $H \to b\overline{b}$, 7, 8, 13 TeV
1.06 ± 0.26		[33] SIRUNYAN	18DB	CMS	$pp \to HW/HZ$, $H \to b\overline{b}$, 13 TeV, 77.2 fb^{-1}
1.01 ± 0.22		[34] SIRUNYAN	18DB	CMS	$pp \to HW/HZ$, $H \to b\overline{b}$, 7, 8, 13 TeV

1.04 ± 0.20	[35] SIRUNYAN	18DB	CMS	$pp \to HX$, ggF, VBF, VH, $t\bar{t}H$ 7, 8, 13 TeV
$2.3\ ^{+1.8}_{-1.6}$	[36] SIRUNYAN	18E	CMS	$pp \to HX$, boosted, 13 TeV
$1.20^{+0.24}_{-0.23}{}^{+0.34}_{-0.28}$	[37] AABOUD	17BA	ATLS	$pp \to HW/ZX$, $H \to b\bar{b}$, 13 TeV, 36.1 fb^{-1}
$0.90 \pm 0.18^{+0.21}_{-0.19}$	[38] AABOUD	17BA	ATLS	$pp \to HW/ZX$, $H \to b\bar{b}$, 7, 8, 13 TeV
$-0.8\ \pm 1.3\ ^{+1.8}_{-1.9}$	[39] AABOUD	16X	ATLS	$pp \to HX$, VBF, 8 TeV
0.62 ± 0.37	[5] AAD	16AN	ATLS	pp, 7, 8 TeV
$0.81^{+0.45}_{-0.43}$	[5] AAD	16AN	CMS	pp, 7, 8 TeV
$0.63^{+0.31}_{-0.30}{}^{+0.24}_{-0.23}$	[40] AAD	16K	ATLS	pp, 7, 8 TeV
$0.52 \pm 0.32 \pm 0.24$	[41] AAD	15G	ATLS	$pp \to HW/ZX$, 7, 8 TeV
$2.8\ ^{+1.6}_{-1.4}$	[42] KHACHATRY...	15Z	CMS	$pp \to HX$, VBF, 8 TeV
$1.03^{+0.44}_{-0.42}$	[43] KHACHATRY...	15Z	CMS	pp, 8 TeV, combined
$1.0\ \pm 0.5$	[44] CHATRCHYAN	14AI	CMS	$pp \to HW/ZX$, 7, 8 TeV
$1.72^{+0.92}_{-0.87}$	[45] AALTONEN	13L	CDF	$p\bar{p} \to HX$, 1.96 TeV
$1.23^{+1.24}_{-1.17}$	[46] ABAZOV	13L	D0	$p\bar{p} \to HX$, 1.96 TeV
$0.5\ \pm 2.2$	[47] AAD	12AI	ATLS	$pp \to HW/ZX$, 7 TeV
	[48] AALTONEN	12T	TEVA	$p\bar{p} \to HW/ZX$, 1.96 TeV
$0.48^{+0.81}_{-0.70}$	[49] CHATRCHYAN	12N	CMS	$pp \to HW/ZX$, 7, 8 TeV

[1] AAD 25Y present measurements of VH, $H \to b\bar{b}$ ($V = W,\ Z$) using 140 fb^{-1} of pp collision data at $E_{\text{cm}} = 13$ TeV. The observed significance for WH and ZH are 5.3 and 4.9 σ, respectively. See their Fig. 12. Cross sections are given in their Table 8 and Figs. 15 and 16, which are based on the simplified template cross section framework (extended stage-1.2).

[2] CMS 22 report combined results (see their Extended Data Table 2) using up to 138 fb^{-1} of data at $E_{\text{cm}} = 13$ TeV, assuming $m_H = 125.38$ GeV. See their Fig. 2 right.

[3] AAD 21AJ present measurements of $H \to b\bar{b}$ in the VBF production mode. The inclusive VBF cross sections with and without the branching ratio of $H \to b\bar{b}$ are $2.07 \pm 0.70^{+0.46}_{-0.37}$ fb and $3.56 \pm 1.21^{+0.80}_{-0.64}$ fb, respectively. The latter is obtained assuming the SM value of B($H \to b\bar{b}$) = 0.5809 and $m_H = 125$ GeV.

[4] AAD 16AN perform fits to the ATLAS and CMS data at $E_{\text{cm}} = 7$ and 8 TeV. The signal strengths for individual production processes are 1.0 ± 0.5 for WH production, 0.4 ± 0.4 for ZH production, and 1.1 ± 1.0 for $t\bar{t}H$ production.

[5] AAD 16AN: In the fit, relative production cross sections are fixed to those in the Standard Model. The quoted signal strength is given for $m_H = 125.09$ GeV.

[6] AALTONEN 13M combine all Tevatron data from the CDF and D0 Collaborations with up to 10.0 fb^{-1} and 9.7 fb^{-1}, respectively, of $p\bar{p}$ collisions at $E_{\text{cm}} = 1.96$ TeV. The quoted signal strength is given for $m_H = 125$ GeV.

[7] HAYRAPETYAN 26 search for $t\bar{t}H$, $H \to c\bar{c}$ together with the $t\bar{t}H$, $H \to b\bar{b}$ measurement using 138 fb^{-1} of pp collision data at $E_{\text{cm}} = 13$ TeV.

[8] CHEKHOVSKY 25A constrain six Wilson coefficients in the Warsaw basis using 138 fb^{-1} of pp collision data at $E_{\text{cm}} = 13$ TeV. The results are shown in their Figs. 7 (for linear and quadratic), 9–13 (two-dimensional likelihood scan). The limits on the energy scale for three different assumptions for each Wilson coefficient are shown in their Fig. 8.

[9] AAD 24F present studies of the VH production mode in the boosted $V \to q\overline{q}$ and $H \to b\overline{b}$ ($p_T(H) > 250$ GeV) using 137 fb^{-1} of pp collision data at $E_{cm} = 13$ TeV. The quoted signal strength is given for $m_H = 125.09$ GeV and corresponds to a significance of 1.7 standard deviations. The corresponding inclusive cross section is $3.1 \pm 1.3^{+1.8}_{-1.4}$ pb. The signal strengths and cross sections are given in their Table I for three $p_T(H)$ regions: 250 < $p_T(H)$ < 450 GeV, 450 < $p_T(H)$ < 650 GeV, 650 GeV < $p_T(H)$ with $|y(H)| < 2$.

[10] HAYRAPETYAN 24AM search for ZH, $H \to b\overline{b}$, $Z \to b\overline{b}$ using 133 fb^{-1} of pp collision data at $E_{cm} = 13$ TeV. The upper limit at 95% CL on the ZH production is 5.0 times the SM prediction.

[11] HAYRAPETYAN 24AY present measurements of boosted $H \to b\overline{b}$ ($p_T > 450$ GeV) via VBF or gluon fusion productions using 138 fb^{-1} of pp collision data at $E_{cm} = 13$ TeV. The result is given for the VBF production. See their Table 3. The VH and $t\overline{t}H$ production rates are fixed to the SM values. The VBF signal strengths and the fiducial cross sections for two different m_{jj} regions and STXS stage 1.2 bins are shown in their Figs. 9 and 10, respectively.

[12] HAYRAPETYAN 24AY present measurements of boosted $H \to b\overline{b}$ ($p_T > 450$ GeV) via VBF or gluon fusion productions using 138 fb^{-1} of pp collision data at $E_{cm} = 13$ TeV. The result is given for the gluon fusion production. See their Table 3. The VH and $t\overline{t}H$ production rates are fixed to the SM values. The gluon fusion signal strengths and the fiducial cross sections for 6 different p_T regions and STXS stage 1.2 bins are shown in their Figs. 9 and 10, respectively.

[13] HAYRAPETYAN 24U present measurements of $H \to b\overline{b}$ in the VBF production mode using 90.8 fb^{-1} of data at $E_{cm} = 13$ TeV constraining the ggF production to be the SM expectation. The quoted signal strength corresponds to a significance of 2.4 standard deviations.

[14] HAYRAPETYAN 24U present measurements of $H \to b\overline{b}$ in the inclusive (ggF+VBF) production mode using 90.8 fb^{-1} of data at $E_{cm} = 13$ TeV. The quoted signal strength corresponds to a significance of 2.6 standard deviations.

[15] HAYRAPETYAN 24U present measurements of $H \to b\overline{b}$ in the ggF and VBF production modes using 90.8 fb^{-1} of data at $E_{cm} = 13$ TeV. The signal strengths for the ggF and VBF production modes are independently obtained. See their Fig. 11.

[16] TUMASYAN 24 report the measurement of VH, $H \to b\overline{b}$ ($V = W, Z$) using 138 fb^{-1} of pp collision data at $E_{cm} = 13$ TeV. The quoted signal strength corresponds to a significance of 6.3 standard deviations. Signal strengths for WH and ZH are given in their Fig. 7. Signal strengths and $\sigma \cdot B$ for 8 different bins defined based on the the simplified template cross section framework are given in their Figs. 8 and 9 and Table VII.

[17] AAD 22X measure cross sections using a boosted $H \to b\overline{b}$ with large-radius jets. The data is 136 fb^{-1} of pp collisions at $E_{cm} = 13$ TeV. All the results are given for $m_H = 125$ GeV. The inclusive signal strength is given using data with a H candidate jet p_T >250 GeV. The fiducial H production cross section ($p_T(H)$>450 GeV and $|y(H)| <2$) is <115 fb (95% CL) and the upper limits for other four different p_T regions are shown in their Fig 12. The measured fiducial H production cross section ($p_T(H)$>1 TeV) is $2.3 \pm 3.9(\text{stat}) \pm 1.3(\text{syst}) \pm 0.5(\text{theory})$ fb.

[18] AAD 21AB search for VH, $H \to b\overline{b}$ ($V = W, Z$) using 139 fb^{-1} of pp collision data at $E_{cm} = 13$ TeV. The results are given for $m_H = 125$ GeV. Cross sections are given in their Table 13 and Fig. 7, which are based on the simplified template cross section framework (reduced stage-1.2). Wilson coefficients of the Warsaw-basis operators are given in their Fig. 9.

[19] AAD 21H present measurements of $H \to b\overline{b}$ with a boosted vector boson ($p_T > 250$ GeV) using 139 fb^{-1} of pp collision data at $E_{cm} = 13$ TeV. Cross sections are given in their Table 6 and Fig. 4, which are based on the simplified template cross section

framework (reduced stage-1.2). Wilson coefficients of the Warsaw-basis operators are given in their Fig. 5.

[20] AAD 21M search for VBF+γ, $H \to b\overline{b}$ using 132 fb^{-1} of pp collision data at E_{cm} = 13 TeV.

[21] SIRUNYAN 20BL search for boosted $H \to b\overline{b}$ (a H candidate jet p_T >450 GeV) using 137 fb^{-1} of pp collision data at E_{cm} = 13 TeV. The quoted signal strength corresponds to a significance of 2.5 standard deviations and is given for m_H = 125 GeV. A differential fiducial cross section as a function of Higgs boson p_T for ggF is shown in their Fig. 7, assuming the other production modes occur at the expected SM rates. The reported value is $3.7 \pm 1.2^{+0.8+0.8}_{-0.7-0.5}$ where the last uncertainty comes from theoretical modeling. We have combined the systematic uncertainties in quadrature.

[22] AABOUD 19U measure cross sections of $pp \to VH$, $H \to b\overline{b}$ production as a function of the gauge boson transverse momentum using data of 79.8 fb^{-1}. The kinematic fiducial volumes used is based on the simplified template cross section framework (reduced stage-1). See their Table 3 and Fig. 3.

[23] SIRUNYAN 19AT perform a combine fit to 35.9 fb^{-1} of data at E_{cm} = 13 TeV.

[24] AABOUD 18BN search for VH, $H \to b\overline{b}$ ($V = W,\ Z$) using 79.8 fb^{-1} of pp collision data at E_{cm} = 13 TeV. The quoted signal strength corresponds to a significance of 4.9 standard deviations and is given for m_H = 125 GeV.

[25] AABOUD 18BN combine results of 79.8 fb^{-1} at E_{cm} = 13 TeV with results of VH at E_{cm} = 7 and 8 TeV.

[26] AABOUD 18BN combine results of VH at E_{cm} = 7, 8 and 13 TeV with results of VBF (+gluon fusion) and $t\overline{t}H$ at E_{cm} = 7, 8, and 13 TeV to perform a search for the $H \to b\overline{b}$ decay. The quoted signal strength assumes a SM production strength and corresponds to a significance of 5.4 standard deviations.

[27] AABOUD 18BQ search for $H \to b\overline{b}$ produced through vector-boson fusion (VBF) and VBF+γ with 30.6 fb^{-1} pp collision data at E_{cm} = 13 TeV. The quoted signal strength is given for m_H = 125 GeV.

[28] The signal strength is measured including all production modes (VBF, ggF, VH, $t\overline{t}H$).

[29] The signal strength is measured for VBF-only and others (ggF, VH, $t\overline{t}H$) are constrained to Standard Model expectations with uncertainties described in their Section VIII B.

[30] AALTONEN 18C use 5.4 fb^{-1} of $p\overline{p}$ collisions at E_{cm} = 1.96 TeV. The upper limit at 95% CL on $p\overline{p} \to H \to b\overline{b}$ is 33 times the SM prediction, which corresponds to a cross section of 40.6 pb.

[31] SIRUNYAN 18AE use 35.9 fb^{-1} of pp collision data at E_{cm} = 13 TeV. The quoted signal strength corresponds to 3.3 standard deviations and is given for m_H = 125.09 GeV.

[32] SIRUNYAN 18AE combine the result of 35.9 fb^{-1} at E_{cm} = 13 TeV with the results obtained from data of up to 5.1 fb^{-1} at E_{cm} = 7 TeV and up to 18.9 fb^{-1} at E_{cm} = 8 TeV (CHATRCHYAN 14AI and KHACHATRYAN 15Z). The quoted signal strength corresponds to 3.8 standard deviations and is given for m_H = 125.09 GeV.

[33] SIRUNYAN 18DB search for VH, $H \to b\overline{b}$ ($V = W,\ Z$) using 77.2 fb^{-1} of pp collision data at E_{cm} = 13 TeV. The quoted signal strength corresponds to a significance of 4.4 standard deviations and is given for m_H = 125.09 GeV.

[34] SIRUNYAN 18DB combine the result of 77.2 fb^{-1} at E_{cm} = 13 TeV with the results obtained from data of up to 5.1 fb^{-1} at E_{cm} = 7 TeV and up to 18.9 fb^{-1} at E_{cm} = 8 TeV. The quoted signal strength corresponds to a significance of 4.8 standard deviations and is given for m_H = 125.09 GeV.

[35] SIRUNYAN 18DB combine results of 77.2 fb^{-1} at E_{cm} = 13 TeV with results of gluon fusion (ggF), VBF and $t\overline{t}H$ at E_{cm} = 7 TeV, 8 TeV and 13 TeV to perform a search for the $H \to b\overline{b}$ decay. The quoted signal strength assumes a SM production strength and corresponds to a significance of 5.6 standard deviations and is given for m_H = 125.09 GeV.

[36] SIRUNYAN 18E use 35.9 fb^{-1} at E_{cm} = 13 TeV. The quoted signal strength is given for m_H = 125 GeV. They measure $\sigma \cdot B$ for gluon fusion production of $H \to b\overline{b}$ with p_T >450 GeV, $|\eta|$ <2.5 to be 74 $\pm$ 48$^{+17}_{-10}$ fb.

[37] AABOUD 17BA use 36.1 fb^{-1} at E_{cm} = 13 TeV. The quoted signal strength is given for m_H = 125 GeV. They give σ(W H)·$B(H \to b\overline{b})$ = 1.08$^{+0.54}_{-0.47}$ pb and σ(Z H)·$B(H \to b\overline{b})$ = 0.57$^{+0.26}_{-0.23}$ pb.

[38] AABOUD 17BA combine 7, 8 and 13 TeV analyses. The quoted signal strength is given for m_H = 125 GeV.

[39] AABOUD 16X search for vector-boson fusion production of H decaying to $b\overline{b}$ in 20.2 fb^{-1} of pp collisions at E_{cm} = 8 TeV. The quoted signal strength is given for m_H = 125 GeV.

[40] AAD 16K use up to 4.7 fb^{-1} of pp collisions at E_{cm} = 7 TeV and up to 20.3 fb^{-1} at E_{cm} = 8 TeV. The quoted signal strength is given for m_H = 125.36 GeV.

[41] AAD 15G use 4.7 fb^{-1} of pp collisions at E_{cm} = 7 TeV and 20.3 fb^{-1} at E_{cm} = 8 TeV. The quoted signal strength is given for m_H = 125.36 GeV.

[42] KHACHATRYAN 15Z search for vector-boson fusion production of H decaying to $b\overline{b}$ in up to 19.8 fb^{-1} of pp collisions at E_{cm} = 8 TeV. The quoted signal strength is given for m_H = 125 GeV.

[43] KHACHATRYAN 15Z combined vector boson fusion, WH, ZH production, and $t\overline{t}H$ production results. The quoted signal strength is given for m_H = 125 GeV.

[44] CHATRCHYAN 14AI use up to 5.1 fb^{-1} of pp collisions at E_{cm} = 7 TeV and up to 18.9 fb^{-1} at E_{cm} = 8 TeV. The quoted signal strength is given for m_H = 125 GeV. See also CHATRCHYAN 14AJ.

[45] AALTONEN 13L combine all CDF results with 9.45–10.0 fb^{-1} of $p\overline{p}$ collisions at E_{cm} = 1.96 TeV. The quoted signal strength is given for m_H = 125 GeV.

[46] ABAZOV 13L combine all D0 results with up to 9.7 fb^{-1} of $p\overline{p}$ collisions at E_{cm} = 1.96 TeV. The quoted signal strength is given for m_H = 125 GeV.

[47] AAD 12AI obtain results based on 4.6–4.8 fb^{-1} of pp collisions at E_{cm} = 7 TeV. The quoted signal strengths are given in their Fig. 10 for m_H = 126 GeV. See also Fig. 13 of AAD 12DA.

[48] AALTONEN 12T combine AALTONEN 12Q, AALTONEN 12R, AALTONEN 12S, ABAZOV 12O, ABAZOV 12P, and ABAZOV 12K. An excess of events over background is observed which is most significant in the region m_H = 120–135 GeV, with a local significance of up to 3.3 σ. The local significance at m_H = 125 GeV is 2.8 σ, which corresponds to $(\sigma(HW) + \sigma(HZ)) \cdot B(H \to b\overline{b})$ = (0.23$^{+0.09}_{-0.08}$) pb, compared to the Standard Model expectation at m_H = 125 GeV of 0.12 $\pm$ 0.01 pb. Superseded by AALTONEN 13M.

[49] CHATRCHYAN 12N obtain results based on 5.0 fb^{-1} of pp collisions at E_{cm}=7 TeV and 5.1 fb^{-1} at E_{cm}=8 TeV. The quoted signal strength is given for m_H=125.5 GeV. See also CHATRCHYAN 13Y.

$\mu^+\mu^-$ final state

VALUE	CL%	DOCUMENT ID		TECN	COMMENT
1.31±0.29 OUR AVERAGE					
1.4 ±0.4		[1] AAD	25AR	ATLS	pp, 13, 13.6 TeV
1.21$^{+0.45}_{-0.42}$		[2] CMS	22	CMS	pp, 13 TeV
• • • We do not use the following data for averages, fits, limits, etc. • • •					
1.6 ±0.6		[3] AAD	25AR	ATLS	pp, 13.6 TeV
1.2 ±0.6		[4] AAD	21	ATLS	pp, 13 TeV
1.19$^{+0.40+0.15}_{-0.39-0.14}$		[5] SIRUNYAN	21C	CMS	pp, 13 TeV

$0.68^{+1.25}_{-1.24}$			[6] SIRUNYAN	19AT	CMS	pp, 13 TeV
$0.7 \pm 1.0\ ^{+0.2}_{-0.1}$			[7] SIRUNYAN	19E	CMS	pp, 13 TeV, 35.9 fb^{-1}
$1.0 \pm 1.0 \pm 0.1$			[7] SIRUNYAN	19E	CMS	pp, 7, 8, 13 TeV
-0.1 ± 1.4			[8] AABOUD	17Y	ATLS	pp, 7, 8, 13 TeV
-0.1 ± 1.5			[8] AABOUD	17Y	ATLS	pp, 13 TeV
0.1 ± 2.5			[9] AAD	16AN	LHC	pp, 7, 8 TeV
-0.6 ± 3.6			[9] AAD	16AN	ATLS	pp, 7, 8 TeV
$0.9\ ^{+3.6}_{-3.5}$			[9] AAD	16AN	CMS	pp, 7, 8 TeV
< 7.4		95	[10] KHACHATRY...	15H	CMS	$pp \to HX$, 7, 8 TeV
< 7.0		95	[11] AAD	14AS	ATLS	$pp \to HX$, 7, 8 TeV

[1] AAD 25AR search for $H \to \mu^+\mu^-$ using 140 fb^{-1} of pp data at $E_{cm} = 13$ TeV and 165 fb^{-1} of pp data at $E_{cm} = 13.6$ TeV. The quoted signal strength corresponds to a significance of 3.4 standard deviations assuming $m_H = 125.09$ GeV.

[2] CMS 22 report combined results (see their Extended Data Table 2) using up to 138 fb^{-1} of data at $E_{cm} = 13$ TeV, assuming $m_H = 125.38$ GeV. See their Fig. 2 right.

[3] AAD 25AR search for $H \to \mu^+\mu^-$ using 165 fb^{-1} of pp collision data at $E_{cm} = 13.6$ TeV. The quoted signal strength corresponds to a significance of 2.8 standard deviations assuming $m_H = 125.09$ GeV.

[4] AAD 21 search for $H \to \mu^+\mu^-$ using 139 fb^{-1} of pp collision data at $E_{cm} = 13$ TeV. The quoted signal strength corresponds to a significance of 2.0 standard deviations and is given for $m_H = 125.09$ GeV. The upper limit on the cross section times branching fraction is 2.2 times the SM prediction at 95% CL, which corresponds to the branching fraction upper limit of 4.7×10^{-4} (assuming SM production cross sections).

[5] SIRUNYAN 21 search for $H \to \mu^+\mu^-$ using 137 fb^{-1} of pp collision data at $E_{cm} = 13$ TeV. The quoted signal strength corresponds to a significance of 3.0 standard deviations and is given for $m_H = 125.38$ GeV.

[6] SIRUNYAN 19AT perform a combine fit to 35.9 fb^{-1} of data at $E_{cm} = 13$ TeV.

[7] SIRUNYAN 19E search for $H \to \mu^+\mu^-$ using 35.9 fb^{-1} of pp collisions at $E_{cm} = 13$ TeV and combine with results of 7 TeV (5.0 fb^{-1}) and 8 TeV (19.7 fb^{-1}). The upper limit at 95% CL on the signal strength is 2.9, which corresponds to the SM Higgs boson branching fraction to a muon pair of 6.4×10^{-4}.

[8] AABOUD 17Y use 36.1 fb^{-1} of pp collisions at $E_{cm} = 13$ TeV, 20.3 fb^{-1} at 8 TeV and 4.5 fb^{-1} at 7 TeV. The quoted signal strength is given for $m_H = 125$ GeV.

[9] AAD 16AN: In the fit, relative production cross sections are fixed to those in the Standard Model. The quoted signal strength is given for $m_H = 125.09$ GeV.

[10] KHACHATRYAN 15H use 5.0 fb^{-1} of pp collisions at $E_{cm} = 7$ TeV and 19.7 fb^{-1} at 8 TeV. The quoted signal strength is given for $m_H = 125$ GeV.

[11] AAD 14AS search for $H \to \mu^+\mu^-$ in 4.5 fb^{-1} of pp collisions at $E_{cm} = 7$ TeV and 20.3 fb^{-1} at $E_{cm} = 8$ TeV. The quoted signal strength is given for $m_H = 125.5$ GeV.

$\tau^+\tau^-$ final state

VALUE	DOCUMENT ID		TECN	COMMENT
0.91±0.09 OUR AVERAGE				
0.85 ± 0.10	[1] CMS	22	CMS	pp, 13 TeV
$1.09^{+0.18}_{-0.17}{}^{+0.26}_{-0.22}{}^{+0.16}_{-0.11}$	[2] AABOUD	19AQ	ATLS	pp, 13 TeV
$1.11^{+0.24}_{-0.22}$	[3,4] AAD	16AN	LHC	pp, 7, 8 TeV
$1.68^{+2.28}_{-1.68}$	[5] AALTONEN	13M	TEVA	$p\overline{p} \to HX$, 1.96 TeV

• • • We do not use the following data for averages, fits, limits, etc. • • •

	[6] AAD	25W	ATLS	pp, 13 TeV	
$1.28^{+0.30}_{-0.29}{}^{+0.25}_{-0.21}$	[7] AAD	24BE	ATLS	$pp \to WH/ZH$, $H \to \tau\tau$, 13 TeV	
$1.64^{+0.68}_{-0.54}$	[8] HAYRAPETY...	24AT	CMS	pp, 13 TeV, boosted $H \to \tau\tau$	
$0.82^{+0.11}_{-0.10}$	[9,10] TUMASYAN	23Y	CMS	pp, 13 TeV	
$0.67^{+0.20}_{-0.18}$	[9,11] TUMASYAN	23Y	CMS	pp, 13 TeV	
$0.81^{+0.17}_{-0.16}$	[9,12] TUMASYAN	23Y	CMS	pp, 13 TeV	
$1.79^{+0.47}_{-0.42}$	[9,13] TUMASYAN	23Y	CMS	pp, 13 TeV	
	[14] AAD	22Q	ATLS	pp, 13 TeV	
	[15] TUMASYAN	22AJ	CMS	pp, 13 TeV	
$2.5\ ^{+1.4}_{-1.3}$	[16] SIRUNYAN	19AF	CMS	$pp \to HW/HZ$, $H \to \tau\tau$, 13 TeV	
$1.24^{+0.29}_{-0.27}$	[17] SIRUNYAN	19AF	CMS	pp, 13 TeV	
$1.02^{+0.26}_{-0.24}$	[18] SIRUNYAN	19AT	CMS	pp, 13 TeV	
$1.09^{+0.27}_{-0.26}$	[19] SIRUNYAN	18Y	CMS	pp, 13 TeV	
0.98 ± 0.18	[20] SIRUNYAN	18Y	CMS	pp, 7, 8, 13 TeV	
$2.3\ \pm 1.6$	[21] AAD	16AC	ATLS	$pp \to HW/ZX$, 8 TeV	
$1.41^{+0.40}_{-0.36}$	[4] AAD	16AN	ATLS	pp, 7, 8 TeV	
$0.88^{+0.30}_{-0.28}$	[4] AAD	16AN	CMS	pp, 7, 8 TeV	
$1.44^{+0.30}_{-0.29}{}^{+0.29}_{-0.23}$	[22] AAD	16K	ATLS	pp, 7, 8 TeV	
$1.43^{+0.27}_{-0.26}{}^{+0.32}_{-0.25} \pm 0.09$	[23] AAD	15AH	ATLS	$pp \to HX$, 7, 8 TeV	
0.78 ± 0.27	[24] CHATRCHYAN	14K	CMS	$pp \to HX$, 7, 8 TeV	
$0.00^{+8.44}_{-0.00}$	[25] AALTONEN	13L	CDF	$p\overline{p} \to HX$, 1.96 TeV	
$3.96^{+4.11}_{-3.38}$	[26] ABAZOV	13L	D0	$p\overline{p} \to HX$, 1.96 TeV	
$0.4\ ^{+1.6}_{-2.0}$	[27] AAD	12AI	ATLS	$pp \to HX$, 7 TeV	
$0.09^{+0.76}_{-0.74}$	[28] CHATRCHYAN	12N	CMS	$pp \to HX$, 7, 8 TeV	

[1] CMS 22 report combined results (see their Extended Data Table 2) using up to 138 fb^{-1} of data at $E_{cm} = 13$ TeV, assuming $m_H = 125.38$ GeV. See their Fig. 2 right.

[2] AABOUD 19AQ use 36.1 fb^{-1} of data. The first, second and third quoted errors are statistical, experimental systematic and theory systematic uncertainties, respectively. The quoted signal strength is given for $m_H = 125$ GeV and corresponds to 4.4 standard deviations. Combining with 7 TeV and 8 TeV results (AAD 15AH), the observed significance is 6.4 standard deviations. The cross sections in the $H \to \tau\tau$ decay channel ($m_H = 125$ GeV) are measured to $3.77^{+0.60}_{-0.59}$ (stat) $^{+0.87}_{-0.74}$ (syst) pb for the inclusive, $0.28 \pm 0.09^{+0.11}_{-0.09}$ pb for VBF, and $3.1 \pm 1.0^{+1.6}_{-1.3}$ pb for gluon-fusion production. See their Table XI for the cross sections in the framework of simplified template cross sections.

[3] AAD 16AN perform fits to the ATLAS and CMS data at $E_{cm} = 7$ and 8 TeV. The signal strengths for individual production processes are 1.0 ± 0.6 for gluon fusion, 1.3 ± 0.4 for

vector boson fusion, -1.4 ± 1.4 for WH production, $2.2^{+2.2}_{-1.8}$ for ZH production, and $-1.9^{+3.7}_{-3.3}$ for $t\bar{t}H$ production.

[4] AAD 16AN: In the fit, relative production cross sections are fixed to those in the Standard Model. The quoted signal strength is given for $m_H = 125.09$ GeV.

[5] AALTONEN 13M combine all Tevatron data from the CDF and D0 Collaborations with up to 10.0 fb^{-1} and 9.7 fb^{-1}, respectively, of $p\overline{p}$ collisions at $E_{\rm cm} = 1.96$ TeV. The quoted signal strength is given for $m_H = 125$ GeV.

[6] AAD 25W measure different types of cross sections with $pp \to H \to \tau\tau$ at $E_{\rm cm} =$ 13 TeV with 140 fb^{-1} data. Their Fig. 5 show $\sigma{\cdot}B$ relative to the SM expectations for the total and per-production-mode, and their Figs. 6 and 8 show those in the simplified template cross section framework. Their Table 7 show the measurements of $\sigma{\cdot}B$ for per-production-mode. The differential fiducial cross sections defined in their Table 8 are given in their Fig. 10. Six Wilson coefficients in the Warsaw basis are in their Figs. 12 and 13 at 95% CL. The constraints on the Wilson coefficients c_{HW} and $c_{H\widetilde{W}}$ are obtained to be $[-1.90, +0.51]$ and $[-0.31, +0.88]$ at 95% CL, respectively, for the interference term alone (the linear term) assuming only one of the Wilson coefficients is non-zero.

[7] AAD 24BE measure the VH Higgs production ($V = W, Z$) with $H \to \tau\tau$ at $E_{\rm cm} =$ 13 TeV with 140 fb^{-1} data. The quoted signal strength corresponds to 4.2 standard deviations. The signal strengths for individual WH and ZH productions are $1.48^{+0.56}_{-0.50}$ and $1.09^{+0.51}_{-0.44}$, respectively. The results are given for $m_H = 125$ GeV. See their Fig. 4.

[8] HAYRAPETYAN 24AT present measurements of the boosted $H \to \tau\tau$ ($p_T > 250$ GeV) using 138 fb^{-1} of pp collision data at $E_{\rm cm} = 13$ TeV. The quoted signal strength corresponds to a significance of 3.5 standard deviations. The fiducial inclusive production cross section is measured to be $3.88^{+1.69}_{-1.35}$ fb. The differential fiducial cross sections as a function of Higgs boson and leading jet p_T are given in their Fig. 3.

[9] TUMASYAN 23Y measure Higgs production with $pp \to H \to \tau\tau$ at $E_{\rm cm} = 13$ TeV with 138 fb^{-1} data. The quoted results are given for $m_H = 125.38$ GeV.

[10] The inclusive $\sigma{\cdot}B$ is 2800^{+356}_{-335} fb (see their Figs. 10 and 14). See their Fig. 15 for the 68 % and 95 % CL contours in the $\kappa_V - \kappa_F$ plane.

[11] The quoted result is for the stage-0 simplified template cross section (STXS) and the $\sigma_{ggF} \cdot B$ is 2030^{+598}_{-555} fb (see their Figs. 10 and 14). Measured cross sections and ratios to the SM predictions in the reduced stage-1.2 STXS (see their Fig. 1) are shown in their Table 9 and Figs. 12 and 14.

[12] The quoted result is for the stage-0 STXS and the $\sigma_{VBF} \cdot B$ is $267^{+53.9}_{-52.6}$ fb (see their Figs. 10 and 14). Measured cross sections and ratios to the SM predictions in the reduced stage-1.2 STXS (see their Fig. 2) are shown in their Table 9 and Figs. 12, 14.

[13] The quoted result is for the stage-0 STXS and the $\sigma_{VH} \cdot B$ is $79.0^{+20.5}_{-18.6}$ fb (see their Figs. 10 and 14). Measured cross sections and ratios to the SM predictions in the reduced stage-1.2 STXS (see their Fig. 3) are shown in their Table 9 and Figs. 12, 14.

[14] AAD 22Q measure cross sections of $pp \to H \to \tau\tau$ at $E_{\rm cm} = 13$ TeV with 139 fb^{-1} data. The quoted results are given for $m_H = 125.09$ GeV and $|y(H)| < 2.5$ is required. The inclusive fiducial $\sigma \cdot B$ is $2.94 \pm 0.21^{+0.37}_{-0.32}$ pb. The fiducial $\sigma \cdot B$ for the four dominant production modes are $2.65 \pm 0.41^{+0.91}_{-0.67}$ pb for ggF, $0.197 \pm 0.028^{+0.032}_{-0.026}$ pb for VBF, $0.115 \pm 0.058^{+0.042}_{-0.040}$ pb for VH, $0.033 \pm 0.031^{+0.022}_{-0.017}$ pb for $t\bar{t}H$. The cross sections using simplified template cross section framework (STXS) are given in their Fig. 14(a) and Table 15. The STXS bins (a reduced stage 1.2) are defined in their Fig. 1.

[15] TUMASYAN 22AJ measure cross sections with $pp \to H \to \tau\tau$ at $E_{\rm cm} = 13$ TeV with 138 fb^{-1} data. The fiducial inclusive $\sigma{\cdot}B$ is 426 ± 102 fb while 408 ± 27 fb is expected

in the Standard Mode for $m_H = 125.38$ GeV. Three differential cross sections are given; see their Fig. 1.

[16] SIRUNYAN 19AF use 35.9 fb^{-1} of data. The quoted signal strength is given for $m_H =$ 125 GeV and corresponds to 2.3 standard deviations.

[17] SIRUNYAN 19AF use 35.9 fb^{-1} of data. HW/Z channels are added with a few updates on gluon fusion and vector boson fusion with respect to SIRUNYAN 18Y. The quoted signal strength is given for $m_H = 125$ GeV and corresponds to 5.5 standard deviations. The signal strengths for the individual production modes are: $1.12^{+0.53}_{-0.50}$ for gluon fusion, $1.13^{+0.45}_{-0.42}$ for vector boson fusion, $3.39^{+1.68}_{-1.54}$ for WH and $1.23^{+1.62}_{-1.35}$ for ZH. See their Fig. 7 for other couplings (κ_V, κ_f).

[18] SIRUNYAN 19AT perform a combine fit to 35.9 fb^{-1} of data at $E_{cm} = 13$ TeV. This combination is based on SIRUNYAN 18Y.

[19] SIRUNYAN 18Y use 35.9 fb^{-1} of pp collisions at $E_{cm} = 13$ TeV. The quoted signal strength is given for $m_H = 125.09$ GeV and corresponds to 4.9 standard deviations.

[20] SIRUNYAN 18Y combine the result of 35.9 fb^{-1} at $E_{cm} = 13$ TeV with the results obtained from data of 4.9 fb^{-1} at $E_{cm} = 7$ TeV and 19.7 fb^{-1} at $E_{cm} = 8$ TeV (KHACHATRYAN 15AM). The quoted signal strength is given for $m_H = 125.09$ GeV and corresponds to 5.9 standard deviations.

[21] AAD 16AC measure the signal strength with $pp \to HW/ZX$ processes using 20.3 fb^{-1} of $E_{cm} = 8$ TeV. The quoted signal strength is given for $m_H = 125$ GeV.

[22] AAD 16K use up to 4.7 fb^{-1} of pp collisions at $E_{cm} = 7$ TeV and up to 20.3 fb^{-1} at $E_{cm} = 8$ TeV. The quoted signal strength is given for $m_H = 125.36$ GeV.

[23] AAD 15AH use 4.5 fb^{-1} of pp collisions at $E_{cm} = 7$ TeV and 20.3 fb^{-1} at $E_{cm} = 8$ TeV. The third uncertainty in the measurement is theory systematics. The signal strength for the gluon fusion mode is $2.0 \pm 0.8^{+1.2}_{-0.8} \pm 0.3$ and that for vector boson fusion and W/ZH production modes is $1.24^{+0.49}_{-0.45}{}^{+0.31}_{-0.29} \pm 0.08$. The quoted signal strength is given for $m_H = 125.36$ GeV.

[24] CHATRCHYAN 14K use 4.9 fb^{-1} of pp collisions at $E_{cm} = 7$ TeV and 19.7 fb^{-1} at $E_{cm} = 8$ TeV. The quoted signal strength is given for $m_H = 125$ GeV. See also CHATRCHYAN 14AJ.

[25] AALTONEN 13L combine all CDF results with 9.45–10.0 fb^{-1} of $p\overline{p}$ collisions at $E_{cm} = 1.96$ TeV. The quoted signal strength is given for $m_H = 125$ GeV.

[26] ABAZOV 13L combine all D0 results with up to 9.7 fb^{-1} of $p\overline{p}$ collisions at $E_{cm} = 1.96$ TeV. The quoted signal strength is given for $m_H = 125$ GeV.

[27] AAD 12AI obtain results based on 4.7 fb^{-1} of pp collisions at $E_{cm} = 7$ TeV. The quoted signal strengths are given in their Fig. 10 for $m_H = 126$ GeV. See also Fig. 13 of AAD 12DA.

[28] CHATRCHYAN 12N obtain results based on 4.9 fb^{-1} of pp collisions at E_{cm}=7 TeV and 5.1 fb^{-1} at E_{cm}=8 TeV. The quoted signal strength is given for m_H=125.5 GeV. See also CHATRCHYAN 13Y .

$Z\gamma$ final state

VALUE	CL%	DOCUMENT ID		TECN	COMMENT
2.2 ±0.7		[1] AAD	24D	LHC	pp, 13 TeV
• • • We do not use the following data for averages, fits, limits, etc. • • •					
2.4 ±0.9		[2] TUMASYAN	23F	CMS	pp, 13 TeV
$2.59^{+1.07}_{-0.96}$		[3] CMS	22	CMS	pp, 13 TeV
< 3.6	95	[4] AAD	20AG	ATLS	pp, 13 TeV
< 7.4	95	[5] SIRUNYAN	18DQ	CMS	pp, 13 TeV
< 6.6	95	[6] AABOUD	17AW	ATLS	pp, 13 TeV
<11	95	[7] AAD	14J	ATLS	pp, 7, 8 TeV
< 9.5	95	[8] CHATRCHYAN	13BK	CMS	pp, 7, 8 TeV

[1] AAD 24D report combined results of ATLAS (AAD 20AG) and CMS (TUMASYAN 23F). The reported signal strength corresponds to a significance of 3.4 σ.

[2] TUMASYAN 23F search for $H \to Z\gamma$, $Z \to ee$, $\mu\mu$ in 138 fb^{-1} of pp collisions at $E_{cm} = 13$ TeV, assuming $m_H = 125.38$ GeV. $\sigma(pp \to H)\cdot B(H \to Z\gamma)$ is measured to be 0.21 ± 0.08 pb. The ratio of branching fractions $B(H \to Z\gamma)/B(H \to \gamma\gamma)$ is measured to be $1.5^{+0.7}_{-0.6}$.

[3] CMS 22 report combined results (see their Extended Data Table 2) using up to 138 fb^{-1} of data at $E_{cm} = 13$ TeV, assuming $m_H = 125.38$ GeV. See their Fig. 2 right.

[4] AAD 20AG search for $H \to Z\gamma$, $Z \to ee$, $\mu\mu$ in 139 fb^{-1} of pp collisions at $E_{cm} = 13$ TeV. The signal strength is $2.0 \pm 0.9^{+0.4}_{-0.3}$ at $m_H = 125.09$ GeV, which corresponds to a significance of 2.2 σ. The upper limit of $\sigma(pp \to H)\cdot B(H \to Z\gamma)$ is 305 fb at 95% CL.

[5] SIRUNYAN 18DQ search for $H \to Z\gamma$, $Z \to ee$, $\mu\mu$ in 35.9 fb^{-1} of pp collisions at $E_{cm} = 13$ TeV. The quoted signal strength (see their Figs. 6 and 7) is given for $m_H = 125$ GeV.

[6] AABOUD 17AW search for $H \to Z\gamma$, $Z \to ee$, $\mu\mu$ in 36.1 fb^{-1} of pp collisions at $E_{cm} = 13$ TeV. The quoted signal strength is given for $m_H = 125.09$ GeV. The upper limit on the branching ratio of $H \to Z\gamma$ is 1.0% at 95% CL assuming the SM Higgs boson production.

[7] AAD 14J search for $H \to Z\gamma \to \ell\ell\gamma$ in 4.5 fb^{-1} of pp collisions at $E_{cm} = 7$ TeV and 20.3 fb^{-1} at $E_{cm} = 8$ TeV. The quoted signal strength is given for $m_H = 125.5$ GeV.

[8] CHATRCHYAN 13BK search for $H \to Z\gamma \to \ell\ell\gamma$ in 5.0 fb^{-1} of pp collisions at $E_{cm} = 7$ TeV and 19.6 fb^{-1} at $E_{cm} = 8$ TeV. A limit on cross section times branching ratio which corresponds to (4–25) times the expected Standard Model cross section is given in the range $m_H = 120$–160 GeV at 95% CL. The quoted limit is given for $m_H = 125$ GeV, where 10 is expected for no signal.

$\gamma^*\gamma$ final state

VALUE	CL%	DOCUMENT ID		TECN	COMMENT
$1.5 \pm 0.5^{+0.2}_{-0.1}$		[1] AAD	21I	ATLS	pp, 13 TeV, $H \to \ell\ell\gamma$, 139 fb^{-1}
• • • We do not use the following data for averages, fits, limits, etc. • • •					
<4.0	95	[2] SIRUNYAN	18DQ	CMS	$pp \to HX$, 13 TeV, $H \to \gamma^*\gamma$
<6.7	95	[3] KHACHATRY...16B		CMS	pp, 8 TeV, $ee\gamma$, $\mu\mu\gamma$

[1] AAD 21I search for $H \to \ell\ell\gamma$ ($\ell = e$, μ) in 139 fb^{-1} of pp collisions at $E_{cm} = 13$ TeV. The mass of dilepton $m_{\ell\ell}$ is smaller than 30 GeV. This region is dominated by the decay through γ^*. The quoted signal strength corresponds to a significance of 3.2 standard deviations and is given for $m_H = 125.09$ GeV. The cross section times the branching ratio of $H \to \ell\ell\gamma$ for $m_{\ell\ell} < 30$ GeV is measured to be $8.7 \pm 2.7^{+0.7}_{-0.6}$ fb.

[2] SIRUNYAN 18DQ search for $H \to \gamma^*\gamma$, $\gamma^* \to \mu\mu$ in 35.9 fb^{-1} of pp collisions at $E_{cm} = 13$ TeV. The mass of γ^* is smaller than 50 GeV except in J/ψ and Υ mass regions. The quoted signal strength (see their Figs. 6 and 7) is given for $m_H = 125$ GeV.

[3] KHACHATRYAN 16B search for $H \to \gamma^*\gamma \to e^+e^-\gamma$ and $\mu^+\mu^-\gamma$ (with $m(e^+e^-) < 3.5$ GeV and $m(\mu^+\mu^-) < 20$ GeV) in 19.7 fb^{-1} of pp collisions at $E_{cm} = 8$ TeV. See their Fig. 6 for limits on individual channels.

HIGGS COUPLINGS

Fermion coupling (κ_F)

VALUE	DOCUMENT ID		TECN	COMMENT
0.94 ±0.05 OUR AVERAGE				
$0.86\ ^{+0.14}_{-0.11}$	[1] TUMASYAN	23W	CMS	pp, 13 TeV, $H \to WW^*$
0.95 ±0.05	[2] ATLAS	22	ATLS	pp, 13 TeV
• • • We do not use the following data for averages, fits, limits, etc. • • •				
$1.00\ ^{+0.16}_{-0.13}$	[3] AAD	23Y	ATLS	pp, 13 TeV, $H \to \gamma\gamma$
0.906	[4] CMS	22	CMS	pp, 13 TeV

[1] TUMASYAN 23W measure Higgs production rates with $H \to WW^*$ at $E_{\text{cm}} = 13$ TeV with 138 fb^{-1} data, assuming $m_H = 125.38$ GeV. See their Fig. 25 for the 68% and 95% CL contours in the $\kappa_V - \kappa_f$ plane.

[2] ATLAS 22 report combined results (see their Extended Data Table 1) using up to 139 fb^{-1} of data at $E_{\text{cm}} = 13$ TeV, assuming $m_H = 125.09$ GeV, $\kappa_V \geq 0$, and $\kappa_F \geq 0$ ($B_{inv} = B_{undetected} = 0$). See their Fig. 4.

[3] AAD 23Y measure Higgs production rates with $H \to \gamma\gamma$ at $E_{\text{cm}} = 13$ TeV with 139 fb^{-1} data, assuming $m_H = 125.09$ GeV. See their Fig. 23 for the 68% and 95% CL contours in the $\kappa_V - \kappa_F$ plane, where $\kappa_F > 0$ is assumed.

[4] CMS 22 report combined results (see their Extended Data Table 2) using up to 138 fb^{-1} of data at $E_{\text{cm}} = 13$ TeV, assuming $m_H = 125.38$ GeV. No uncertainty is given while their Fig. 3 left shows 68% and 95% CL contours.

Gauge boson coupling (κ_V)

VALUE	CL%	DOCUMENT ID		TECN	COMMENT
1.023±0.026 OUR AVERAGE					
0.99 ±0.05		[1] TUMASYAN	23W	CMS	13 TeV, $H \to WW^*$
1.035±0.031		[2] ATLAS	22	ATLS	pp, 13 TeV
• • • We do not use the following data for averages, fits, limits, etc. • • •					
−3.7 to 3.8	95	[3] HAYRAPETY...24AW		CMS	13 TeV, VHH, $HH \to b\bar{b}b\bar{b}$
$1.02\ ^{+0.06}_{-0.05}$		[4] AAD	23Y	ATLS	13 TeV, $H \to \gamma\gamma$
1.014		[5] CMS	22	CMS	pp, 13 TeV

[1] TUMASYAN 23W measure Higgs production rates with $H \to WW^*$ at $E_{\text{cm}} = 13$ TeV with 138 fb^{-1} data, assuming $m_H = 125.38$ GeV. See their Fig. 25 for the 68% and 95% CL contours in the $\kappa_V - \kappa_f$ plane.

[2] ATLAS 22 report combined results (see their Extended Data Table 1) using up to 139 fb^{-1} of data at $E_{\text{cm}} = 13$ TeV, assuming $m_H = 125.09$ GeV, $\kappa_V \geq 0$, and $\kappa_F \geq 0$ ($B_{inv} = B_{undetected} = 0$). See their Fig. 4.

[3] HAYRAPETYAN 24AW search for non-resonant HH production in association with a vector boson using $HH \to b\bar{b}b\bar{b}$ with data of 138 fb^{-1} at $E_{\text{cm}} = 13$ TeV. The vector boson decays both leptonically ($W \to \ell\nu$, $Z \to \ell\ell$, $\nu\nu$, $\ell = e,\ \mu$) and hadronically. See their Fig. 19. All other Higgs couplings are fixed to the SM values.

[4] AAD 23Y measure Higgs production rates with $H \to \gamma\gamma$ at $E_{\text{cm}} = 13$ TeV with 139 fb^{-1} data, assuming $m_H = 125.09$ GeV. See their Fig. 23 for the 68% and 95% CL contours in the $\kappa_V - \kappa_F$ plane, where $\kappa_F > 0$ is assumed.

[5] CMS 22 report combined results (see their Extended Data Table 2) using up to 138 fb^{-1} of data at $E_{\text{cm}} = 13$ TeV, assuming $m_H = 125.38$ GeV. See their Fig. 3 left.

W boson coupling (κ_W)

VALUE	DOCUMENT ID		TECN	COMMENT
• • • We do not use the following data for averages, fits, limits, etc. • • •				
	[1] HAYRAPETY...25B		CMS	pp, 13 TeV, VBF WH, coupling sign
	[2] AAD	24BM	ATLS	pp, 13 TeV, VBF WH, coupling sign
1.02 ± 0.05	[3,4] ATLAS	22	ATLS	pp, 13 TeV
1.05 ± 0.06	[3,5] ATLAS	22	ATLS	pp, 13 TeV
$1.00^{+0.00}_{-0.02}$	[3,6] ATLAS	22	ATLS	pp, 13 TeV
1.06 ± 0.07	[7,8] CMS	22	CMS	pp, 13 TeV
1.02 ± 0.08	[7,9] CMS	22	CMS	pp, 13 TeV

[1] HAYRAPETYAN 25B present the determination of the relative sign of κ_W and κ_Z with VBF WH, $H \to b\overline{b}$ using 138 fb^{-1} of data at $E_{\text{cm}} = 13$ TeV. The opposite-sign coupling hypothesis is excluded with a significance beyond 5σ.

[2] AAD 24BM present the determination of the relative sign of κ_W and κ_Z with VBF WH, $H \to b\overline{b}$ using 140 fb^{-1} of data at $E_{\text{cm}} = 13$ TeV. The opposite-sign coupling hypothesis is excluded with a significance beyond 5σ.

[3] ATLAS 22 report combined results (see their Extended Data Table 1) using up to 139 fb^{-1} of data at $E_{\text{cm}} = 13$ TeV, assuming $m_H = 125.09$ GeV.

[4] All modifiers(κ) > 0, and $\kappa_c = \kappa_t$ ($B_{inv} = B_{undetected} = 0$) are assumed. Only SM particles assume to contribute to the loop-induced processes.See their Fig. 5, which shows both $\kappa_c = \kappa_t$ andκ_c floating.

[5] $B_{inv} = B_{undetected} = 0$ is assumed. Coupling strength modifiers including effective photon, $Z\gamma$ and gluon are measured. See their Fig. 6.

[6] B_{inv} floating, $B_{undetected} \geq 0$, and $\kappa_V \leq 1$ are assumed. Coupling strength modifiers including effective photon, $Z\gamma$ and gluon are measured. See their Fig. 6.

[7] CMS 22 report combined results (see their Extended Data Table 2) using up to 138 fb^{-1} of data at $E_{\text{cm}} = 13$ TeV, assuming $m_H = 125.38$ GeV.

[8] Only SM particles assume to contribute to the loop-induced processes. See their Fig. 3 right.

[9] Coupling strength modifiers including effective photon, $Z\gamma$ and gluon are measured. See their Fig. 4 left.

Z boson coupling (κ_Z)

VALUE	DOCUMENT ID		TECN	COMMENT
• • • We do not use the following data for averages, fits, limits, etc. • • •				
	[1] HAYRAPETY...25B		CMS	pp, 13 TeV, VBF WH, coupling sign
	[2] AAD	24BM	ATLS	pp, 13 TeV, VBF WH, coupling sign
$0.99^{+0.06}_{-0.05}$	[3,4] ATLAS	22	ATLS	pp, 13 TeV
0.99 ± 0.06	[3,5] ATLAS	22	ATLS	pp, 13 TeV
$0.98^{+0.02}_{-0.05}$	[3,6] ATLAS	22	ATLS	pp, 13 TeV
1.04 ± 0.07	[7,8] CMS	22	CMS	pp, 13 TeV
1.04 ± 0.07	[7,9] CMS	22	CMS	pp, 13 TeV

[1] HAYRAPETYAN 25B present the determination of the relative sign of κ_W and κ_Z with VBF WH, $H \to b\overline{b}$ using 138 fb^{-1} of data at $E_{\text{cm}} = 13$ TeV. The opposite-sign coupling hypothesis is excluded with a significance beyond 5σ.

[2] AAD 24BM present the determination of the relative sign of κ_W and κ_Z with VBF WH, $H \to b\overline{b}$ using 140 fb^{-1} of data at $E_{\text{cm}} = 13$ TeV. The opposite-sign coupling hypothesis is excluded with a significance beyond 5σ.

[3] ATLAS 22 report combined results (see their Extended Data Table 1) using up to 139 fb^{-1} of data at $E_{cm} = 13$ TeV, assuming $m_H = 125.09$ GeV.

[4] All modifiers(κ) > 0, and $\kappa_c = \kappa_t$ ($B_{inv} = B_{undetected} = 0$) are assumed. Only SM particles assume to contribute to the loop-induced processes.See their Fig. 5, which shows both $\kappa_c = \kappa_t$ andκ_c floating.

[5] $B_{inv} = B_{undetected} = 0$ is assumed. Coupling strength modifiers including effective photon, $Z\gamma$ and gluon are measured. See their Fig. 6.

[6] B_{inv} floating, $B_{undetected} \geq 0$, and $\kappa_V \leq 1$ are assumed. Coupling strength modifiers including effective photon, $Z\gamma$ and gluon are measured. See their Fig. 6.

[7] CMS 22 report combined results (see their Extended Data Table 2) using up to 138 fb^{-1} of data at $E_{cm} = 13$ TeV, assuming $m_H = 125.38$ GeV.

[8] Only SM particles assume to contribute to the loop-induced processes. See their Fig. 3 right.

[9] Coupling strength modifiers including effective photon, $Z\gamma$ and gluon are measured. See their Fig. 4 left.

top Yukawa coupling (κ_t)

VALUE	CL%	DOCUMENT ID		TECN	COMMENT
• • • We do not use the following data for averages, fits, limits, etc. • • •					
		[1] HAYRAPETY...25R		CMS	$t\bar{t}H$, tH, $H \to b\bar{b}$, 13 TeV
$0.84^{+0.30}_{-0.46}$		[2] AAD	24J	ATLS	$t\bar{t}H$, tH, $H \to b\bar{b}$, 13 TeV
<1.9	95	[3] AAD	23BC	ATLS	pp, 13 TeV
0.87–1.20	95	[4] AAD	23Y	ATLS	pp, 13 TeV
0.65–1.25	95	[5] AAD	23Y	ATLS	pp, 13 TeV
-1.09– $-$ 0.74 or 0.77–1.3	95	[6] TUMASYAN	23P	CMS	pp, 13 TeV
0.86–1.26		[6,7] TUMASYAN	23P	CMS	pp, 13 TeV
0.95 ± 0.07		[8,9] ATLAS	22	ATLS	pp, 13 TeV
0.94 ± 0.11		[8,10] ATLAS	22	ATLS	pp, 13 TeV
0.94 ± 0.11		[8,11] ATLAS	22	ATLS	pp, 13 TeV
$0.95^{+0.07}_{-0.08}$		[12,13] CMS	22	CMS	pp, 13 TeV
$1.01^{+0.11}_{-0.10}$		[12,14] CMS	22	CMS	pp, 13 TeV
-0.9– $-$ 0.7 or 0.7–1.1	95	[15] SIRUNYAN	21R	CMS	pp, 13 TeV
<1.7	95	[16] SIRUNYAN	20C	CMS	pp, 13 TeV
<1.67	95	[17] SIRUNYAN	19BY	CMS	pp, 13 TeV
<2.1	95	[18] SIRUNYAN	18BU	CMS	pp, 13 TeV

[1] HAYRAPETYAN 25R measure the $t\bar{t}H$ and tH productions with $H \to b\bar{b}$ decay channel using 138 fb^{-1} of data at $E_{cm} = 13$ TeV. Two-dimensional likelihood scan of (κ_t, κ_V) is shown in their Fig. 15. Assuming $\kappa_V = 1$, κ_t is measured to be [-0.55, -0.24] and [0.20, 0.72] at 68% CL.

[2] AAD 24J measure the *CP* structure of the top Yukawa coupling using 139 fb^{-1} of data at $E_{cm} = 13$ TeV. The top Yukawa coupling strength modifier κ_t is measured with the *CP*-mixing angle α. See their Fig. 3.

[3] AAD 23BC measure the production of four top quarks with same-sign and multilepton final states with 140 fb^{-1} pp collision data at $E_{cm} = 13$ TeV. The results constraint the ratio of the top quark Yukawa coupling y_t to its Standard Model value, yielding $|y_t/y_t^{SM}| < 1.9$ (see their erratum) at 95% CL. See their Fig. 8 as a function of κ_t and *CP*-mixing angle.

[4] AAD 23Y constrain κ_t from Higgs production rates with $H \to \gamma\gamma$ with 139 fb^{-1} pp collision data at $E_{\rm cm} = 13$ TeV. The quoted result is obtained assuming the SM loop structure in $gg \to H$ and $H \to \gamma\gamma$. See their Fig. 14.

[5] AAD 23Y constrain κ_t from Higgs production rates with $H \to \gamma\gamma$ with 139 fb^{-1} pp collision data at $E_{\rm cm} = 13$ TeV. The quoted result is obtained assuming effective couplings κ_{gluon} and κ_γ for $gg \to H$ and $H \to \gamma\gamma$, respectively. See their Fig. 14.

[6] TUMASYAN 23P constrain κ_t from $t\bar{t}H$ and tH decaying $H \to WW^*$ and $H \to \tau\tau$ (multilepton decay mode) with 138 fb^{-1} pp collision data at $E_{\rm cm} = 13$ TeV. The κ_t is obtained by fixing $\widetilde{\kappa}_t = 0$ and other couplings (κ_V etc.) to the SM values. See their Fig. 9 for 2-dim contours and Table 6.

[7] The quoted result is obtained by combining with other $t\bar{t}H$ decaying $H \to \gamma\gamma$ (SIRUNYAN 20AS) and $H \to 4\ell$ (SIRUNYAN 21AE) and $\widetilde{\kappa}_t = 0$. See their Fig. 12 for 2-dim contours and Table 7.

[8] ATLAS 22 report combined results (see their Extended Data Table 1) using up to 139 fb^{-1} of data at $E_{\rm cm} = 13$ TeV, assuming $m_H = 125.09$ GeV.

[9] All modifiers(κ) > 0, and $\kappa_c = \kappa_t$ (B_{inv} =$B_{undetected} = 0$) are assumed. Only SM particles assume to contribute to the loop-induced processes.See their Fig. 5, which shows both $\kappa_c = \kappa_t$ andκ_c floating.

[10] $B_{inv} = B_{undetected} = 0$ is assumed. Coupling strength modifiers including effective photon, $Z\gamma$ and gluon are measured. See their Fig. 6.

[11] B_{inv} floating, $B_{undetected} \geq 0$, and $\kappa_V \leq 1$ are assumed. Coupling strength modifiers including effective photon, $Z\gamma$ and gluon are measured. See their Fig. 6.

[12] CMS 22 report combined results (see their Extended Data Table 2) using up to 138 fb^{-1} of data at $E_{\rm cm} = 13$ TeV, assuming $m_H = 125.38$ GeV.

[13] Only SM particles assume to contribute to the loop-induced processes. See their Fig. 3 right.

[14] Coupling strength modifiers including effective photon, $Z\gamma$ and gluon are measured. See their Fig. 4 left.

[15] SIRUNYAN 21R constrain the ratio of the top quark Yukawa coupling y_t to its Standard Model value from $t\bar{t}H$ and tH production rates using 137 fb^{-1} pp collision data at $E_{\rm cm} = 13$ TeV. Assuming a SM Higgs couplings to τ's, the joint interval $-0.9 < \kappa_t(=y_t/y_t^{SM}) < -0.7$ and $0.7 < \kappa_t < 1.1$ is obtained at 95% CL (see their Fig. 17).

[16] SIRUNYAN 20C search for the production of four top quarks with same-sign and multilepton final states with 137 fb^{-1} pp collision data at $E_{\rm cm} = 13$ TeV. The results constraint the ratio of the top quark Yukawa coupling y_t to its Standard Model value by comparing to the central value of a theoretical prediction (see their Refs. [1-2]), yielding $|y_t/y_t^{SM}| < 1.7$ at 95% CL. See their Fig. 5.

[17] SIRUNYAN 19BY measure the top quark Yukawa coupling from $t\bar{t}$ kinematic distributions, the invariant mass of the top quark pair and the rapidity difference between t and $\bar{t}$, in the ℓ+jets final state with 35.8 fb^{-1} pp collision data at $E_{\rm cm} = 13$ TeV. The results constraint the ratio of the top quark Yukawa coupling to its the Standard Model to be $1.07^{+0.34}_{-0.43}$ with an upper limit of 1.67 at 95% CL (see their Table III).

[18] SIRUNYAN 18BU search for the production of four top quarks with same-sign and multilepton final states with 35.9 fb^{-1} pp collision data at $E_{\rm cm} = 13$ TeV. The results constraint the ratio of the top quark Yukawa coupling y_t to its the Standard Model by comparing to the central value of a theoretical prediction (see their Ref. [16]), yielding $|y_t/y_t^{SM}| < 2.1$ at 95% CL.

bottom quark Yukawa coupling (κ_b)

VALUE	CL%	DOCUMENT ID		TECN	COMMENT
• • • We do not use the following data for averages, fits, limits, etc. • • •					
$0.65 < \lvert\kappa_b\rvert < 1.37$	95	[1] AAD	25Y	ATLS	$pp \to VH$, $H \to b\overline{b}$, 13 TeV
-1.09 to -0.86 OR 0.81 to 1.09	95	[2] AAD	23C	ATLS	pp, 13 TeV, $\gamma\gamma$, $ZZ^* \to 4\ell$ cross sections
		[3] AAD	23CD	ATLS	pp, 13 TeV, $H \to \Upsilon(\text{nS})\gamma$
-1.1 to 1.1	95	[4] HAYRAPETY...23		CMS	pp, 13 TeV, $ZZ^* \to 4\ell$ cross sections
0.90 ± 0.11		[5,6] ATLAS	22	ATLS	pp, 13 TeV
0.89 ± 0.11		[5,7] ATLAS	22	ATLS	pp, 13 TeV
$0.82^{+0.09}_{-0.08}$		[5,8] ATLAS	22	ATLS	pp, 13 TeV
$1.02^{+0.15}_{-0.17}$		[9,10] CMS	22	CMS	pp, 13 TeV
$0.99^{+0.17}_{-0.16}$		[9,11] CMS	22	CMS	pp, 13 TeV

[1] AAD 25Y present measurements of VH, $H \to b\overline{b}$ and $H \to c\overline{c}$ ($V = W,\ Z$) using 140 fb^{-1} of pp collision data at $E_{\text{cm}} = 13$ TeV. The quoted value is obtained assuming $\kappa_c = 1$, all other couplings to their SM predictions, and only SM decays.

[2] AAD 23C combine results of $H \to \gamma\gamma$ and $H \to ZZ^* \to 4\ell$ ($\ell = e,\ \mu$) using 139 fb^{-1} at $E_{\text{cm}} = 13$ TeV. The Higgs boson transverse momentum (p_T^H) distribution constrains κ_b and κ_c, assuming other couplings fixed to the SM values. The κ_b is obtained using the p_T^H shape and normalisation. Other cases are given in their Tables 6 and 7.

[3] AAD 23CD search for $H \to \Upsilon(\text{nS})\gamma$, $\Upsilon(\text{nS}) \to \mu^+\mu^-$ (n=1,2,3) with 138 fb^{-1} of pp collision data at $E_{\text{cm}} = 13$ TeV. They interpret the $H \to \Upsilon(\text{nS})\gamma$ search to constraint the bottom Yukawa coupling by comparing to $H \to \gamma\gamma$. An observed 95% CL interval of (-37, 40) is obtained for κ_b/κ_γ.

[4] HAYRAPETYAN 23 measure the cross sections for $pp \to H \to ZZ^* \to 4\ell$ ($\ell = e,\ \mu$) using 138 fb^{-1} at $E_{\text{cm}} = 13$ TeV. The κ_b is obtained from the p_T differential cross section of the ggF production employing the dependence of the branching fraction on κ_b and κ_c.

[5] ATLAS 22 report combined results (see their Extended Data Table 1) using up to 139fb^{-1} of data at $E_{\text{cm}} = 13$ TeV, assuming $m_H = 125.09$ GeV.

[6] All modifiers (κ) > 0, and $\kappa_c = \kappa_t$ ($B_{inv} = B_{undetected} = 0$) are assumed. Only SM particles assume to contribute to the loop-induced processes. See their Fig. 5, which shows both $\kappa_c = \kappa_t$ and κ_c floating.

[7] $B_{inv} = B_{undetected} = 0$ is assumed. Coupling strength modifiers including effective photon, $Z\gamma$ and gluon are measured. See their Fig. 6.

[8] B_{inv} floating, $B_{undetected} \geq 0$, and $\kappa_V \leq 1$ are assumed. Coupling strength modifiers including effective photon, $Z\gamma$ and gluon are measured. See their Fig. 6.

[9] CMS 22 report combined results (see their Extended Data Table 2) using up to 138 fb^{-1} of data at $E_{\text{cm}} = 13$ TeV, assuming $m_H = 125.38$ GeV.

[10] Only SM particles assume to contribute to the loop-induced processes. See their Fig. 3 right.

[11] Coupling strength modifiers including effective photon, $Z\gamma$ and gluon are measured. See their Fig. 4 left.

charm quark Yukawa coupling (κ_c)

VALUE	CL%	DOCUMENT ID		TECN	COMMENT
• • • We do not use the following data for averages, fits, limits, etc. • • •					
$\lvert\kappa_c\rvert < 3.5$	95	[1] HAYRAPETY...26		CMS	pp, $t\bar{t}H$, $H \to c\bar{c}$, 13 TeV
$\lvert\kappa_c\rvert < 4.2$	95	[2] AAD	25Y	ATLS	$pp \to VH$, 13 TeV
$0.0\ ^{+2.3}_{-2.8}$		[3] CHEKHOVSKY	25G	CMS	pp, 13 TeV, $H\gamma$, $H \to ZZ^* \to 4\ell$
$\lvert\kappa_c\rvert < 38.1$	95	[4] CHEKHOVSKY	25L	CMS	pp, 13 TeV, $H \to \gamma\gamma$
-166 to 208	95	[5] HAYRAPETY...25H		CMS	pp, 13 TeV, $H \to J/\psi\gamma$
$\lvert\kappa_c\rvert < 190$	95	[6] HAYRAPETY...24D		CMS	pp, 13 TeV, $H\gamma$, $H \to WW^* \to e\nu\mu\nu$
$\lvert\kappa_c\rvert < 2.27$	95	[7] AAD	23C	ATLS	pp, 13 TeV, $\gamma\gamma$, $ZZ^* \to 4\ell$ cross sections
		[8] AAD	23CD	ATLS	pp, 13 TeV, $H \to J/\psi\gamma$
$-$ 5.3 to 5.2	95	[9] HAYRAPETY...23		CMS	pp, 13 TeV, $ZZ^* \to 4\ell$ cross sections
$1.1 < \lvert\kappa_c\rvert < 5.5$	95	[10] TUMASYAN	23AH	CMS	$pp \to WH/ZH$, 13 TeV
$0.03^{+3.02}_{-0.03}$		[11] ATLAS	22	ATLS	pp, 13 TeV

[1] HAYRAPETYAN 26 search for $t\bar{t}H$, $H \to c\bar{c}$ together with the $t\bar{t}H$, $H \to b\bar{b}$ measurement using 138 fb^{-1} of pp collision data at $E_{\text{cm}} = 13$ TeV. The quoted value is obtained by combining with the VH channel and assuming $\kappa_b = 1$.

[2] AAD 25Y present measurements of VH, $H \to b\bar{b}$ and $H \to c\bar{c}$ ($V = W,\ Z$) using 140 fb^{-1} of pp collision data at $E_{\text{cm}} = 13$ TeV. The quoted value is obtained assuming $\kappa_b = 1$, all other couplings to their SM predictions, and only SM decays. The ratio of κ_b and κ_c is measured to be $\lvert\kappa_c/\kappa_b\rvert < 3.6$ at 95% CL.

[3] CHEKHOVSKY 25G search for the $H\gamma$ production with $H \to ZZ^* \to 4\ell$ ($\ell = e,\ \mu$) decay channel with data of 138 fb^{-1} at $E_{\text{cm}} = 13$ TeV. Coupling modifiers κ_u, κ_d, κ_s and κ_c are simultaneously obtained assuming the SM Yukawa couplings for the bottom and top quarks ($\kappa_b = 1$, $\kappa_t = 1$) and constraining the HVV couplings ($\kappa^2_{ZZ} \leq 1$, $\kappa^2_{WW} = \kappa^2_{ZZ}$). See their Tables III.

[4] CHEKHOVSKY 25L search for the production of a Higgs boson and one or more charm quarks (H+c) with $H \to \gamma\gamma$ using 138 fb^{-1} of data at $E_{\text{cm}} = 13$ TeV. The quoted value is obtained assuming the SM rates for all other Higgs production processes.

[5] HAYRAPETYAN 25H search for $H \to J/\psi\gamma$, $J/\psi \to \mu^+\mu^-$ with 123 fb^{-1} of pp collision data at $E_{\text{cm}} = 13$ TeV. They interpret the $H \to J/\psi\gamma$ search to constrain the charm Yukawa coupling by comparing to $H \to \gamma\gamma$. An observed 95% CL interval of (-157, 199) is obtained for κ_c/κ_γ. The quoted value is obtained assuming $\kappa_\gamma = 1$.

[6] HAYRAPETYAN 24D search for the $H\gamma$ production using $H \to WW^* \to e\nu\mu\nu$ with 138 fb^{-1} of pp collision data at $E_{\text{cm}} = 13$ TeV. They interpret the $H\gamma$ search to constraint the charm Yukawa coupling assuming that the charm quark and the Higgs interaction vertex shown in their Fig. 1 is the only parameter. See their Table II.

[7] AAD 23C combine results of $H \to \gamma\gamma$ and $H \to ZZ^* \to 4\ell$ ($\ell = e,\ \mu$) using 139 fb^{-1} at $E_{\text{cm}} = 13$ TeV. The Higgs boson transverse momentum (p^H_T) distribution constrains κ_b and κ_c, assuming other couplings fixed to the SM values. The κ_c is obtained using the p^H_T shape and normalisation. Other cases are given in their Tables 6 and 7. See their Table 8 for results combined with VH, $H \to b\bar{b}$ and $c\bar{c}$.

[8] AAD 23CD search for $H \to J/\psi\gamma$, $J/\psi \to \mu^+\mu^-$ with 138 fb^{-1} of pp collision data at $E_{\text{cm}} = 13$ TeV. They interpret the $H \to J/\psi\gamma$ search to constraint the charm Yukawa coupling by comparing to $H \to \gamma\gamma$. An observed 95% CL interval of (-133, 175) is obtained for κ_c/κ_γ.

[9] HAYRAPETYAN 23 measure the cross sections for $pp \to H \to ZZ^* \to 4\ell$ ($\ell = e$, μ) using 138 fb^{-1} at $E_{cm} = 13$ TeV. The κ_c is obtained from the p_T differential cross section of the ggF production employing the dependence of the branching fraction of κ_b and κ_c.

[10] TUMASYAN 23AH search for VH, $H \to c\overline{c}$ ($V = W, Z$) using 138 fb^{-1} of pp collision data at $E_{cm} = 13$ TeV. The quoted values are obtained from the measured signal strength in the κ-framework, where only the Higgs decay width for $H \to c\overline{c}$ is changed while assuming all the other decay widths and the production cross section to be SM ones. The quoted values are given for $m_H = 125.38$ GeV.

[11] ATLAS 22 report combined results (see their Extended Data Table 1) using up to 139 fb^{-1} of data at $E_{cm} = 13$ TeV, assuming $m_H = 125.09$ GeV, and all modifiers (κ) > 0 ($B_{inv} = B_{undetected} = 0$). Only SM particles assume to contribute to the loop-induced processes. See their Fig. 5, which shows both $\kappa_c = \kappa_t$ and κ_c floating.

strange quark Yukawa coupling (κ_s)

VALUE	CL%	DOCUMENT ID	TECN	COMMENT
• • • We do not use the following data for averages, fits, limits, etc. • • •				
0^{+30}_{-32}		[1] CHEKHOVSKY25G	CMS	pp, 13 TeV, $H\gamma$, $H \to ZZ^* \to 4\ell$
$\lvert\kappa_s\rvert < 1700$	95	[2] HAYRAPETY...24D	CMS	pp, 13 TeV, $H\gamma$, $H \to WW^* \to e\nu\mu\nu$

[1] CHEKHOVSKY 25G search for the $H\gamma$ production with $H \to ZZ^* \to 4\ell$ ($\ell = e$, μ) decay channel with data of 138 fb^{-1} at $E_{cm} = 13$ TeV. Coupling modifiers κ_u, κ_d, κ_s and κ_c are simultaneously obtained assuming the SM Yukawa couplings for the bottom and top quarks ($\kappa_b = 1$, $\kappa_t = 1$) and constraining the HVV couplings ($\kappa^2_{ZZ} \leq 1$, $\kappa^2_{WW} = \kappa^2_{ZZ}$). See their Tables III.

[2] HAYRAPETYAN 24D search for the $H\gamma$ production using $H \to WW^* \to e\nu\mu\nu$ with 138 fb^{-1} of pp collision data at $E_{cm} = 13$ TeV. They interpret the $H\gamma$ search to constraint the strange quark Yukawa coupling assuming that the strange quark and the Higgs interaction vertex shown in their Fig. 1 is the only parameter. See their Table II.

down quark Yukawa coupling (κ_d)

VALUE (units 10^2)	CL%	DOCUMENT ID	TECN	COMMENT
• • • We do not use the following data for averages, fits, limits, etc. • • •				
$0.0^{+6.7}_{-6.8}$		[1] CHEKHOVSKY25G	CMS	pp, 13 TeV, $H\gamma$, $H \to ZZ^* \to 4\ell$
-170 to 170	95	[2] HAYRAPETY...24D	CMS	pp, 13 TeV, $H\gamma$, $H \to WW^* \to e\nu\mu\nu$

[1] CHEKHOVSKY 25G search for the $H\gamma$ production with $H \to ZZ^* \to 4\ell$ ($\ell = e$, μ) decay channel with data of 138 fb^{-1} at $E_{cm} = 13$ TeV. Coupling modifiers κ_u, κ_d, κ_s and κ_c are simultaneously obtained assuming the SM Yukawa couplings for the bottom and top quarks ($\kappa_b = 1$, $\kappa_t = 1$) and constraining the HVV couplings ($\kappa^2_{ZZ} \leq 1$, $\kappa^2_{WW} = \kappa^2_{ZZ}$). See their Tables III.

[2] HAYRAPETYAN 24D search for the $H\gamma$ production using $H \to WW^* \to e\nu\mu\nu$ with 138 fb^{-1} of pp collision data at $E_{cm} = 13$ TeV. They interpret the $H\gamma$ search to constraint the down quark Yukawa coupling assuming that the down quark and the Higgs interaction vertex shown in their Fig. 1 is the only parameter. See their Table II.

up quark Yukawa coupling (κ_u)

VALUE (units 10^3)	*CL%*	*DOCUMENT ID*		*TECN*	*COMMENT*
• • • We do not use the following data for averages, fits, limits, etc. • • •					
0.0 ± 1.5		[1] CHEKHOVSKY 25G		CMS	pp, 13 TeV, $H\gamma$, $H \to ZZ^* \to 4\ell$
-16 to 16	95	[2] HAYRAPETY...24D		CMS	pp, 13 TeV, $H\gamma$, $H \to WW^* \to e\nu\mu\nu$

[1] CHEKHOVSKY 25G search for the $H\gamma$ production with $H \to ZZ^* \to 4\ell$ ($\ell = e, \mu$) decay channel with data of 138 fb^{-1} at $E_{\text{cm}} = 13$ TeV. Coupling modifiers κ_u, κ_d, κ_s and κ_c are simultaneously obtained assuming the SM Yukawa couplings for the bottom and top quarks ($\kappa_b = 1$, $\kappa_t = 1$) and constraining the HVV couplings ($\kappa^2_{ZZ} \leq 1$, $\kappa^2_{WW} = \kappa^2_{ZZ}$). See their Tables III.

[2] HAYRAPETYAN 24D search for the $H\gamma$ production using $H \to WW^* \to e\nu\mu\nu$ with 138 fb^{-1} of pp collision data at $E_{\text{cm}} = 13$ TeV. They interpret the $H\gamma$ search to constraint the up quark Yukawa coupling assuming that the up quark and the Higgs interaction vertex shown in their Fig. 1 is the only parameter. See their Table II.

tau Yukawa coupling (κ_τ)

VALUE	*DOCUMENT ID*		*TECN*	*COMMENT*
• • • We do not use the following data for averages, fits, limits, etc. • • •				
0.94 ± 0.07	[1,2] ATLAS	22	ATLS	pp, 13 TeV
0.93 ± 0.07	[1,3] ATLAS	22	ATLS	pp, 13 TeV
$0.91^{+0.07}_{-0.06}$	[1,4] ATLAS	22	ATLS	pp, 13 TeV
0.93 ± 0.08	[5,6] CMS	22	CMS	pp, 13 TeV
0.92 ± 0.08	[5,7] CMS	22	CMS	pp, 13 TeV

[1] ATLAS 22 report combined results (see their Extended Data Table 1) using up to 139 fb^{-1} of data at $E_{\text{cm}} = 13$ TeV, assuming $m_H = 125.09$ GeV.

[2] All modifiers(κ) > 0, and $\kappa_c = \kappa_t$ ($B_{inv} = B_{undetected} = 0$) are assumed. Only SM particles assume to contribute to the loop-induced processes.See their Fig. 5, which shows both $\kappa_c = \kappa_t$ andκ_c floating.

[3] $B_{inv} = B_{undetected} = 0$ is assumed. Coupling strength modifiers including effective photon, $Z\gamma$ and gluon are measured. See their Fig. 6.

[4] B_{inv} floating, $B_{undetected} \geq 0$, and $\kappa_V \leq 1$ are assumed. Coupling strength modifiers including effective photon, $Z\gamma$ and gluon are measured. See their Fig. 6.

[5] CMS 22 report combined results (see their Extended Data Table 2) using up to 138 fb^{-1} of data at $E_{\text{cm}} = 13$ TeV, assuming $m_H = 125.38$ GeV.

[6] Only SM particles assume to contribute to the loop-induced processes. See their Fig. 3 right.

[7] Coupling strength modifiers including effective photon, $Z\gamma$ and gluon are measured. See their Fig. 4 left.

muon Yukawa couping (κ_μ)

VALUE	*DOCUMENT ID*		*TECN*	*COMMENT*
• • • We do not use the following data for averages, fits, limits, etc. • • •				
$1.07^{+0.25}_{-0.31}$	[1,2] ATLAS	22	ATLS	pp, 13 TeV
$1.06^{+0.25}_{-0.30}$	[1,3] ATLAS	22	ATLS	pp, 13 TeV
$1.04^{+0.23}_{-0.30}$	[1,4] ATLAS	22	ATLS	pp, 13 TeV

1.12 ± 0.20	[5,6] CMS	22	CMS	pp, 13 TeV	
$1.12^{+0.21}_{-0.22}$	[5,7] CMS	22	CMS	pp, 13 TeV	

[1] ATLAS 22 report combined results (see their Extended Data Table 1) using up to 139 fb^{-1} of data at $E_{\text{cm}} = 13$ TeV, assuming $m_H = 125.09$ GeV.

[2] All modifiers(κ) > 0, and $\kappa_c = \kappa_t$ ($B_{inv} = B_{undetected} = 0$) are assumed. Only SM particles assume to contribute to the loop-induced processes.See their Fig. 5, which shows both $\kappa_c = \kappa_t$ andκ_c floating.

[3] $B_{inv} = B_{undetected} = 0$ is assumed. Coupling strength modifiers including effective photon, $Z\gamma$ and gluon are measured. See their Fig. 6.

[4] B_{inv} floating, $B_{undetected} \geq 0$, and $\kappa_V \leq 1$ are assumed. Coupling strength modifiers including effective photon, $Z\gamma$ and gluon are measured. See their Fig. 6.

[5] CMS 22 report combined results (see their Extended Data Table 2) using up to 138 fb^{-1} of data at $E_{\text{cm}} = 13$ TeV, assuming $m_H = 125.38$ GeV.

[6] Only SM particles assume to contribute to the loop-induced processes. See their Fig. 3 right.

[7] Coupling strength modifiers including effective photon, $Z\gamma$ and gluon are measured. See their Fig. 4 left.

photon effective coupling (κ_γ)

VALUE	DOCUMENT ID		TECN	COMMENT
• • • We do not use the following data for averages, fits, limits, etc. • • •				
$1.02^{+0.08}_{-0.07}$	[1] AAD	23Y	ATLS	pp, 13 TeV
1.01 ± 0.06	[2,3] ATLAS	22	ATLS	pp, 13 TeV
0.98 ± 0.05	[2,4] ATLAS	22	ATLS	pp, 13 TeV
1.10 ± 0.08	[5] CMS	22	CMS	pp, 13 TeV

[1] AAD 23Y constrain κ_γ from Higgs production rates with $H \to \gamma\gamma$ with 139 fb^{-1} pp collision data at $E_{\text{cm}} = 13$ TeV. The quoted result is obtained assuming effective couplings κ_{gluon} and κ_γ for $gg \to H$ and $H \to \gamma\gamma$, respectively and other couplings fixed to the SM values. See their Fig. 15.

[2] ATLAS 22 report combined results (see their Extended Data Table 1) using up to 139 fb^{-1} of data at $E_{\text{cm}} = 13$ TeV, assuming $m_H = 125.09$ GeV. Coupling strength modifiers including effective photon, $Z\gamma$ and gluon are measured. See their Fig. 6.

[3] $B_{inv} = B_{undetected} = 0$ is assumed.

[4] B_{inv} floating, $B_{undetected} \geq 0$, and $\kappa_V \leq 1$ are assumed.

[5] CMS 22 report combined results (see their Extended Data Table 2) using up to 138 fb^{-1} of data at $E_{\text{cm}} = 13$ TeV, assuming $m_H = 125.38$ GeV. Coupling strength modifiers including effective photon, $Z\gamma$ and gluon are measured. See their Fig. 4 left.

gluon effective coupling (κ_{gluon})

VALUE	DOCUMENT ID		TECN	COMMENT
• • • We do not use the following data for averages, fits, limits, etc. • • •				
$1.01^{+0.11}_{-0.09}$	[1] AAD	23Y	ATLS	pp, 13 TeV
0.95 ± 0.07	[2,3] ATLAS	22	ATLS	pp, 13 TeV
$0.94^{+0.07}_{-0.06}$	[2,4] ATLAS	22	ATLS	pp, 13 TeV
0.92 ± 0.08	[5] CMS	22	CMS	pp, 13 TeV

[1] AAD 23Y constrain κ_{gluon} from Higgs production rates with $H \to \gamma\gamma$ with 139 fb^{-1} pp collision data at $E_{\text{cm}} = 13$ TeV. The quoted result is obtained assuming effective

couplings κ_{gluon} and κ_γ for $gg \to H$ and $H \to \gamma\gamma$, respectively and other couplings fixed to the SM values. See their Fig. 15.

[2] ATLAS 22 report combined results (see their Extended Data Table 1) using up to 139fb^{-1} of data at $E_{cm} = 13$ TeV, assuming $m_H = 125.09$ GeV. Coupling strength modifiers including effective photon, $Z\gamma$ andgluon are measured. See their Fig. 6.

[3] $B_{inv} = B_{undetected} = 0$ is assumed.

[4] B_{inv} floating, $B_{undetected} \geq 0$, and $\kappa_V \leq 1$ are assumed.

[5] CMS 22 report combined results (see their Extended Data Table 2) using up to 138 fb^{-1} of data at $E_{cm} = 13$ TeV, assuming $m_H = 125.38$ GeV. Coupling strength modifiers including effective photon, $Z\gamma$ and gluon are measured. See their Fig. 4 left.

$Z\gamma$ effective coupling ($\kappa_{Z\gamma}$)

VALUE	DOCUMENT ID		TECN	COMMENT
• • • We do not use the following data for averages, fits, limits, etc. • • •				
$1.38^{+0.31}_{-0.37}$	[1,2] ATLAS	22	ATLS	pp, 13 TeV
$1.35^{+0.29}_{-0.36}$	[1,3] ATLAS	22	ATLS	pp, 13 TeV
$1.65^{+0.34}_{-0.37}$	[4] CMS	22	CMS	pp, 13 TeV

[1] ATLAS 22 report combined results (see their Extended Data Table 1) using up to 139 fb^{-1} of data at $E_{cm} = 13$ TeV, assuming $m_H = 125.09$ GeV. Coupling strength modifiers including effective photon, $Z\gamma$ and gluon are measured. See their Fig. 6.

[2] $B_{inv} = B_{undetected} = 0$ is assumed.

[3] B_{inv} floating, $B_{undetected} \geq 0$, and $\kappa_V \leq 1$ are assumed.

[4] CMS 22 report combined results (see their Extended Data Table 2) using up to 138 fb^{-1} of data at $E_{cm} = 13$ TeV, assuming $m_H = 125.38$ GeV. Coupling strength modifiers including effective photon, $Z\gamma$ and gluon are measured. See their Fig. 4 left.

OTHER H PRODUCTION PROPERTIES

$t\bar{t}H$ production

Signal strength relative to the Standard Model cross section.

VALUE	DOCUMENT ID		TECN	COMMENT
$0.91^{+0.20}_{-0.18}$ OUR AVERAGE	Error includes scale factor of 1.6. See the ideogram below.			
$0.81^{+0.22}_{-0.19}$	[1] AAD	25AJ	ATLS	pp, 13 TeV, $H \to b\bar{b}$
0.33 ± 0.26	[2] HAYRAPETY...	25R	CMS	pp, 13 TeV, $H \to b\bar{b}$
$0.92 \pm 0.19^{+0.17}_{-0.13}$	[3] SIRUNYAN	21R	CMS	pp, 13 TeV, $H \to \tau\tau$, WW^*, ZZ^*
$1.43^{+0.33+0.21}_{-0.31-0.15}$	[4] AAD	20Z	ATLS	pp, 13 TeV, $H \to \gamma\gamma$
$1.6\ ^{+0.5}_{-0.4}$	[5] AABOUD	18AC	ATLS	pp, 13 TeV, $H \to \tau\tau$, WW^*, ZZ^*
$1.9\ ^{+0.8}_{-0.7}$	[6] AAD	16AN	ATLS	pp, 7, 8 TeV
• • • We do not use the following data for averages, fits, limits, etc. • • •				
-1.6 ± 4.5	[7] HAYRAPETY...26		CMS	pp, 13 TeV, $H \to c\bar{c}$
$0.91^{+0.26}_{-0.22}$	[7] HAYRAPETY...26		CMS	pp, 13 TeV, $H \to b\bar{b}$
$-0.27^{+0.86}_{-0.83}$	[8] TUMASYAN	23AI	ATLS	pp, 13 TeV, boosted $H \to b\bar{b}$

$0.35^{+0.36}_{-0.34}$	[9] AAD	22M	ATLS	pp, 13 TeV, $H \to b\overline{b}$
$1.38^{+0.36}_{-0.29}$	[10] SIRUNYAN	20AS	CMS	pp, 13 TeV, $H \to \gamma\gamma$
$0.72 \pm 0.24 \pm 0.38$	[11] SIRUNYAN	19R	CMS	pp, 13 TeV, $H \to b\overline{b}$
1.2 ± 0.3	[12] AABOUD	18AC	ATLS	pp, 13 TeV, $H \to b\overline{b}\,\tau\tau$, $\gamma\gamma$, WW^*, ZZ^*
	[13] AABOUD	18BK	ATLS	pp, 13 TeV, $H \to b\overline{b}\,\tau\tau$, $\gamma\gamma$, WW^*, ZZ^*
$0.84^{+0.64}_{-0.61}$	[14] AABOUD	18T	ATLS	pp, 13 TeV, $H \to b\overline{b}$
0.9 ± 1.5	[15] SIRUNYAN	18BD	CMS	pp, 13 TeV, $H \to b\overline{b}$
$1.23^{+0.45}_{-0.43}$	[16] SIRUNYAN	18BQ	CMS	pp, 13 TeV, $H \to \tau\tau$, WW^*, ZZ^*
$1.26^{+0.31}_{-0.26}$	[17] SIRUNYAN	18L	CMS	pp, 7, 8, 13 TeV, $H \to b\overline{b}$, $\tau\tau$, $\gamma\gamma$, WW^*, ZZ^*
1.7 ± 0.8	[18] AAD	16AL	ATLS	pp, 7, 8 TeV, $H \to b\overline{b}$, $\tau\tau$, $\gamma\gamma$, WW^*, and ZZ^*
$2.3\ ^{+0.7}_{-0.6}$	[6,19] AAD	16AN	LHC	pp, 7, 8 TeV
$2.9\ ^{+1.0}_{-0.9}$	[6] AAD	16AN	CMS	pp, 7, 8 TeV
$1.81^{+0.52}_{-0.50}{}^{+0.58}_{-0.55}{}^{+0.31}_{-0.12}$	[20] AAD	16K	ATLS	pp, 7, 8 TeV
$1.4\ ^{+2.1}_{-1.4}\ ^{+0.6}_{-0.3}$	[21] AAD	15	ATLS	pp, 7, 8 TeV
1.5 ± 1.1	[22] AAD	15BC	ATLS	pp, 8 TeV
$2.1\ ^{+1.4}_{-1.2}$	[23] AAD	15T	ATLS	pp, 8 TeV
$1.2\ ^{+1.6}_{-1.5}$	[24] KHACHATRY...	15AN	CMS	pp, 8 TeV
$2.8\ ^{+1.0}_{-0.9}$	[25] KHACHATRY...	14H	CMS	pp, 7, 8 TeV
$9.49^{+6.60}_{-6.28}$	[26] AALTONEN	13L	CDF	$p\overline{p}$, 1.96 TeV
< 5.8 at 95% CL	[27] CHATRCHYAN	13X	CMS	pp, 7, 8 TeV, $H \to b\overline{b}$

[1] AAD 25AJ measure the $t\overline{t}H$ production with $H \to b\overline{b}$ decay channel using 140 fb^{-1} of data at $E_{\rm cm} = 13$ TeV. The $t\overline{t}H$ cross section is measured to be 411^{+101}_{-92} fb for a Higgs boson mass of 125.09 GeV. The signal strengths with simplified template cross section bins are given in their Fig. 3.

[2] HAYRAPETYAN 25R measure the $t\overline{t}H$ and tH productions with $H \to b\overline{b}$ decay channel using 138 fb^{-1} of data at $E_{\rm cm} = 13$ TeV. The quoted value is obtained assuming the tH contribution predicted in the SM. The signal strengths with simplified template cross section bins are given in their Fig. 12. Two-dimensional likelihood scan of $(\mu_{tH}, \mu_{t\overline{t}H})$ is shown in their Fig. 14.

[3] SIRUNYAN 21R search for $t\overline{t}H$ in final states with electrons, muons and hadronically decaying τ leptons ($H \to WW^*$, ZZ^*, $\tau\tau$) with 137 fb^{-1} of pp collision data at $E_{\rm cm} = 13$ TeV. The quoted signal strength corresponds to a significance of 4.7 standard deviations and is given for $m_H = 125$ GeV.

[4] AAD 20Z measure $\sigma_{t\overline{t}H} \cdot \mathrm{B}(H \to \gamma\gamma)$ to be $1.64^{+0.38}_{-0.36}{}^{+0.17}_{-0.14}$ fb in 139 fb^{-1} of data at $E_{\rm cm} = 13$ TeV.

[5] AABOUD 18AC search for $t\overline{t}H$ production with H decaying to $\tau\tau$, $WW^*(\to\ \ell\nu\ell\nu$, $\ell\nu q\overline{q})$, $ZZ^*(\to\ \ell\ell\nu\nu$, $\ell\ell q\overline{q})$ in 36.1 fb^{-1} of pp collisions at $E_{\rm cm} = 13$ TeV. The quoted signal strength is given for $m_H = 125$ GeV. See their Table 13 and Fig. 13.

[6] AAD 16AN: In the fit, relative branching ratios are fixed to those in the Standard Model. The quoted signal strength is given for $m_H = 125.09$ GeV.

[7] HAYRAPETYAN 26 search for $t\overline{t}H$, $H \to\ c\overline{c}$ together with the $t\overline{t}H$, $H \to\ b\overline{b}$ measurement using 138 fb^{-1} of pp collision data at $E_{\rm cm} = 13$ TeV.

[8] TUMASYAN 23AI measure boosted $H \to\ b\overline{b}$ ($p_T\ >200$ GeV) in $t\overline{t}H$ production using 138 fb^{-1} of data at $E_{\rm cm} = 13$ TeV. The differential cross section for the Higgs p_T is shown in their Fig. 8 and Table V. Limits on eight Wilson coefficients at 68% and 95% CL are shown in their Fig. 10 and Table VI.

[9] AAD 22M measure $H \to\ b\overline{b}$ in $t\overline{t}H$ production using 139 fb^{-1} of data at $E_{\rm cm} = 13$ TeV. See their Fig. 14. The signal strengths and 95% CL cross section upper limits with simplified template cross section bins are given in their Figs. 18 and 19, respectively.

[10] SIRUNYAN 20AS measure $\sigma_{t\overline{t}H} \cdot {\rm B}(H \to\ \gamma\gamma)$ to be $1.56^{+0.34}_{-0.32}$ fb in 137 fb^{-1} of data at $E_{\rm cm} = 13$ TeV.

[11] SIRUNYAN 19R search for $t\overline{t}H$ production with H decaying to $b\overline{b}$ in 35.9 fb^{-1} of data at $E_{\rm cm} = 13$ TeV. The quoted signal strength is given for $m_H = 125$ GeV.

[12] AABOUD 18AC combine results of $t\overline{t}H$, $H \to\ \tau\tau$, $WW^*(\to\ \ell\nu\ell\nu$, $\ell\nu q\overline{q})$, $ZZ^*(\to\ \ell\ell\nu\nu$, $\ell\ell q\overline{q})$ with results of $t\overline{t}H$, $H \to\ b\overline{b}$ (AABOUD 18T), $\gamma\gamma$ (AABOUD 18BO), $ZZ^*(\to\ 4\ell)$ (AABOUD 18AJ) in 36.1 fb^{-1} of pp collisions at $E_{\rm cm} = 13$ TeV. The quoted signal strength is given for $m_H = 125$ GeV. See their Table 14.

[13] AABOUD 18BK use 79.8 fb^{-1} data for $t\overline{t}H$ production with $H \to\ \gamma\gamma$ and $ZZ^* \to\ 4\ell$ ($\ell = e$, μ) and 36.1 fb^{-1} for other decay channels at $E_{\rm cm} = 13$ TeV. A significance of 5.8 standard deviations is observed for $m_H = 125.09$ GeV and its signal strength without the uncertainty of the $t\overline{t}H$ cross section is $1.32^{+0.28}_{-0.26}$. Combining with results of 7 and 8 TeV (AAD 16K), the significance is 6.3 standard deviations. Assuming Standard Model branching fractions, the total $t\overline{t}H$ production cross section at 13 TeV is measured to be $670 \pm 90^{+110}_{-100}$ fb.

[14] AABOUD 18T search for $t\overline{t}H$ production with H decaying to $b\overline{b}$ in 36.1 fb^{-1} of pp collisions at $E_{\rm cm} = 13$ TeV. The quoted signal strength is given for $m_H = 125$ GeV.

[15] SIRUNYAN 18BD search for $t\overline{t}H$, $H \to\ b\overline{b}$ in the all-jet final state with 35.9 fb^{-1} pp collision data at $E_{\rm cm} = 13$ TeV. The quoted signal strength is given for $m_H = 125$ GeV.

[16] SIRUNYAN 18BQ search for $t\overline{t}H$ in final states with electrons, muons and hadronically decaying τ leptons ($H \to\ WW^*$, ZZ^*, $\tau\tau$) with 35.9 fb^{-1} of pp collision data at $E_{\rm cm} = 13$ TeV. The quoted signal strength corresponds to a significance of 3.2 standard deviations and is given for $m_H = 125$ GeV.

[17] SIRUNYAN 18L use up to 5.1, 19.7 and 35.9 fb^{-1} of pp collisions at $E_{\rm cm} = 7$, 8, and 13 TeV, respectively. The quoted signal strength corresponds to a significance of 5.2 standard deviations and is given for $m_H = 125.09$ GeV. H decay channels of WW^*, ZZ^*, $\gamma\gamma$, $\tau\tau$, and $b\overline{b}$ are used. See their Table 1 and Fig. 2 for results on individual channels.

[18] AAD 16AL search for $t\overline{t}H$ production with H decaying to $\gamma\gamma$ in 4.5 fb^{-1} of pp collisions at $E_{\rm cm} = 7$ TeV and $b\overline{b}$, $\tau\tau$, $\gamma\gamma$, WW^*, and ZZ^* in 20.3 fb^{-1} at $E_{\rm cm} = 8$ TeV. The quoted signal strength is given for $m_H = 125$ GeV. This paper combines the results of previous papers, and the new result of this paper only is: $\mu = 1.6 \pm 2.6$.

[19] AAD 16AN perform fits to the ATLAS and CMS data at $E_{\rm cm} = 7$ and 8 TeV.

[20] AAD 16K use up to 4.7 fb^{-1} of pp collisions at $E_{\rm cm} = 7$ TeV and up to 20.3 fb^{-1} at $E_{\rm cm} = 8$ TeV. The third uncertainty in the measurement is theory systematics. The quoted signal strength is given for $m_H = 125.36$ GeV.

[21] AAD 15 search for $t\overline{t}H$ production with H decaying to $\gamma\gamma$ in 4.5 fb^{-1} of pp collisions at $E_{\rm cm}$ = 7 TeV and 20.3 fb^{-1} at $E_{\rm cm}$ = 8 TeV. The quoted result on the signal strength is equivalent to an upper limit of 6.7 at 95% CL and is given for m_H = 125.4 GeV.

[22] AAD 15BC search for $t\overline{t}H$ production with H decaying to $b\overline{b}$ in 20.3 fb^{-1} of pp collisions at $E_{\rm cm}$ = 8 TeV. The corresponding upper limit is 3.4 at 95% CL. The quoted signal strength is given for m_H = 125 GeV.

[23] AAD 15T search for $t\overline{t}H$ production with H resulting in multilepton final states (mainly from WW^*, $\tau\tau$, ZZ^*) in 20.3 fb^{-1} of pp collisions at $E_{\rm cm}$ = 8 TeV. The quoted result on the signal strength is given for m_H = 125 GeV and corresponds to an upper limit of 4.7 at 95% CL. The data sample is independent from AAD 15 and AAD 15BC.

[24] KHACHATRYAN 15AN search for $t\overline{t}H$ production with H decaying to $b\overline{b}$ in 19.5 fb^{-1} of pp collisions at $E_{\rm cm}$ = 8 TeV. The quoted result on the signal strength is equivalent to an upper limit of 4.2 at 95% CL and is given for m_H = 125 GeV.

[25] KHACHATRYAN 14H search for $t\overline{t}H$ production with H decaying to $b\overline{b}$, $\tau\tau$, $\gamma\gamma$, WW^*, and ZZ^*, in 5.1 fb^{-1} of pp collisions at $E_{\rm cm}$ = 7 TeV and 19.7 fb^{-1} at $E_{\rm cm}$ = 8 TeV. The quoted signal strength is given for m_H = 125.6 GeV.

[26] AALTONEN 13L combine all CDF results with 9.45–10.0 fb^{-1} of $p\overline{p}$ collisions at $E_{\rm cm}$ = 1.96 TeV. The quoted signal strength is given for m_H = 125 GeV.

[27] CHATRCHYAN 13X search for $t\overline{t}H$ production followed by $H \to b\overline{b}$, one top decaying to $\ell\nu$ and the other to either $\ell\nu$ or $q\overline{q}$ in 5.0 fb^{-1} and 5.1 fb^{-1} of pp collisions at $E_{\rm cm}$ = 7 and 8 TeV. A limit on cross section times branching ratio which corresponds to (4.0–8.6) times the expected Standard Model cross section is given for m_H = 110–140 GeV at 95% CL. The quoted limit is given for m_H = 125 GeV, where 5.2 is expected for no signal.

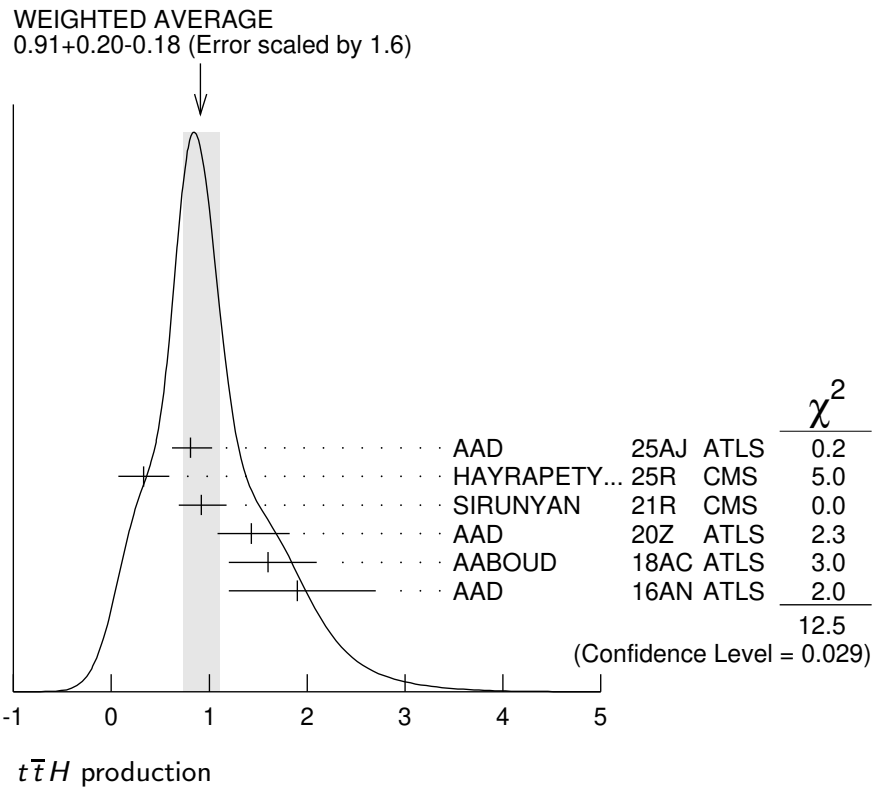

$b\bar{b}H$ production

VALUE	CL%	DOCUMENT ID	TECN	COMMENT
<3.7	95	[1] HAYRAPETY...25	CMS	pp, 13 TeV, $H \to \tau\tau$, WW^*

[1] HAYRAPETYAN 25 search for $b\bar{b}H$ and bH in final states with leptons using 138 fb^{-1} of data at $E_{cm} = 13$ TeV. $H \to \tau\tau$ or $H \to WW^* \to \ell\nu\ell\nu$ are considered. Upper limits at 95% CL on the signal strength for each final state are found in their Fig. 3. Combing with TUMASYAN 23Y, two-dimensional exclusion regions as a function of the κ_b and κ_t parameters are shown in their Fig. 4. The best fit value is (κ_t, κ_b) = (-0.73, 1.58). All other Higgs couplings are fixed to the SM values.

tH production

VALUE	CL%	DOCUMENT ID		TECN	COMMENT
7.1±2.5 OUR AVERAGE					
8.1±2.6±2.0		[1] AAD	25BD	ATLS	pp, 13 TeV
5.7±2.7±3.0		[2] SIRUNYAN	21R	CMS	pp, 13 TeV
• • • We do not use the following data for averages, fits, limits, etc. • • •					
<13.9	95	[3] AAD	25BD	ATLS	pp, 13 TeV
<14.6	95	[4] HAYRAPETY...25R		CMS	pp, 13 TeV
<12	95	[5] AAD	20Z	ATLS	pp, 13 TeV
		[6] SIRUNYAN	19BK	CMS	pp, 13 TeV
		[7] KHACHATRY...16AU		CMS	pp, 8 TeV

[1] AAD 25BD search for tH in final states with leptons (electron or muon) ($H \to b\bar{b}$, WW^*, ZZ^*, $\tau\tau$) with 140 fb^{-1} of pp collision data at $E_{cm} = 13$ TeV. The quoted signal strength corresponds to the cross-section of $\sigma(tH) = 720 \pm 270$ fb and a significance of 2.8 standard deviations.

[2] SIRUNYAN 21R search for tH in final states with electrons, muons and hadronically decaying τ leptons ($H \to WW^*$, ZZ^*, $\tau\tau$) with 137 fb^{-1} of pp collision data at $E_{cm} = 13$ TeV. The quoted signal strength corresponds to a significance of 1.4 standard deviations and is given for $m_H = 125$ GeV.

[3] AAD 25BD search for tH in final states with leptons (electron or muon) ($H \to b\bar{b}$, WW^*, ZZ^*, $\tau\tau$) with 140 fb^{-1} of pp collision data at $E_{cm} = 13$ TeV.

[4] HAYRAPETYAN 25R measure the $t\bar{t}H$ and tH productions with $H \to b\bar{b}$ decay channel using 138 fb^{-1} of data at $E_{cm} = 13$ TeV. The quoted value is obtained assuming the $t\bar{t}H$ contribution predicted in the SM. Two-dimensional likelihood scan of (μ_{tH}, $\mu_{t\bar{t}H}$) is shown in their Fig. 14.

[5] AAD 20Z search for the tH associated production using $H \to \gamma\gamma$ in 139 fb^{-1} of data at $E_{cm} = 13$ TeV. An upper limit on its rate is set to be 12 times the Standard Model at 95% CL ($m_H = 125.09$ GeV).

[6] SIRUNYAN 19BK search for the tH associated production using multilepton signatures ($H \to WW^*$, $H \to \tau\tau$, $H \to ZZ^*$) and signatures with a single lepton and a $b\bar{b}$ pair ($H \to b\bar{b}$) using 35.9 fb^{-1} at $E_{cm} = 13$ TeV. Results are combined with $H \to \gamma\gamma$ (SIRUNYAN 18DS). The observed 95% CL upper limit on the tH production cross section times $H \to WW^* + \tau\tau + ZZ^* + b\bar{b} + \gamma\gamma$ branching fraction is 1.94 pb (assuming SM $t\bar{t}H$ production cross section). See their Table X and Fig. 14. The values outside the ranges of [−0.9, −0.5] and [1.0, 2.1] times the standard model top quark Yukawa coupling are excluded at 95% CL.

[7] KHACHATRYAN 16AU search for the tH associated production in 19.7 fb^{-1} at E_{cm} = 8 TeV. The 95% CL upper limits on the tH associated production cross section is measured to be 600–1000 fb depending on the assumed $\gamma\gamma$ branching ratios of the Higgs boson. The $\gamma\gamma$ branching ratio is varied to be by a factor of 0.5–3.0 of the Standard Model Higgs boson ($m_H = 125$ GeV). The results of the signal strengths for a negative Higgs-boson trilinear coupling are given. The results are given for $m_H = 125$ GeV.

cH production

VALUE	CL%	DOCUMENT ID		TECN	COMMENT
• • • We do not use the following data for averages, fits, limits, etc. • • •					
		[1] AAD	25R	ATLS	pp, 13 TeV, $H \to \gamma\gamma$
<243	95	[2] CHEKHOVSKY	25L	CMS	pp, 13 TeV, $H \to \gamma\gamma$

[1] AAD 25R search for the production of a Higgs boson and one or more charm quarks (H+c) with $H \to \gamma\gamma$ using 140 fb^{-1} of data at $E_{cm} = 13$ TeV. The observed H+c cross section is 5.3 ± 3.2 pb. The observed upper limit on the H+c cross section at 95% CL is 10.6 pb.

[2] CHEKHOVSKY 25L search for the production of a Higgs boson and one or more charm quarks (H+c) with $H \to \gamma\gamma$ using 138 fb^{-1} of data at $E_{cm} = 13$ TeV. The quoted value is obtained assuming the SM rates for all other Higgs production processes.

VBS/VBF WH production

WH production through vector boson scattering (VBS) or vector boson fusion (VBF). The VBS/VBF WH production cross section related to the SM prediction.

VALUE	CL%	DOCUMENT ID		TECN	COMMENT
• • • We do not use the following data for averages, fits, limits, etc. • • •					
<14.3	95	[1] HAYRAPETY...25B		CMS	pp, 13 TeV, VBF WH, coupling sign
< 9.0	95	[2] AAD	24BM	ATLS	pp, 13 TeV, VBF WH, coupling sign

[1] HAYRAPETYAN 25B present the determination of the relative sign of κ_W and κ_Z with VBF WH, $H \to b\overline{b}$ using 148 fb^{-1} of data at $E_{cm} = 13$ TeV. The upper limit at 95% CL on the cross section for VBF WH production is obtained. The signal strength is measured to be $2.2^{+6.1}_{-5.8}$.

[2] AAD 24BM present the determination of the relative sign of κ_W and κ_Z with VBF WH, $H \to b\overline{b}$ using 140 fb^{-1} of data at $E_{cm} = 13$ TeV. The upper limit at 95% CL on the cross section for VBF WH production is obtained. The signal strength is measured to be $0.9^{+4.0}_{-4.3}$.

γH production

VALUE	DOCUMENT ID		TECN	COMMENT
• • • We do not use the following data for averages, fits, limits, etc. • • •				
	[1] CHEKHOVSKY	25G	CMS	pp, 13 TeV, $H \to b\overline{b}$, $H \to ZZ^* \to 4\ell$

[1] CHEKHOVSKY 25G search for the γH production using a boosted Higgs boson recoiling against a high-energy photon with data of 138 fb^{-1} at $E_{cm} = 13$ TeV. The production cross section is constraint to be $\sigma_{\gamma H} < 16.4$ fb at 95% CL. Constraints on four anomalous couplings involving $HZ\gamma$ and $H\gamma\gamma$ are shown in their Table I.

HH production

The HH production cross section relative to the SM prediction.

VALUE	CL%	DOCUMENT ID		TECN	COMMENT
< 2.4	95	[1] AAD	23AT	ATLS	13 TeV, $b\overline{b}b\overline{b}$, $b\overline{b}\tau\tau$, $b\overline{b}\gamma\gamma$
• • • We do not use the following data for averages, fits, limits, etc. • • •					
< 5.9	95	[2] AAD	24AZ	ATLS	13 TeV, $b\overline{b}\tau\tau$
< 17	95	[3] AAD	24BG	ATLS	13 TeV, $b\overline{b}ZZ^*$, $VVVV$, $VV\tau\tau$, $\tau\tau\tau\tau$, $\gamma\gamma VV$, $\gamma\gamma\tau\tau$

$<$ 2.9	95	[4] AAD	24BL ATLS	13 TeV, $b\overline{b}b\overline{b}$, $b\overline{b}\tau\tau$, $b\overline{b}\gamma\gamma$, multilepton , $b\overline{b}\ell\ell$
$<$ 4.0	95	[5] AAD	24X ATLS	13 TeV, $b\overline{b}\gamma\gamma$
$<$ 9.7	95	[6] AAD	24Y ATLS	13 TeV, $b\overline{b}WW^*$, $b\overline{b}ZZ^*$, $b\overline{b}\tau\tau$, multilepton
$<$ 14	95	[7] HAYRAPETY...	24AE CMS	13 TeV, $b\overline{b}WW^*$
$<$294	95	[8] HAYRAPETY...	24AW CMS	13 TeV, VHH, $HH \rightarrow b\overline{b}b\overline{b}$
$<$183	95	[9] AAD	23AD ATLS	13 TeV, VHH, $HH \rightarrow b\overline{b}b\overline{b}$
$<$ 5.4	95	[10] AAD	23BK ATLS	13 TeV, $b\overline{b}b\overline{b}$
$<$ 4.7	95	[11] AAD	23Z ATLS	13 TeV, $b\overline{b}\tau\tau$
$<$ 9.9	95	[12] TUMASYAN	23AE CMS	13 TeV, $b\overline{b}b\overline{b}$
$<$ 3.3	95	[13,14] TUMASYAN	23D CMS	13 TeV, $b\overline{b}\tau\tau$
$<$124	95	[13,15] TUMASYAN	23D CMS	13 TeV, $b\overline{b}\tau\tau$
$<$ 32.4	95	[16] TUMASYAN	23I CMS	13 TeV, $b\overline{b}ZZ^*$ ($ZZ^* \rightarrow 4\ell$)
$<$ 21.3	95	[17] TUMASYAN	23O CMS	13 TeV, WW^*WW^*, $WW^*\tau\tau$, $\tau\tau\tau\tau$
$<$ 4.2	95	[18] AAD	22Y ATLS	13 TeV, $\gamma\gamma b\overline{b}$
$<$ 3.4	95	[19] CMS	22 CMS	13 TeV, $b\overline{b}ZZ^*$, $b\overline{b}\gamma\gamma$, $b\overline{b}\tau\tau$, $b\overline{b}b\overline{b}$, multilepton
$<$ 3.9	95	[20] TUMASYAN	22AN CMS	13 TeV, $b\overline{b}b\overline{b}$
$<$ 7.7	95	[21] SIRUNYAN	21K CMS	13 TeV, $\gamma\gamma b\overline{b}$
$<$ 6.9	95	[22] AAD	20C ATLS	13 TeV, $b\overline{b}\gamma\gamma$, $b\overline{b}\tau\tau$, $b\overline{b}b\overline{b}$, $b\overline{b}WW^*$, $WW^*\gamma\gamma$, WW^*WW^*
$<$ 40	95	[23] AAD	20E ATLS	13 TeV, $HH \rightarrow b\overline{b}\ell\nu\ell\nu$
$<$840	95	[24] AAD	20X ATLS	13 TeV, VBF, $b\overline{b}b\overline{b}$
$<$ 12.9	95	[25] AABOUD	19A ATLS	13 TeV, $b\overline{b}b\overline{b}$
$<$300	95	[26] AABOUD	19O ATLS	13 TeV, $b\overline{b}WW^*$
$<$160	95	[27] AABOUD	19T ATLS	13 TeV, WW^*WW^*
$<$ 24	95	[28] SIRUNYAN	19 CMS	13 TeV, $\gamma\gamma b\overline{b}$
$<$ 75	95	[29] SIRUNYAN	19AB CMS	13 TeV, $b\overline{b}b\overline{b}$
$<$ 22.2	95	[30] SIRUNYAN	19BE CMS	13 TeV, $b\overline{b}\gamma\gamma$ $b\overline{b}\tau\tau$, $b\overline{b}b\overline{b}$, $b\overline{b}WW^*$, $b\overline{b}ZZ^*$
$<$179	95	[31] SIRUNYAN	19H CMS	13 TeV, $b\overline{b}b\overline{b}$
$<$230	95	[32] AABOUD	18BU ATLS	13 TeV, $\gamma\gamma WW^*$
$<$ 12.7	95	[33] AABOUD	18CQ ATLS	13 TeV, $b\overline{b}\tau\tau$
$<$ 22	95	[34] AABOUD	18CW ATLS	13 TeV, $\gamma\gamma b\overline{b}$
$<$ 30	95	[35] SIRUNYAN	18A CMS	13 TeV, $b\overline{b}\tau\tau$
$<$ 79	95	[36] SIRUNYAN	18F CMS	13 TeV, $b\overline{b}\ell\nu\ell\nu$
$<$ 43	95	[37] SIRUNYAN	17CN CMS	8 TeV, $b\overline{b}\tau\tau$, $\gamma\gamma b\overline{b}$, $b\overline{b}b\overline{b}$
$<$108	95	[38] AABOUD	16I ATLS	13 TeV, $b\overline{b}b\overline{b}$
$<$ 74	95	[39] KHACHATRY...	16BQ CMS	8 TeV, $\gamma\gamma b\overline{b}$
$<$ 70	95	[40] AAD	15CE ATLS	8 TeV, $b\overline{b}b\overline{b}$, $b\overline{b}\tau\tau$, $\gamma\gamma b\overline{b}$, $\gamma\gamma WW$

[1] AAD 23AT combine results from 126–139 fb^{-1} of data at $E_{cm} = 13$ TeV for $pp \rightarrow HH \rightarrow b\overline{b}b\overline{b}$ (AAD 23BK), $b\overline{b}\tau\tau$ (AAD 23Z), and $b\overline{b}\gamma\gamma$ (AAD 22Y).

[2] AAD 24AZ search for non-resonant HH production using $HH \rightarrow b\overline{b}\tau\tau$ with data of 140 fb^{-1} at $E_{cm} = 13$ TeV. The result is interpreted: limits on Wilson coefficients of the Higgs effective field theory (HEFT) and the SM effective field theory (SMEFT) are shown in their Table IV and Figs. 11 and 12; the ggF HH production cross sections (7 benchmark points) of HEFT are shown in their Fig. 10. In those interpretations the VBF HH production is neglected.

[3] AAD 24BG search for non-resonant HH production targeting the $b\overline{b}ZZ^*$, $VVVV$, $VV\tau\tau$, $\tau\tau\tau\tau$, $\gamma\gamma VV$, $\gamma\gamma\tau\tau$ decay channels with data of 140 fb^{-1} at $E_{\rm cm} = 13$ TeV. Signal strengths for the 11 different signal regions are given in their Fig. 8.

[4] AAD 24BL combine results from 126–140 fb^{-1} of data at $E_{\rm cm} = 13$ TeV for $pp \to HH \to b\overline{b}b\overline{b}$ (AAD 23BK, AAD 24BV), $b\overline{b}\tau\tau$ (AAD 24AZ), $b\overline{b}\gamma\gamma$ (AAD 24X), multilepton (AAD 24BG), and $b\overline{b}\ell\ell$ (AAD 24Y). See their Fig. 2. The signal strength is measured to be $0.5^{+1.2}_{-1.0}$. Constraints for three interaction parameters (c_{tthh}, c_{gghh}, c_{hhh}) in the Higgs effective field theory are set. See their Fig. 4.

[5] AAD 24X search for non-resonant HH production using $HH \to b\overline{b}\gamma\gamma$ with data of 140 fb^{-1} at $E_{\rm cm} = 13$ TeV. The result is interpreted: limits on three Wilson coefficients and the ggF HH production cross sections (7 benchmark points shown in their Table 5) of the Higgs effective field theory are shown in their Table 4 and Fig. 8, respectively; limits on two Wilson coefficients of the SM effective field theory are shown in their Table 6 and Fig. 9. In those interpretations only the ggF HH production is considered instead of both ggF and VBF.

[6] AAD 24Y search for non-resonant HH production in $2b + 2\ell + \nu$s final state ($\ell = e$, μ) targeting $b\overline{b}WW^*$, $b\overline{b}ZZ^*$, and $b\overline{b}\tau\tau$ decay channels with data of 140 fb^{-1} at $E_{\rm cm} = 13$ TeV. The signal strength is measured to be $-8.5^{+7.7}_{-8.4}$. See their Fig. 6.

[7] HAYRAPETYAN 24AE search for non-resonant HH production using $HH \to b\overline{b}WW^*$ with data of 138 fb^{-1} at $E_{\rm cm} = 13$ TeV. The result is interpreted: the ggF HH production cross sections (20 benchmark points) of the Higgs effective field theory are shown in their Fig. 16; the coupling between two top quarks and two Higgs bosons is constrained between [-0.8, 1.3] at 95%CL (see their Fig. 17) with all other Higgs couplings fixed to the SM values.

[8] HAYRAPETYAN 24AW search for non-resonant HH production in association with a vector boson using $HH \to b\overline{b}b\overline{b}$ with data of 138 fb^{-1} at $E_{\rm cm} = 13$ TeV. The vector boson decays both leptonically ($W \to \ell\nu$, $Z \to \ell\ell$, $\nu\nu$, $\ell = e$, μ) and hadronically. The quoted value is the upper limit of the VHH cross section. See their Figs. 13 and 16 (left) for the best fit and the upper limit of the VHH cross section, respectively. In addition, upper limits at 95% CL on VHH and HH cross sections are shown as a function of κ_λ, κ_{2V}, and κ_V in their Figs. 17, 18, and 19.

[9] AAD 23AD search for non-resonant HH production in association with a vector boson using $HH \to b\overline{b}b\overline{b}$ with data of 139 fb^{-1} at $E_{\rm cm} = 13$ TeV. The vector boson decays leptonically ($W \to \ell\nu$, $Z \to \ell\ell$, $\nu\nu$, $\ell = e$, μ).

[10] AAD 23BK search for non-resonant HH production using $HH \to b\overline{b}b\overline{b}$ with data of 126 fb^{-1} at $E_{\rm cm} = 13$ TeV.

[11] AAD 23Z search for non-resonant HH production using $HH \to b\overline{b}\tau\tau$ with data of 139 fb^{-1} at $E_{\rm cm} = 13$ TeV. The upper limit on the $pp \to HH$ production cross section at 95% CL is measured to be 140 fb, which corresponds to 4.7 times the SM prediction (see their Table 6).

[12] TUMASYAN 23AE search for HH production using $HH \to b\overline{b}b\overline{b}$, where both $b\overline{b}$ pairs are highly boosted, with data of 138 fb^{-1} at $E_{\rm cm} = 13$ TeV.

[13] TUMASYAN 23D search for non-resonant HH production using $HH \to b\overline{b}\tau\tau$ with data of 138 fb^{-1} at $E_{\rm cm} = 13$ TeV.

[14] The upper limit on the $pp \to HH$ production cross section (gluon fusion and VBF) at 95% CL is measured to be 102 fb, which corresponds to 3.3 times the SM prediction (see their Table 2).

[15] The upper limit on the VBF $pp \to HH$ production cross section at 95% CL is measured to be 212 fb, which corresponds to 124 times the SM prediction (see their Table 3).

[16] TUMASYAN 23I search for non-resonant HH production using $HH \to b\overline{b}ZZ^*$ ($ZZ^* \to 4\ell$, $\ell = e$, μ) with data of 138 fb^{-1} at $E_{\rm cm} = 13$ TeV.

[17] TUMASYAN 23O search for non-resonant HH production using $HH \to WW^*WW^*$, $WW^*\tau\tau$, and $\tau\tau\tau\tau$ (multilepton) with data of 138 fb^{-1} at $E_{cm} = 13$ TeV. See their Fig. 9 for different final states and these combination.

[18] AAD 22Y search for non-resonant HH production using $HH \to \gamma\gamma b\overline{b}$ with data of 139 fb^{-1} at $E_{cm} = 13$ TeV. The upper limit on the $pp \to HH$ production cross section at 95% CL is measured to be 130 fb, which corresponds to 4.2 times the SM prediction.

[19] CMS 22 report combined results (see their Extended Data Table 2) using 138 fb^{-1} of data at $E_{cm} = 13$ TeV. See their Fig. 5 (left) for different final states and these combination.

[20] TUMASYAN 22AN search for non-resonant HH production using $HH \to b\overline{b}b\overline{b}$ with data of 138 fb^{-1} at $E_{cm} = 13$ TeV. The upper limit on the $pp \to HH$ production cross section at 95% CL is measured to be 120 fb, which corresponds to 3.9 times the SM prediction.

[21] SIRUNYAN 21K search for non-resonant HH production using $HH \to \gamma\gamma b\overline{b}$ with data of 137 fb^{-1} at $E_{cm} = 13$ TeV. The upper limit on the $pp \to HH \to \gamma\gamma b\overline{b}$ production cross section at 95% CL is measured to be 0.67 fb, which corresponds to about 7.7 times the SM prediction.

[22] AAD 20C combine results of up to 36.1 fb^{-1} data at $E_{cm} = 13$ TeV for $pp \to HH \to b\overline{b}\gamma\gamma$, $b\overline{b}\tau\tau$, $b\overline{b}b\overline{b}$, $b\overline{b}WW^*$, $WW^*\gamma\gamma$, WW^*WW^* (AABOUD 18CW, AABOUD 18CQ, AABOUD 19A, AABOUD 19O, AABOUD 18BU, and AABOUD 19T).

[23] AAD 20E search non-resonant for HH production using $HH \to b\overline{b}\ell\nu\ell\nu$, where one of the Higgs bosons decays to $b\overline{b}$ and the other decays to either WW^*, ZZ^*, or $\tau\tau$, with data of 139 fb^{-1} at $E_{cm} = 13$ TeV. The upper limit on the $pp \to HH$ production cross section at 95% CL is measured to be 1.2 pb, which corresponds to about 40 times the SM prediction.

[24] AAD 20X search for $HH \to b\overline{b}b\overline{b}$ process via VBF with data of 126 fb^{-1} at $E_{cm} =$ 13 TeV. The upper limit on the SM non-resonant HH production cross section is 1460 fb at 95% CL, which corresponds to 840 times the SM prediction.

[25] AABOUD 19A search for HH production using $HH \to b\overline{b}b\overline{b}$ with data of 36.1 fb^{-1} at $E_{cm} = 13$ TeV. The upper limit on the $pp \to HH \to b\overline{b}b\overline{b}$ production cross section at 95% is measured to be 147 fb, which corresponds to about 12.9 times the SM prediction.

[26] AABOUD 19O search for HH production using $HH \to b\overline{b}WW^*$ with data of 36.1 fb^{-1} at $E_{cm} = 13$ TeV. The upper limit on the $pp \to HH$ production cross section at 95% CL is calculated to be 10 pb from the observed upper limit on the $pp \to HH \to b\overline{b}WW^*$ production cross section of 2.5 pb assuming the SM branching fractions. The former corresponds to about 300 times the SM prediction.

[27] AABOUD 19T search for HH production using $HH \to WW^*WW^*$ with data of 36.1 fb^{-1} at $E_{cm} = 13$ TeV. The upper limit on the $pp \to HH$ production cross section at 95% is measured to be 5.3 pb, which corresponds to about 160 times the SM prediction.

[28] SIRUNYAN 19 search for HH production using $HH \to \gamma\gamma b\overline{b}$ with data of 35.9 fb^{-1} at $E_{cm} = 13$ TeV. The upper limit on the $pp \to HH \to \gamma\gamma b\overline{b}$ production cross section at 95% CL is measured to be 2.0 fb, which corresponds to about 24 times the SM prediction.

[29] SIRUNYAN 19AB search for HH production using $HH \to b\overline{b}b\overline{b}$, where 4 heavy flavor jets from two Higgs bosons are resolved, with data of 35.9 fb^{-1} at $E_{cm} = 13$ TeV. The upper limit on the $pp \to HH \to b\overline{b}b\overline{b}$ production cross section at 95% is measured to be 847 fb, which corresponds to about 75 times the SM prediction.

[30] SIRUNYAN 19BE combine results of 13 TeV 35.9 fb^{-1} data: SIRUNYAN 19, SIRUNYAN 18A, SIRUNYAN 19AB, SIRUNYAN 19H, and SIRUNYAN 18F.

[31] SIRUNYAN 19H search for HH production using $HH \to b\overline{b}b\overline{b}$, where one of $b\overline{b}$ pairs is highly boosted and the other one is resolved, with data of 35.9 fb^{-1} at $E_{cm} = 13$ TeV. The upper limit on the $pp \to HH \to b\overline{b}b\overline{b}$ production cross section at 95% is measured to be 1980 fb, which corresponds to about 179 times the SM prediction.

[32] AABOUD 18BU search for HH production using $\gamma\gamma WW^*$ with the final state of $\gamma\gamma\ell\nu jj$ using data of 36.1 fb^{-1} at $E_{cm} = 13$ TeV. The upper limit on the $pp \to HH$ production cross section at 95% CL is measured to be 7.7 pb, which corresponds to about 230 times the SM prediction. The upper limit on the $pp \to HH \to \gamma\gamma WW^*$ at 95% CL is measured to be 7.5 fb (see thier Table 6).

[33] AABOUD 18CQ search for HH production using $HH \to b\overline{b}\tau\tau$ with data of 36.1 fb^{-1} at $E_{cm} = 13$ TeV. The upper limit on the $pp \to HH \to b\overline{b}\tau\tau$ production cross section at 95% is measured to be 30.9 fb, which corresponds to about 12.7 times the SM prediction.

[34] AABOUD 18CW search for HH production using $HH \to \gamma\gamma b\overline{b}$ with data of 36.1 fb^{-1} at $E_{cm} = 13$ TeV. The upper limit on the $pp \to HH$ production cross section at 95% is measured to be 0.73 pb, which corresponds to about 22 times the SM prediction.

[35] SIRUNYAN 18A search for HH production using $HH \to b\overline{b}\tau\tau$ with data of 35.9 fb^{-1} at $E_{cm} = 13$ TeV. The upper limit on the $gg \to HH \to b\overline{b}\tau\tau$ production cross section is measured to be 75.4 fb, which corresponds to about 30 times the SM prediction.

[36] SIRUNYAN 18F search non-resonant for HH production using $HH \to b\overline{b}\ell\nu\ell\nu$, where $\ell\nu\ell\nu$ is either $WW \to \ell\nu\ell\nu$ or $ZZ \to \ell\ell\nu\nu$ (ℓ is e, μ or a leptonically decaying τ), with data of 35.9 fb^{-1} at $E_{cm} = 13$ TeV. The upper limit on the $HH \to b\overline{b}\ell\nu\ell\nu$ production cross section at 95% CL is measured to be 72 fb, which corresponds to about 79 times the SM prediction.

[37] SIRUNYAN 17CN search for HH production using $HH \to b\overline{b}\tau\tau$ with data of 18.3 fb^{-1} at $E_{cm} = 8$ TeV. Results are then combined with the published results of the $HH \to \gamma\gamma b\overline{b}$ and $HH \to b\overline{b}b\overline{b}$, which use data of up to 19.7 fb^{-1} at $E_{cm} = 8$ TeV. The upper limit on the $gg \to HH$ production cross section is measured to be 0.59 pb from $b\overline{b}\tau\tau$, which corresponds to about 59 times the SM prediction (gluon fusion). The combined upper limit is 0.43 pb, which is about 43 times the SM prediction. The quoted values are given for $m_H = 125$ GeV.

[38] AABOUD 16I search for HH production using $HH \to b\overline{b}b\overline{b}$ with data of 3.2 fb^{-1} at $E_{cm} = 13$ TeV. The upper limit on the $pp \to HH \to b\overline{b}b\overline{b}$ production cross section is measured to be 1.22 pb. This result corresponds to about 108 times the SM prediction (gluon fusion), which is $11.3^{+0.9}_{-1.0}$ fb (NNLO+NNLL) including top quark mass effects. The quoted values are given for $m_H = 125$ GeV.

[39] KHACHATRYAN 16BQ search for HH production using $HH \to \gamma\gamma b\overline{b}$ with data of 19.7 fb^{-1} at $E_{cm} = 8$ TeV. The upper limit on the $gg \to HH \to \gamma\gamma b\overline{b}$ production is measured to be 1.85 fb, which corresponds to about 74 times the SM prediction and is translated into 0.71 pb for $gg \to HH$ production cross section.

[40] AAD 15CE search for HH production using $HH \to b\overline{b}\tau\tau$ and $HH \to \gamma\gamma WW$ with data of 20.3 fb^{-1} at $E_{cm} = 8$ TeV. These results are then combined with the published results of the $HH \to \gamma\gamma b\overline{b}$ and $HH \to b\overline{b}b\overline{b}$, which use data of up to 20.3 fb^{-1} at $E_{cm} = 8$ TeV. The upper limits on the $gg \to HH$ production cross section are measured to be 1.6 pb, 11.4 pb, 2.2 pb and 0.62 pb from $b\overline{b}\tau\tau$, $\gamma\gamma WW$, $\gamma\gamma b\overline{b}$ and $b\overline{b}b\overline{b}$, respectively. The combined upper limit is 0.69 pb, which corresponds to about 70 times the SM prediction. The quoted results are given for $m_H = 125.4$ GeV. See their Table 4.

HHH production

The HHH production cross section relative to the SM prediction.

VALUE	CL%	DOCUMENT ID		TECN	COMMENT
<760	95	[1] AAD	25J	ATLS	13 TeV, $b\overline{b}b\overline{b}b\overline{b}$

[1] AAD 25J search for non-resonant HHH production using $HHH \to b\overline{b}b\overline{b}b\overline{b}$ with data of 126 fb^{-1} at $E_{cm} = 13$ TeV. The upper limit on the $pp \to HHH$ production cross section at 95% CL is measured to be 59 fb.

Higgs trilinear self coupling modifier κ_λ

Signal strength relative to the SM prediction, $\kappa_\lambda = \kappa_3 = \lambda_{HHH} / \lambda^{SM}_{HHH}$.

VALUE	CL%	DOCUMENT ID		TECN	COMMENT
3.8 $^{+2.1}_{=3.6}$		[1] AAD	24BL	ATLS	13 TeV, $b\bar{b}b\bar{b}$, $b\bar{b}\tau\tau$, $b\bar{b}\gamma\gamma$, multilepton , $b\bar{b}\ell\ell$
• • • We do not use the following data for averages, fits, limits, etc. • • •					
−11 to 17	95	[2] AAD	25J	ATLS	13 TeV, $b\bar{b}b\bar{b}b\bar{b}$
− 1.2 to 7.5	95	[3] HAYRAPETY...	25F	CMS	13 TeV, single and double Higgs production
− 3.1 to 9.0	95	[4] AAD	24AZ	ATLS	13 TeV, $b\bar{b}\tau\tau$
− 6.2 to 11.6	95	[5] AAD	24BG	ATLS	13 TeV, $b\bar{b}ZZ^*$, $VVVV$, $VV\tau\tau$, $\tau\tau\tau\tau$, $\gamma\gamma VV$, $\gamma\gamma\tau\tau$
− 1.2 to 7.2	95	[1] AAD	24BL	ATLS	13 TeV, $b\bar{b}b\bar{b}$, $b\bar{b}\tau\tau$, $b\bar{b}\gamma\gamma$, multilepton , $b\bar{b}\ell\ell$
− 1.4 to 6.9	95	[6] AAD	24X	ATLS	13 TeV, $b\bar{b}\gamma\gamma$
− 6.2 to 13.3	95	[7] AAD	24Y	ATLS	13 TeV, $b\bar{b}WW^*$, $b\bar{b}ZZ^*$, $b\bar{b}\tau\tau$, multilepton
− 7.2 to 13.8	95	[8] HAYRAPETY...	24AE	CMS	13 TeV, $b\bar{b}WW^*$
−37.7 to 37.2	95	[9] HAYRAPETY...	24AW	CMS	13 TeV, VHH, $HH \to b\bar{b}b\bar{b}$
−34.4 to 33.3	95	[10] AAD	23AD	ATLS	13 TeV, VHH, $HH \to b\bar{b}b\bar{b}$
− 0.6 to 6.6	95	[11] AAD	23AT	ATLS	13 TeV, $b\bar{b}b\bar{b}$, $b\bar{b}\tau\tau$, $b\bar{b}\gamma\gamma$
− 0.4 to 6.3	95	[12] AAD	23AT	ATLS	13 TeV, $b\bar{b}b\bar{b}$, $b\bar{b}\tau\tau$, $b\bar{b}\gamma\gamma$
− 3.5 to 11.3	95	[13] AAD	23BK	ATLS	13 TeV, $b\bar{b}b\bar{b}$
− 5.4 to 14.9	95	[14] HAYRAPETY...	23	CMS	13 TeV, $ZZ^* \to 4\ell$ cross sections
− 9.9 to 16.9	95	[15] TUMASYAN	23AE	CMS	13 TeV, $b\bar{b}b\bar{b}$
− 1.7 to 8.7	95	[16] TUMASYAN	23D	CMS	13 TeV, $b\bar{b}\tau\tau$
− 8.8 to 13.4	95	[17] TUMASYAN	23I	CMS	13 TeV, $b\bar{b}ZZ^*$ ($ZZ^* \to 4\ell$)
− 6.9 to 11.1	95	[18] TUMASYAN	23O	CMS	13 TeV, WW^*WW^*, $WW^*\tau\tau$, $\tau\tau\tau\tau$
− 1.5 to 6.7	95	[19] AAD	22Y	ATLS	13 TeV, $\gamma\gamma b\bar{b}$
− 1.24 to 6.49	95	[20] CMS	22	CMS	13 TeV, $b\bar{b}ZZ^*$, $b\bar{b}\gamma\gamma$, $b\bar{b}\tau\tau$, $b\bar{b}b\bar{b}$, multilepton
− 2.3 to 9.4	95	[21] TUMASYAN	22AN	CMS	13 TeV, $b\bar{b}b\bar{b}$
− 3.3 to 8.5	95	[22] SIRUNYAN	21K	CMS	13 TeV, $\gamma\gamma b\bar{b}$
− 5.0 to 12.0	95	[23] AAD	20C	ATLS	13 TeV, $b\bar{b}\gamma\gamma$, $b\bar{b}\tau\tau$, $b\bar{b}b\bar{b}$, $b\bar{b}WW^*$, $WW^*\gamma\gamma$, WW^*WW^*
−11 to 17	95	[24] SIRUNYAN	19	CMS	13 TeV, $\gamma\gamma b\bar{b}$
−11.8 to 18.8	95	[25] SIRUNYAN	19BE	CMS	13 TeV, $b\bar{b}\gamma\gamma$ $b\bar{b}\tau\tau$, $b\bar{b}b\bar{b}$, $b\bar{b}WW^*$, $b\bar{b}ZZ^*$
− 8.2 to 13.2	95	[26] AABOUD	18CW	ATLS	13 TeV, $\gamma\gamma b\bar{b}$
		[27] SIRUNYAN	18A	CMS	13 TeV, $b\bar{b}\tau\tau$
−17 to 22.5	95	[28] KHACHATRY...	16BQ	CMS	8 TeV, $\gamma\gamma b\bar{b}$

[1] AAD 24BL combine results from 126–140 fb^{-1} of data at $E_{cm} = 13$ TeV for $pp \to HH \to b\bar{b}b\bar{b}$ (AAD 23BK, AAD 24BV), $b\bar{b}\tau\tau$ (AAD 24AZ), $b\bar{b}\gamma\gamma$ (AAD 24X), multilepton (AAD 24BG), and $b\bar{b}\ell\ell$ (AAD 24Y). See their Fig. 3. All other Higgs couplings are fixed to the SM values.

[2] AAD 25J search for non-resonant HHH production using $HHH \to b\overline{b}b\overline{b}b\overline{b}$ with data of 126 fb^{-1} at $E_{\rm cm} = 13$ TeV. Two-dimensional likelihood scan of (κ_3 ($=\kappa_\lambda$), κ_4) is shown in their Fig. 9. The quoted values are obtained by assuming $\kappa_4 = 1$. Note that the quoted values are calculated using the kappa framework, which outside the unitarity bounds requires additional modification to preserve unitarity for their results.

[3] HAYRAPETYAN 25F constrain the Higgs trilinear self-coupling using single and double Higgs production with data at $E_{\rm cm} = 13$ TeV. The production modes and decay channels used are listed in their Tables 1 and 2 for single- and double-Higgs, respectively. Only single- and double-Higgs channels give $-1.8 < \kappa_\lambda < 12.0$ and $-1.7 < \kappa_\lambda < 7.0$, respectively. All the other Higgs boson couplings are fixed to their SM values. Their Table 3 shows results with some of the couplings are loosened. Two-dimensional likelihood scan of (κ_λ, κ_t) is shown in their Fig. 5.

[4] AAD 24AZ search for non-resonant HH production using $HH \to b\overline{b}\tau\tau$ with data of 140 fb^{-1} at $E_{\rm cm} = 13$ TeV. Two-dimensional exclusion regions as a function of the κ_λ and κ_{2V} couplings are shown in their Fig. 9. All other Higgs couplings are fixed to the SM values.

[5] AAD 24BG search for non-resonant HH production targeting the $b\overline{b}ZZ^*$, $VVVV$, $VV\tau\tau$, $\tau\tau\tau\tau$, $\gamma\gamma VV$, $\gamma\gamma\tau\tau$ decay channels with data of 140 fb^{-1} at $E_{\rm cm} = 13$ TeV. The limits are obtained with the values of all other couplings fixed to their SM value.

[6] AAD 24X search for non-resonant HH production using $HH \to b\overline{b}\gamma\gamma$ with data of 140 fb^{-1} at $E_{\rm cm} = 13$ TeV. Two-dimensional exclusion regions as a function of the κ_λ and κ_{2V} couplings are shown in their Fig. 6. All other Higgs couplings are fixed to the SM values.

[7] AAD 24Y search for non-resonant HH production in $2b + 2\ell + \nu$s final state ($\ell = e$, μ) targeting $b\overline{b}WW^*$, $b\overline{b}ZZ^*$, and $b\overline{b}\tau\tau$ decay channels with data of 140 fb^{-1} at $E_{\rm cm} = 13$ TeV. All other coupling modifiers are set to their SM values.

[8] HAYRAPETYAN 24AE search for non-resonant HH production using $HH \to b\overline{b}WW^*$ with data of 138 fb^{-1} at $E_{\rm cm} = 13$ TeV. Two-dimensional exclusion regions as a function of the (κ_λ, κ_{2V}) and (κ_λ, κ_t) are shown in their Figs. 13 and 15. All other Higgs couplings are fixed to the SM values.

[9] HAYRAPETYAN 24AW search for non-resonant HH production in association with a vector boson using $HH \to b\overline{b}b\overline{b}$ with data of 138 fb^{-1} at $E_{\rm cm} = 13$ TeV. The vector boson decays both leptonically ($W \to \ell\nu$, $Z \to \ell\ell$, $\nu\nu$, $\ell = e$, μ) and hadronically. All other Higgs couplings are fixed to the SM values. Two-dimensional exclusion regions as a function of the κ_{2V} and κ_λ parameters are shown in their Fig. 14, with other couplings fixed to the SM values. The best fit value is (κ_λ, κ_{2V}) = (-2.6, 10.1).

[10] AAD 23AD search for non-resonant HH production in association with a vector boson using $HH \to b\overline{b}b\overline{b}$ with data of 139 fb^{-1} at $E_{\rm cm} = 13$ TeV. The vector boson decays leptonically ($W \to \ell\nu$, $Z \to \ell\ell$, $\nu\nu$, $\ell = e$, μ). The quoted κ_λ is measured assuming all other Higgs boson couplings are at their SM value.

[11] AAD 23AT combine results from 126–139 fb^{-1} of data at $E_{\rm cm} = 13$ TeV for $pp \to HH \to b\overline{b}b\overline{b}$ (AAD 23BK), $b\overline{b}\tau\tau$ (AAD 23Z), and $b\overline{b}\gamma\gamma$ (AAD 22Y). The quoted values are obtained from the profile likelihood scan as a function of κ_λ as shown in their Fig. 5(a). All other coupling modifiers are assumed to have their SM values.

[12] AAD 23AT combine results from 126–139 fb^{-1} of data at $E_{\rm cm} = 13$ TeV for $pp \to HH \to b\overline{b}b\overline{b}$ (AAD 23BK), $b\overline{b}\tau\tau$ (AAD 23Z), and $b\overline{b}\gamma\gamma$ (AAD 22Y) with single-Higgs boson analyses ($\gamma\gamma$, ZZ^*, WW^*, $\tau\tau$, $b\overline{b}$, see their Table 1). The quoted values are obtained from the profile likelihood scan as a function of κ_λ as shown in their Fig. 5(a), assuming that all other Higgs boson couplings are at their SM values. Results with other assumptions are shown in their Table 2.

[13] AAD 23BK search for non-resonant HH production using $HH \to b\overline{b}b\overline{b}$ with data of 126 fb^{-1} at $E_{\rm cm} = 13$ TeV. The quoted values are obtained from the one-dimensional profile likelihood scan as a function of κ_λ. See their Fig. 12 (a). The $\mu_{ggF+VBF}$

measurement for different values of κ_λ constrains -3.9 $< \kappa_\lambda <$ 11.1 at 95% CL as shown in their Fig. 10 (a). $\kappa_{2V} = \kappa_V = 1$ is assumed in both cases.

[14] HAYRAPETYAN 23 measure the cross sections for $pp \to H \to ZZ^* \to 4\ell$ ($\ell = e$, μ) using 138 fb^{-1} at $E_{\rm cm} = 13$ TeV.

[15] TUMASYAN 23AE search for HH production using $HH \to b\overline{b}b\overline{b}$, where both $b\overline{b}$ pairs are highly boosted, with data of 138 fb^{-1} at $E_{\rm cm} = 13$ TeV. The quoted κ_λ is measured assuming all other Higgs boson couplings are at their SM values.

[16] TUMASYAN 23D search for non-resonant HH production using $HH \to b\overline{b}\tau\tau$ with data of 138 fb^{-1} at $E_{\rm cm} = 13$ TeV. The quoted values are obtained from the upper limit on the HH production cross section times the $b\overline{b}\tau\tau$ branching fraction for different values of κ_λ. See their Fig. 8 (left). All other coupling modifiers are assumed to be 1. In addition, two-dimensional exclusion regions as a function of the κ_λ and κ_t couplings, with $\kappa_{2V} = \kappa_V = 1$, are shown in their Fig. 9 (left). The one-dimensional likelihood scan as a function of κ_λ is given in their Fig 10 (left), from which a 95% confidence interval of -1.77 $< \kappa_\lambda <$ 8.73 is extracted.

[17] TUMASYAN 23AI search for non-resonant HH production using $HH \to b\overline{b}ZZ^*$ ($ZZ^* \to 4\ell$, ℓ=e,μ) with data of 138 fb^{-1} at $E_{\rm cm} = 13$ TeV. See their Fig. 4.

[18] TUMASYAN 23O search for non-resonant HH production using $HH \to WW^*WW^*$, $WW^*\tau\tau$, and $\tau\tau\tau\tau$ (multilepton) with data of 138 fb^{-1} at $E_{\rm cm} = 13$ TeV. See their Fig. 10 for different final states and these combination. Limits are set on a variety of new-physics models using an effective field theory approach. See their Figs. 11, 12, and 13.

[19] AAD 22Y search for non-resonant HH production using $HH \to \gamma\gamma b\overline{b}$ with data of 139 fb^{-1} at $E_{\rm cm} = 13$ TeV. The quoted κ_λ is obtained from their Fig. 12 where the theory uncertainties are not included while a negative log-likelihood scan vs. $\kappa_\lambda$is shown in their Fig. 13 with the theory uncertainties, which provides $\kappa_\lambda = 2.8^{+2.0}_{-2.2}$ for the 1σ confidence interval.

[20] CMS 22 report combined results (see their Extended Data Table 2) using 138 fb^{-1} of data at $E_{\rm cm} = 13$ TeV. See their Fig. 6 (left).

[21] TUMASYAN 22AN search for non-resonant HH production using $HH \to b\overline{b}b\overline{b}$ with data of 138 fb^{-1} at $E_{\rm cm} = 13$ TeV. The upper limit on the $pp \to HH$ production cross section at 95% CL is shown as a function of κ_λ in their Fig. 2 (top).

[22] SIRUNYAN 21K search for non-resonant HH production using $HH \to \gamma\gamma b\overline{b}$ with data of 137 fb^{-1} at $E_{\rm cm} = 13$ TeV.

[23] AAD 20C combine results of up to 36.1 fb^{-1} data at $E_{\rm cm} = 13$ TeV for $pp \to HH \to b\overline{b}\gamma\gamma$, $b\overline{b}\tau\tau$, $b\overline{b}b\overline{b}$, $b\overline{b}WW^*$, $WW^*\gamma\gamma$, WW^*WW^* (AABOUD 18CW, AABOUD 18CQ, AABOUD 19A, AABOUD 19O, AABOUD 18BU, and AABOUD 19T).

[24] SIRUNYAN 19 search for HH production using $HH \to \gamma\gamma b\overline{b}$ with data of 35.9 fb^{-1} at $E_{\rm cm} = 13$ TeV. The quoted κ_λ is measured assuming all other Higgs boson couplings are at their SM value.

[25] SIRUNYAN 19BE combine results of 13 TeV 35.9 fb^{-1} data: SIRUNYAN 19, SIRUNYAN 18A, SIRUNYAN 19AB, SIRUNYAN 19H, and SIRUNYAN 18F.

[26] AABOUD 18CW search for HH production using $HH \to \gamma\gamma b\overline{b}$ with data of 36.1 fb^{-1} at $E_{\rm cm} = 13$ TeV. The quoted κ_λ is measured assuming all other Higgs boson couplings are at their SM value.

[27] SIRUNYAN 18A search for HH production using $HH \to b\overline{b}\tau\tau$ with data of 35.9 fb^{-1} at $E_{\rm cm} = 13$ TeV. The upper limit on production cross section times branching fraction at 95% CL is shown as a function of κ_λ/κ_t in their Fig. 6 (top) where $\kappa_t = y_t \,/\, y_t{}^{SM}$ (top Yukawa coupling y_t).

[28] KHACHATRYAN 16BQ search for HH production using $HH \to \gamma\gamma b\overline{b}$ with data of 19.7 fb^{-1} at $E_{\rm cm} = 8$ TeV.

Higgs quartic self coupling modifier κ_4

Signal strength relative to the SM prediction, $\kappa_4 = \lambda_{HHHH}/\lambda^{\mathrm{SM}}_{HHHH}$.

VALUE	CL%	DOCUMENT ID		TECN	COMMENT
• • • We do not use the following data for averages, fits, limits, etc. • • •					
−230 to 240	95	[1] AAD	25J	ATLS	13 TeV, $b\overline{b}b\overline{b}b\overline{b}$

[1] AAD 25J search for non-resonant HHH production using $HHH \to b\overline{b}b\overline{b}b\overline{b}$ with data of 126 fb^{-1} at $E_{\mathrm{cm}} = 13$ TeV. Two-dimensional likelihood scan of (κ_3 (=κ_λ), κ_4) is shown in their Fig. 9. The quoted values are obtained by assuming $\kappa_3 = 1$. Note that the quoted values are calculated using the kappa framework, which outside the unitarity bounds requires additional modification to preserve unitarity for their results.

Higgs-gauge boson quartic coupling modifier κ_{2V}

Signal strength relative to the SM prediction, $\kappa_{2V} = \lambda_{VVHH} \,/\, \lambda^{SM}_{VVHH}$, $V = W, Z$.

VALUE	CL%	DOCUMENT ID		TECN	COMMENT
$\mathbf{1.02^{+0.22}_{-0.23}}$		[1] AAD	24BL	ATLS	13 TeV, $b\overline{b}b\overline{b}$, $b\overline{b}\tau\tau$, $b\overline{b}\gamma\gamma$, multilepton , $b\overline{b}\ell\ell$
• • • We do not use the following data for averages, fits, limits, etc. • • •					
		[2] HAYRAPETY...25F		CMS	13 TeV, single and double Higgs production
− 0.5 to 2.7	95	[3] AAD	24AZ	ATLS	13 TeV, $b\overline{b}\tau\tau$
− 2.5 to 4.6	95	[4] AAD	24BG	ATLS	13 TeV, $b\overline{b}ZZ^*$, $VVVV$, $VV\tau\tau$, $\tau\tau\tau\tau$, $\gamma\gamma VV$, $\gamma\gamma\tau\tau$
0.6 to 1.5	95	[1] AAD	24BL	ATLS	13 TeV, $b\overline{b}b\overline{b}$, $b\overline{b}\tau\tau$, $b\overline{b}\gamma\gamma$, multilepton , $b\overline{b}\ell\ell$
0.55 to 1.49	95	[5] AAD	24BV	ATLS	13 TeV, $b\overline{b}b\overline{b}$
0.52 to 1.52	95	[6] AAD	24BV	ATLS	13 TeV, $b\overline{b}b\overline{b}$
− 0.5 to 2.7	95	[7] AAD	24X	ATLS	13 TeV, $b\overline{b}\gamma\gamma$
− 0.17 to 2.4	95	[8] AAD	24Y	ATLS	13 TeV, $b\overline{b}WW^*$, $b\overline{b}ZZ^*$, $b\overline{b}\tau\tau$, multilepton
− 1.1 to 3.2	95	[9] HAYRAPETY...24AE		CMS	13 TeV, $b\overline{b}WW^*$
−12.2 to 13.5	95	[10] HAYRAPETY...24AW		CMS	13 TeV, VHH, $HH \to b\overline{b}b\overline{b}$
− 8.6 to 10.0	95	[11] AAD	23AD	ATLS	13 TeV, VHH, $HH \to b\overline{b}b\overline{b}$
0.1 to 2.0	95	[12] AAD	23AT	ATLS	13 TeV, $b\overline{b}b\overline{b}$, $b\overline{b}\tau\tau$, $b\overline{b}\gamma\gamma$
0.0 to 2.1	95	[13] AAD	23BK	ATLS	13 TeV, $b\overline{b}b\overline{b}$
0.62 to 1.41	95	[14] TUMASYAN	23AE	CMS	13 TeV, $b\overline{b}b\overline{b}$
− 0.4 to 2.6	95	[15] TUMASYAN	23D	CMS	13 TeV, $b\overline{b}\tau\tau$
0.67 to 1.38	95	[16] CMS	22	CMS	13 TeV, $b\overline{b}ZZ^*$, $b\overline{b}\gamma\gamma$, $b\overline{b}\tau\tau$, $b\overline{b}b\overline{b}$, multilepton
− 0.1 to 2.2	95	[17] TUMASYAN	22AN	CMS	13 TeV, $b\overline{b}b\overline{b}$
− 1.3 to 3.5	95	[18] SIRUNYAN	21K	CMS	13 TeV, $\gamma\gamma b\overline{b}$
− 0.43 to 2.56	95	[19] AAD	20X	ATLS	13 TeV, VBF, $b\overline{b}b\overline{b}$

[1] AAD 24BL combine results from 126–140 fb^{-1} of data at $E_{\mathrm{cm}} = 13$ TeV for $pp \to HH \to b\overline{b}b\overline{b}$ (AAD 23BK, AAD 24BV), $b\overline{b}\tau\tau$ (AAD 24AZ), $b\overline{b}\gamma\gamma$ (AAD 24X), multilepton (AAD 24BG), and $b\overline{b}\ell\ell$ (AAD 24Y). See their Fig. 3. All other Higgs couplings are fixed to the SM values.

[2] HAYRAPETYAN 25F constrain the Higgs trilinear self-coupling using single and double Higgs production with data at $E_{\mathrm{cm}} = 13$ TeV. The production modes and decay channels used are listed in their Tables 1 and 2 for single- and double-Higgs, respectively. Two-dimensional likelihood scan of (κ_V, κ_{2V}) is shown in their Fig. 6.

[3] AAD 24AZ search for non-resonant HH production using $HH \to b\overline{b}\tau\tau$ with data of 140 fb^{-1} at $E_{\rm cm} = 13$ TeV. Two-dimensional exclusion regions as a function of the κ_λ and κ_{2V} couplings are shown in their Fig. 9. All other Higgs couplings are fixed to the SM values.

[4] AAD 24BG search for non-resonant HH production targeting the $b\overline{b}ZZ^*$, $VVVV$, $VV\tau\tau$, $\tau\tau\tau\tau$, $\gamma\gamma VV$, $\gamma\gamma\tau\tau$ decay channels with data of 140 fb^{-1} at $E_{\rm cm} = 13$ TeV. The limits are obtained with the values of all other couplings fixed to their SM value.

[5] AAD 24BV search for non-resonant HH production via vector boson fusion in the $b\overline{b}b\overline{b}$ final state using two boosted Higgs ($p_T > 250$ GeV) with data of 140 fb^{-1} at $E_{\rm cm} = 13$ TeV. The result is obtained by combining with the resolved result (AAD 23BK). The value $\kappa_{2V} = 0$ is excluded with a significance of 3.8 σ with other Higgs couplings fixed to their SM values. Two-dimensional exclusion regions as a function of the κ_λ and κ_{2V} parameters are shown in their Fig. 6. All other Higgs couplings are fixed to the SM values.

[6] AAD 24BV search for non-resonant HH production via vector boson fusion in the $b\overline{b}b\overline{b}$ final state using two boosted Higgs ($p_T > 250$ GeV) with data of 140 fb^{-1} at $E_{\rm cm} = 13$ TeV. The value $\kappa_{2V} = 0$ is excluded with a significance of 3.4 σ with other Higgs couplings fixed to their SM values.

[7] AAD 24X search for non-resonant HH production using $HH \to b\overline{b}\gamma\gamma$ with data of 140 fb^{-1} at $E_{\rm cm} = 13$ TeV. Two-dimensional exclusion regions as a function of the κ_λ and κ_{2V} couplings are shown in their Fig. 6. All other Higgs couplings are fixed to the SM values.

[8] AAD 24Y search for non-resonant HH production in $2b + 2\ell + \nu$s final state ($\ell = e$, μ) targeting $b\overline{b}WW^*$, $b\overline{b}ZZ^*$, and $b\overline{b}\tau\tau$ decay channels with data of 140 fb^{-1} at $E_{\rm cm} = 13$ TeV. All other coupling modifiers are set to their SM values.

[9] HAYRAPETYAN 24AE search for non-resonant HH production using $HH \to b\overline{b}WW^*$ with data of 138 fb^{-1} at $E_{\rm cm} = 13$ TeV. Two-dimensional exclusion regions as a function of the (κ_λ, κ_{2V}) and (κ_V, κ_{2V}) are shown in their Figs. 13 and 14. All other Higgs couplings are fixed to the SM values.

[10] HAYRAPETYAN 24AW search for non-resonant HH production in association with a vector boson using $HH \to b\overline{b}b\overline{b}$ with data of 138 fb^{-1} at $E_{\rm cm} = 13$ TeV. The vector boson decays both leptonically ($W \to \ell\nu$, $Z \to \ell\ell$, $\nu\nu$, $\ell = e$, μ) and hadronically. All other Higgs couplings are fixed to the SM values. Two-dimensional exclusion regions as a function of the κ_{2V} and κ_λ parameters are shown in their Fig. 14, with other couplings fixed to the SM values. The best fit value is (κ_λ, κ_{2V}) = (-2.6, 10.1). The constraints on κ_{2W} and κ_{2Z} are separately measured to be -14.0 $< \kappa_{2W} <$ 15.4 and -17.4 $< \kappa_{2Z} <$ 18.5 (95% CL). The quoted κ_{2V} ($V = W$, Z) is measured assuming all other Higgs boson couplings are at their SM value. See their Table 7.

[11] AAD 23AD search for non-resonant HH production in association with a vector boson using $HH \to b\overline{b}b\overline{b}$ with data of 139 fb^{-1} at $E_{\rm cm} = 13$ TeV. The vector boson decays leptonically ($W \to \ell\nu$, $Z \to \ell\ell$, $\nu\nu$, $\ell = e$, μ). The constraints on κ_{2W} and κ_{2Z} are separately measured to be -12.3 $< \kappa_{2W} <$ 13.5 and -9.9 $< \kappa_{2Z} <$ 11.3 (95% CL). The quoted κ_{2V} ($V = W$, Z) is measured assuming all other Higgs boson couplings are at their SM value.

[12] AAD 23AT combine results from 126–139 fb^{-1} of data at $E_{\rm cm} = 13$ TeV for $pp \to HH \to b\overline{b}b\overline{b}$ (AAD 23BK), $b\overline{b}\tau\tau$ (AAD 23Z), and $b\overline{b}\gamma\gamma$ (AAD 22Y). The quoted values are obtained from the 95% CL VBF HH cross-section upper limit as a function of κ_{2V} as shown in their Fig. 4(b). All other coupling modifiers are assumed to have their SM values.

[13] AAD 23BK search for non-resonant HH production using $HH \to b\overline{b}b\overline{b}$ with data of 126 fb^{-1} at $E_{\rm cm} = 13$ TeV. The quoted values are obtained from the one-dimensional profile likelihood scan as a function of κ_{2V}. See their Fig. 12 (b). The μ_{VBF} measurement for different values of κ_{2V} constrains -0.03 $< \kappa_{2V} <$ 2.11 at 95% CL as shown in their Fig. 10 (b). $\kappa_\lambda = \kappa_V = 1$ is assumed in both cases.

[14] TUMASYAN 23AE search for HH production using $HH \to b\overline{b}b\overline{b}$, where both $b\overline{b}$ pairs are highly boosted, with data of 138 fb^{-1} at $E_{cm} = 13$ TeV. The $\kappa_{2V} = 0$ is excluded at 6.3 σ assuming all other Higgs boson couplings are at their SM values.

[15] TUMASYAN 23D search for non-resonant HH production using $HH \to b\overline{b}\tau\tau$ with data of 138 fb^{-1} at $E_{cm} = 13$ TeV. The quoted values are obtained from the upper limits on the HH production cross section times the $b\overline{b}\tau\tau$ branching fraction for different values of κ_{2V}. See their Fig. 8 (right). All other coupling modifiers are assumed to be 1. In addition, two-dimensional exclusion regions as a function of the κ_{2V} and κ_V couplings, with $\kappa_\lambda = \kappa_t = 1$, are shown in their Fig. 9 (right). The one-dimensional likelihood scan as a function of κ_{2V} is given in their Fig. 10 (right), from which a 95% confidence interval of -0.34 $< \kappa_{2V} <$ 2.49 is extracted.

[16] CMS 22 report combined results (see their Extended Data Table 2) using 138 fb^{-1} of data at $E_{cm} = 13$ TeV. See their Fig. 6 (right).

[17] TUMASYAN 22AN search for non-resonant HH production using $HH \to b\overline{b}b\overline{b}$ with data of 138 fb^{-1} at $E_{cm} = 13$ TeV. The upper limit on the $pp \to HH$ production cross section at 95% CL is shown as a function of κ_{2V} in their Fig. 2 (bottom).

[18] SIRUNYAN 21K search for non-resonant HH production using $HH \to \gamma\gamma b\overline{b}$ with data of 137 fb^{-1} at $E_{cm} = 13$ TeV.

[19] AAD 20X search for $HH \to b\overline{b}b\overline{b}$ process via VBF with data of 126 fb^{-1} at $E_{cm} =$ 13 TeV.

H production cross section in pp collisions at $\sqrt{s} = 13$ TeV

VALUE (pb)	*DOCUMENT ID*		*TECN*	*COMMENT*
56.8± 3.4 OUR AVERAGE				
$55.5^{+\ 4.0}_{-\ 3.8}$	[1] AAD	23C	ATLS	pp, 13 TeV, $\gamma\gamma$, $ZZ^* \to 4\ell$ ($\ell = e,\ \mu$)
61.1± 6.0±3.7	[2] SIRUNYAN	19BA	CMS	pp, 13 TeV, $\gamma\gamma$, $ZZ^* \to 4\ell$ ($\ell = e,\ \mu$)
• • • We do not use the following data for averages, fits, limits, etc. • • •				
58 ± 4 ±4	[3] AAD	22N	ATLS	pp, 13 TeV, $\gamma\gamma$
53.5± 4.9±2.1	[4] AAD	20BA	ATLS	pp, 13 TeV, $ZZ^* \to 4\ell$ ($\ell = e,\ \mu$)
$57.0^{+\ 6.0+4.0}_{-\ 5.9-3.3}$	[5] AABOUD	18CG	ATLS	pp, 13 TeV, $\gamma\gamma$, $ZZ^* \to 4\ell$ ($\ell = e,\ \mu$)
$47.9^{+\ 9.1}_{-\ 8.6}$	[5] AABOUD	18CG	ATLS	pp, 13 TeV, $\gamma\gamma$
$68\ ^{+11}_{-10}$	[5] AABOUD	18CG	ATLS	pp, 13 TeV, $ZZ^* \to 4\ell$ ($\ell = e,\ \mu$)
$69\ ^{+10}_{-\ 9}$ ±5	[6] AABOUD	17CO	ATLS	pp, 13 TeV, $ZZ^* \to 4\ell$

[1] AAD 23C combine AAD 22N and AAD 20BA, where both use 139 fb^{-1} of pp collisions at $E_{cm} = 13$ TeV. The Higgs production cross sections at $E_{cm} = 7$ and 8 TeV are obtained to be 34^{+11}_{-10} pb and $33.3^{+5.8}_{-5.4}$ pb, respectively. The quoted value is given for $m_H = 125.09$ GeV. The differential cross sections are given in their Figs. 3 and 4.

[2] SIRUNYAN 19BA use 35.9 fb^{-1} of pp collisions at $E_{cm} = 13$ TeV. The quoted value is given for $m_H = 125.09$ GeV.

[3] AAD 22N use 139 fb^{-1} of pp collisions at $E_{cm} = 13$ TeV. The quoted value is given for $m_H = 125.09$ GeV.

[4] AAD 20BA use 139 fb^{-1} of pp collisions at $E_{cm} = 13$ TeV with $H \to ZZ^* \to 4\ell$ where $\ell = e,\ \mu$. The quoted value is given for $m_H = 125$ GeV and assumes the Standard Model branching ratio.

[5] AABOUD 18CG use 36.1 fb^{-1} of pp collisions at $E_{cm} = 13$ TeV. All the quoted values are given for $m_H = 125.09$ GeV.

[6] AABOUD 17CO use 36.1 fb^{-1} of pp collisions at $E_{cm} = 13$ TeV with $H \to ZZ^* \to 4\ell$ where $\ell = e,\ \mu$ for $m_H = 125$ GeV. Differential cross sections for the Higgs boson transverse momentum, Higgs boson rapidity, and other related quantities are measured as shown in their Figs. 8 and 9.

H production cross section in pp collisions at $\sqrt{s} = 13.6$ TeV

VALUE (pb)	*DOCUMENT ID*		*TECN*	*COMMENT*
58.2±8.7	[1] AAD	24AQ	ATLS	pp, 13.6 TeV, $\gamma\gamma$, $ZZ^* \to 4\ell$ ($\ell = e,\ \mu$)

[1] AAD 24AQ measure the total cross section to be 67^{+12}_{-11} pb and 46 ± 12 pb using $H \to \gamma\gamma$ and $H \to ZZ^* \to 4\ell$, respectively, with data of 31.4 fb^{-1} and 29.0 fb^{-1} of pp collisions at $E_{cm} = 13.6$ TeV. The SM expected value is 59.9 ± 2.6 pb. All the values are given for $m_H = 125.09$ GeV.

H REFERENCES

HAYRAPETY...	26	PRL 136 011801	A. Hayrapetyan *et al.*	(CMS Collab.)
AAD	25AG	JHEP 2508 034	G. Aad *et al.*	(ATLAS Collab.)
AAD	25AJ	EPJ C85 210	G. Aad *et al.*	(ATLAS Collab.)
AAD	25AP	PL B865 139449 (errat.)	G. Aad *et al.*	(ATLAS Collab.)
AAD	25AQ	RPP 88 057803	G. Aad *et al.*	(ATLAS Collab.)
AAD	25AR	PRL 135 231802	G. Aad *et al.*	(ATLAS Collab.)
AAD	25AT	PL B868 139671	G. Aad *et al.*	(ATLAS Collab.)
AAD	25AV	PL B870 139898	G. Aad *et al.*	(ATLAS Collab.)
AAD	25BC	JHEP 2510 092	G. Aad *et al.*	(ATLAS Collab.)
AAD	25BD	JHEP 2510 093	G. Aad *et al.*	(ATLAS Collab.)
AAD	25BK	EPJ C85 1403	G. Aad *et al.*	(ATLAS Collab.)
AAD	25E	PL B861 139277	G. Aad *et al.*	(ATLAS Collab.)
AAD	25J	PR D111 032006	G. Aad *et al.*	(ATLAS Collab.)
AAD	25R	JHEP 2502 045	G. Aad *et al.*	(ATLAS Collab.)
AAD	25W	JHEP 2503 010	G. Aad *et al.*	(ATLAS Collab.)
AAD	25Y	JHEP 2504 075	G. Aad *et al.*	(ATLAS Collab.)
CHEKHOVSKY	25A	JHEP 2503 114	V. Chekhovsky *et al.*	(CMS Collab.)
CHEKHOVSKY	25B	JHEP 2505 079	V. Chekhovsky *et al.*	(CMS Collab.)
CHEKHOVSKY	25G	PR D112 112001	V. Chekhovsky *et al.*	(CMS Collab.)
CHEKHOVSKY	25L	JHEP 2511 060	V. Chekhovsky *et al.*	(CMS Collab.)
HAYRAPETY...	25	PL B860 139173	A. Hayrapetyan *et al.*	(CMS Collab.)
HAYRAPETY...	25AC	PRL 135 091802	A. Hayrapetyan *et al.*	(CMS Collab.)
HAYRAPETY...	25AL	JHEP 2509 070	A. Hayrapetyan *et al.*	(CMS Collab.)
HAYRAPETY...	25B	PL B860 139202	A. Hayrapetyan *et al.*	(CMS Collab.)
HAYRAPETY...	25F	PL B861 139210	A. Hayrapetyan *et al.*	(CMS Collab.)
HAYRAPETY...	25G	PL B862 139296	A. Hayrapetyan *et al.*	(CMS Collab.)
HAYRAPETY...	25H	PL B865 139462	A. Hayrapetyan *et al.*	(CMS Collab.)
HAYRAPETY...	25L	PR D111 092014	A. Hayrapetyan *et al.*	(CMS Collab.)
HAYRAPETY...	25R	JHEP 2502 097	A. Hayrapetyan *et al.*	(CMS Collab.)
AAD	24AG	JHEP 2405 105	G. Aad *et al.*	(ATLAS Collab.)
AAD	24AQ	EPJ C84 78	G. Aad *et al.*	(ATLAS Collab.)
AAD	24AZ	PR D110 032012	G. Aad *et al.*	(ATLAS Collab.)
AAD	24BE	PL B855 138817	G. Aad *et al.*	(ATLAS Collab.)
AAD	24BG	JHEP 2408 164	G. Aad *et al.*	(ATLAS Collab.)
AAD	24BH	JHEP 2408 153	G. Aad *et al.*	(ATLAS Collab.)
AAD	24BL	PRL 133 101801	G. Aad *et al.*	(ATLAS Collab.)
AAD	24BM	PRL 133 141801	G. Aad *et al.*	(ATLAS Collab.)
AAD	24BV	PL B858 139007	G. Aad *et al.*	(ATLAS Collab.)
AAD	24D	PRL 132 021803	G. Aad *et al.*	(ATLAS and CMS Collabs.)
AAD	24F	PRL 132 131802	G. Aad *et al.*	(ATLAS Collab.)
AAD	24J	PL B849 138469	G. Aad *et al.*	(ATLAS Collab.)
AAD	24R	PL B855 138762	G. Aad *et al.*	(ATLAS Collab.)
AAD	24X	JHEP 2401 066	G. Aad *et al.*	(ATLAS Collab.)
AAD	24Y	JHEP 2402 037	G. Aad *et al.*	(ATLAS Collab.)
HAYRAPETY...	24AE	JHEP 2407 293	A. Hayrapetyan *et al.*	(CMS Collab.)
HAYRAPETY...	24AG	EPJ C84 779	A. Hayrapetyan *et al.*	(CMS Collab.)
HAYRAPETY...	24AM	EPJ C84 712	A. Hayrapetyan *et al.*	(CMS Collab.)

HAYRAPETY...	24AT	PL B857 138964	A. Hayrapetyan *et al.*	(CMS Collab.)
HAYRAPETY...	24AW	JHEP 2410 061	A. Hayrapetyan *et al.*	(CMS Collab.)
HAYRAPETY...	24AY	JHEP 2412 035	A. Hayrapetyan *et al.*	(CMS Collab.)
HAYRAPETY...	24D	PRL 132 121901	A. Hayrapetyan *et al.*	(CMS Collab.)
HAYRAPETY...	24U	JHEP 2401 173	A. Hayrapetyan *et al.*	(CMS Collab.)
TUMASYAN	24	PR D109 092011	A. Tumasyan *et al.*	(CMS Collab.)
AABOUD	23A	JHEP 2312 158 (errat.)	M. Aaboud *et al.*	(ATLAS Collab.)
AAD	23A	PL B842 137963	G. Aad *et al.*	(ATLAS Collab.)
AAD	23AD	EPJ C83 519	G. Aad *et al.*	(ATLAS Collab.)
AAD	23AF	EPJ C83 503	G. Aad *et al.*	(ATLAS Collab.)
AAD	23AK	EPJ C83 563	G. Aad *et al.*	(ATLAS Collab.)
AAD	23AN	PRL 131 061802	G. Aad *et al.*	(ATLAS Collab.)
AAD	23AP	PR D108 032005	G. Aad *et al.*	(ATLAS Collab.)
AAD	23AT	PL B843 137745	G. Aad *et al.*	(ATLAS Collab.)
AAD	23AU	PL B843 137880	G. Aad *et al.*	(ATLAS Collab.)
AAD	23BC	EPJ C83 496	G. Aad *et al.*	(ATLAS Collab.)
Also		EPJ C84 156 (errat.)	G. Aad *et al.*	(ATLAS Collab.)
AAD	23BK	PR D108 052003	G. Aad *et al.*	(ATLAS Collab.)
AAD	23BP	PRL 131 251802	G. Aad *et al.*	(ATLAS Collab.)
AAD	23BR	PL B846 138223	G. Aad *et al.*	(ATLAS Collab.)
Also		PL B854 138734 (errat.)	G. Aad *et al.*	(ATLAS Collab.)
Also		PL B865 139449 (errat.)	G. Aad *et al.*	(ATLAS Collab.)
AAD	23BS	PL B847 138292	G. Aad *et al.*	(ATLAS Collab.)
AAD	23BU	PL B847 138315	G. Aad *et al.*	(ATLAS Collab.)
AAD	23BV	PR D108 072003	G. Aad *et al.*	(ATLAS Collab.)
AAD	23C	JHEP 2305 028	G. Aad *et al.*	(ATLAS Collab.)
AAD	23CD	EPJ C83 781	G. Aad *et al.*	(ATLAS Collab.)
AAD	23Q	JHEP 2307 166	G. Aad *et al.*	(ATLAS Collab.)
AAD	23Y	JHEP 2307 088	G. Aad *et al.*	(ATLAS Collab.)
AAD	23Z	JHEP 2307 040	G. Aad *et al.*	(ATLAS Collab.)
HAYRAPETY...	23	JHEP 2308 040	A. Hayrapetyan *et al.*	(CMS Collab.)
HAYRAPETY...	23C	PR D108 072004	A. Hayrapetyan *et al.*	(CMS Collab.)
TUMASYAN	23AD	PRL 131 041801	A. Tumasyan *et al.*	(CMS Collab.)
TUMASYAN	23AE	PRL 131 041803	A. Tumasyan *et al.*	(CMS Collab.)
TUMASYAN	23AH	PRL 131 061801	A. Tumasyan *et al.*	(CMS Collab.)
TUMASYAN	23AI	PR D108 032008	A. Tumasyan *et al.*	(CMS Collab.)
TUMASYAN	23AJ	PR D108 032013	A. Tumasyan *et al.*	(CMS Collab.)
TUMASYAN	23AU	PL B846 137783	A. Tumasyan *et al.*	(CMS Collab.)
TUMASYAN	23BA	EPJ C83 933	A. Tumasyan *et al.*	(CMS Collab.)
TUMASYAN	23C	PL B842 137534	A. Tumasyan *et al.*	(CMS Collab.)
TUMASYAN	23D	PL B842 137531	A. Tumasyan *et al.*	(CMS Collab.)
TUMASYAN	23F	JHEP 2305 233	A. Tumasyan *et al.*	(CMS Collab.)
TUMASYAN	23I	JHEP 2306 130	A. Tumasyan *et al.*	(CMS Collab.)
TUMASYAN	23O	JHEP 2307 095	A. Tumasyan *et al.*	(CMS Collab.)
TUMASYAN	23P	JHEP 2307 092	A. Tumasyan *et al.*	(CMS Collab.)
TUMASYAN	23Q	JHEP 2307 091	A. Tumasyan *et al.*	(CMS Collab.)
TUMASYAN	23W	EPJ C83 667	A. Tumasyan *et al.*	(CMS Collab.)
TUMASYAN	23Y	EPJ C83 562	A. Tumasyan *et al.*	(CMS Collab.)
AAD	22D	PL B829 137066	G. Aad *et al.*	(ATLAS Collab.)
AAD	22M	JHEP 2206 097	G. Aad *et al.*	(ATLAS Collab.)
AAD	22N	JHEP 2208 027	G. Aad *et al.*	(ATLAS Collab.)
AAD	22P	JHEP 2208 104	G. Aad *et al.*	(ATLAS Collab.)
AAD	22Q	JHEP 2208 175	G. Aad *et al.*	(ATLAS Collab.)
AAD	22S	EPJ C82 105	G. Aad *et al.*	(ATLAS Collab.)
AAD	22V	EPJ C82 622	G. Aad *et al.*	(ATLAS Collab.)
AAD	22W	EPJ C82 717	G. Aad *et al.*	(ATLAS Collab.)
AAD	22X	PR D105 092003	G. Aad *et al.*	(ATLAS Collab.)
AAD	22Y	PR D106 052001	G. Aad *et al.*	(ATLAS Collab.)
ATLAS	22	NAT 607 52	ATLAS Collaboration	(ATLAS Collab.)
Also		NAT 612 E24 (errat.)	ATLAS Collaboration	(ATLAS Collab.)
CMS	22	NAT 607 60	CMS Collaboration	(CMS Collab.)
TUMASYAN	22AJ	PRL 128 081805	A. Tumasyan *et al.*	(CMS Collab.)
TUMASYAN	22AM	NATP 18 1329	A. Tumasyan *et al.*	(CMS Collab.)
TUMASYAN	22AN	PRL 129 081802	A. Tumasyan *et al.*	(CMS Collab.)
TUMASYAN	22G	PR D105 092007	A. Tumasyan *et al.*	(CMS Collab.)
TUMASYAN	22Y	JHEP 2206 012	A. Tumasyan *et al.*	(CMS Collab.)
AAD	21	PL B812 135980	G. Aad *et al.*	(ATLAS Collab.)
AAD	21AB	EPJ C81 178	G. Aad *et al.*	(ATLAS Collab.)
AAD	21AJ	EPJ C81 537	G. Aad *et al.*	(ATLAS Collab.)
AAD	21F	PR D103 112006	G. Aad *et al.*	(ATLAS Collab.)
AAD	21H	PL B816 136204	G. Aad *et al.*	(ATLAS Collab.)

AAD	21I	PL B819 136412	G. Aad *et al.*	(ATLAS Collab.)
AAD	21M	JHEP 2103 268	G. Aad *et al.*	(ATLAS Collab.)
SIRUNYAN	21	PL B812 135992	A.M. Sirunyan *et al.*	(CMS Collab.)
SIRUNYAN	21A	EPJ C81 13	A.M. Sirunyan *et al.*	(CMS Collab.)
Also		EPJ C81 333 (errat.)	A.M. Sirunyan *et al.*	(CMS Collab.)
SIRUNYAN	21AE	PR D104 052004	A.M. Sirunyan *et al.*	(CMS Collab.)
SIRUNYAN	21B	EPJ C81 3	A.M. Sirunyan *et al.*	(CMS Collab.)
SIRUNYAN	21C	JHEP 2101 148	A.M. Sirunyan *et al.*	(CMS Collab.)
SIRUNYAN	21K	JHEP 2103 257	A.M. Sirunyan *et al.*	(CMS Collab.)
SIRUNYAN	21L	JHEP 2103 011	A.M. Sirunyan *et al.*	(CMS Collab.)
SIRUNYAN	21O	JHEP 2107 027	A.M. Sirunyan *et al.*	(CMS Collab.)
SIRUNYAN	21R	EPJ C81 378	A.M. Sirunyan *et al.*	(CMS Collab.)
SIRUNYAN	21S	EPJ C81 488	A.M. Sirunyan *et al.*	(CMS Collab.)
SIRUNYAN	21Z	PR D104 032013	A.M. Sirunyan *et al.*	(CMS Collab.)
TUMASYAN	21D	JHEP 2111 153	A. Tumasyan *et al.*	(CMS Collab.)
AAD	20	PR D101 012002	G. Aad *et al.*	(ATLAS Collab.)
AAD	20A	PL B800 135069	G. Aad *et al.*	(ATLAS Collab.)
AAD	20AE	PRL 125 221802	G. Aad *et al.*	(ATLAS Collab.)
AAD	20AG	PL B809 135754	G. Aad *et al.*	(ATLAS Collab.)
AAD	20AQ	EPJ C80 957	G. Aad *et al.*	(ATLAS Collab.)
Also		EPJ C81 29 (errat.)	G. Aad *et al.*	(ATLAS Collab.)
Also		EPJ C81 398 (errat.)	G. Aad *et al.*	(ATLAS Collab.)
AAD	20BA	EPJ C80 942	G. Aad *et al.*	(ATLAS Collab.)
AAD	20C	PL B800 135103	G. Aad *et al.*	(ATLAS Collab.)
AAD	20E	PL B801 135145	G. Aad *et al.*	(ATLAS Collab.)
AAD	20F	PL B801 135148	G. Aad *et al.*	(ATLAS Collab.)
AAD	20N	PL B805 135426	G. Aad *et al.*	(ATLAS Collab.)
AAD	20X	JHEP 2007 108	G. Aad *et al.*	(ATLAS Collab.)
Also		JHEP 2101 145 (errat.)	G. Aad *et al.*	(ATLAS Collab.)
Also		JHEP 2105 207 (errat.)	G. Aad *et al.*	(ATLAS Collab.)
AAD	20Z	PRL 125 061802	G. Aad *et al.*	(ATLAS Collab.)
SIRUNYAN	20AE	JHEP 2003 131	A.M. Sirunyan *et al.*	(CMS Collab.)
SIRUNYAN	20AH	JHEP 2005 032	A.M. Sirunyan *et al.*	(CMS Collab.)
SIRUNYAN	20AS	PRL 125 061801	A.M. Sirunyan *et al.*	(CMS Collab.)
SIRUNYAN	20BK	JHEP 2011 039	A.M. Sirunyan *et al.*	(CMS Collab.)
SIRUNYAN	20BL	JHEP 2012 085	A.M. Sirunyan *et al.*	(CMS Collab.)
SIRUNYAN	20C	EPJ C80 75	A.M. Sirunyan *et al.*	(CMS Collab.)
SIRUNYAN	20L	PL B805 135425	A.M. Sirunyan *et al.*	(CMS Collab.)
AABOUD	19A	JHEP 1901 030	M. Aaboud *et al.*	(ATLAS Collab.)
AABOUD	19AI	PL B793 499	M. Aaboud *et al.*	(ATLAS Collab.)
AABOUD	19AL	PRL 122 231801	M. Aaboud *et al.*	(ATLAS Collab.)
AABOUD	19AQ	PR D99 072001	M. Aaboud *et al.*	(ATLAS Collab.)
AABOUD	19F	PL B789 508	M. Aaboud *et al.*	(ATLAS Collab.)
AABOUD	19N	JHEP 1904 048	M. Aaboud *et al.*	(ATLAS Collab.)
AABOUD	19O	JHEP 1904 092	M. Aaboud *et al.*	(ATLAS Collab.)
AABOUD	19T	JHEP 1905 124	M. Aaboud *et al.*	(ATLAS Collab.)
AABOUD	19U	JHEP 1905 141	M. Aaboud *et al.*	(ATLAS Collab.)
AAD	19A	PL B798 134949	G. Aad *et al.*	(ATLAS Collab.)
SIRUNYAN	19	PL B788 7	A.M. Sirunyan *et al.*	(CMS Collab.)
SIRUNYAN	19AB	JHEP 1904 112	A.M. Sirunyan *et al.*	(CMS Collab.)
SIRUNYAN	19AF	JHEP 1906 093	A.M. Sirunyan *et al.*	(CMS Collab.)
SIRUNYAN	19AJ	EPJ C79 94	A.M. Sirunyan *et al.*	(CMS Collab.)
SIRUNYAN	19AT	EPJ C79 421	A.M. Sirunyan *et al.*	(CMS Collab.)
SIRUNYAN	19AX	PL B791 96	A.M. Sirunyan *et al.*	(CMS Collab.)
SIRUNYAN	19BA	PL B792 369	A.M. Sirunyan *et al.*	(CMS Collab.)
SIRUNYAN	19BE	PRL 122 121803	A.M. Sirunyan *et al.*	(CMS Collab.)
SIRUNYAN	19BK	PR D99 092005	A.M. Sirunyan *et al.*	(CMS Collab.)
SIRUNYAN	19BL	PR D99 112003	A.M. Sirunyan *et al.*	(CMS Collab.)
SIRUNYAN	19BO	PL B793 520	A.M. Sirunyan *et al.*	(CMS Collab.)
SIRUNYAN	19BR	PL B797 134811	A.M. Sirunyan *et al.*	(CMS Collab.)
SIRUNYAN	19BY	PR D100 072007	A.M. Sirunyan *et al.*	(CMS Collab.)
SIRUNYAN	19BZ	PR D100 112002	A.M. Sirunyan *et al.*	(CMS Collab.)
SIRUNYAN	19CG	JHEP 1910 139	A.M. Sirunyan *et al.*	(CMS Collab.)
SIRUNYAN	19E	PRL 122 021801	A.M. Sirunyan *et al.*	(CMS Collab.)
SIRUNYAN	19H	JHEP 1901 040	A.M. Sirunyan *et al.*	(CMS Collab.)
SIRUNYAN	19L	JHEP 1901 183	A.M. Sirunyan *et al.*	(CMS Collab.)
SIRUNYAN	19R	JHEP 1903 026	A.M. Sirunyan *et al.*	(CMS Collab.)
AABOUD	18	PL B776 318	M. Aaboud *et al.*	(ATLAS Collab.)
AABOUD	18AC	PR D97 072003	M. Aaboud *et al.*	(ATLAS Collab.)
AABOUD	18AJ	JHEP 1803 095	M. Aaboud *et al.*	(ATLAS Collab.)

AABOUD	18AU	JHEP 1807 127	M. Aaboud *et al.*	(ATLAS Collab.)
Also		JHEP 2312 158 (errat.)	M. Aaboud *et al.*	(ATLAS Collab.)
AABOUD	18BK	PL B784 173	M. Aaboud *et al.*	(ATLAS Collab.)
AABOUD	18BL	PL B786 134	M. Aaboud *et al.*	(ATLAS Collab.)
AABOUD	18BM	PL B784 345	M. Aaboud *et al.*	(ATLAS Collab.)
AABOUD	18BN	PL B786 59	M. Aaboud *et al.*	(ATLAS Collab.)
AABOUD	18BO	PR D98 052005	M. Aaboud *et al.*	(ATLAS Collab.)
AABOUD	18BP	PL B786 223	M. Aaboud *et al.*	(ATLAS Collab.)
AABOUD	18BQ	PR D98 052003	M. Aaboud *et al.*	(ATLAS Collab.)
AABOUD	18BU	EPJ C78 1007	M. Aaboud *et al.*	(ATLAS Collab.)
AABOUD	18CA	JHEP 1810 180	M. Aaboud *et al.*	(ATLAS Collab.)
AABOUD	18CG	PL B786 114	M. Aaboud *et al.*	(ATLAS Collab.)
AABOUD	18CQ	PRL 121 191801	M. Aaboud *et al.*	(ATLAS Collab.)
AABOUD	18CW	JHEP 1811 040	M. Aaboud *et al.*	(ATLAS Collab.)
AABOUD	18M	PRL 120 211802	M. Aaboud *et al.*	(ATLAS Collab.)
AABOUD	18T	PR D97 072016	M. Aaboud *et al.*	(ATLAS Collab.)
AAIJ	18AM	EPJ C78 1008	R. Aaij *et al.*	(LHCb Collab.)
AALTONEN	18C	PR D98 072002	T. Aaltonen *et al.*	(CDF Collab.)
SIRUNYAN	18A	PL B778 101	A.M. Sirunyan *et al.*	(CMS Collab.)
SIRUNYAN	18AE	PL B780 501	A.M. Sirunyan *et al.*	(CMS Collab.)
SIRUNYAN	18BD	JHEP 1806 101	A.M. Sirunyan *et al.*	(CMS Collab.)
SIRUNYAN	18BH	JHEP 1806 001	A.M. Sirunyan *et al.*	(CMS Collab.)
SIRUNYAN	18BQ	JHEP 1808 066	A.M. Sirunyan *et al.*	(CMS Collab.)
SIRUNYAN	18BU	EPJ C78 140	A.M. Sirunyan *et al.*	(CMS Collab.)
SIRUNYAN	18BV	EPJ C78 291	A.M. Sirunyan *et al.*	(CMS Collab.)
SIRUNYAN	18DB	PRL 121 121801	A.M. Sirunyan *et al.*	(CMS Collab.)
SIRUNYAN	18DQ	JHEP 1811 152	A.M. Sirunyan *et al.*	(CMS Collab.)
SIRUNYAN	18DS	JHEP 1811 185	A.M. Sirunyan *et al.*	(CMS Collab.)
SIRUNYAN	18E	PRL 120 071802	A.M. Sirunyan *et al.*	(CMS Collab.)
SIRUNYAN	18F	JHEP 1801 054	A.M. Sirunyan *et al.*	(CMS Collab.)
SIRUNYAN	18L	PRL 120 231801	A.M. Sirunyan *et al.*	(CMS Collab.)
SIRUNYAN	18S	PR D97 092005	A.M. Sirunyan *et al.*	(CMS Collab.)
SIRUNYAN	18Y	PL B779 283	A.M. Sirunyan *et al.*	(CMS Collab.)
AABOUD	17AW	JHEP 1710 112	M. Aaboud *et al.*	(ATLAS Collab.)
AABOUD	17BA	JHEP 1712 024	M. Aaboud *et al.*	(ATLAS Collab.)
AABOUD	17BD	EPJ C77 765	M. Aaboud *et al.*	(ATLAS Collab.)
AABOUD	17CO	JHEP 1710 132	M. Aaboud *et al.*	(ATLAS Collab.)
AABOUD	17Y	PRL 119 051802	M. Aaboud *et al.*	(ATLAS Collab.)
AAD	17	EPJ C77 70	G. Aad *et al.*	(ATLAS Collab.)
KHACHATRY...	17F	JHEP 1702 135	V. Khachatryan *et al.*	(CMS Collab.)
SIRUNYAN	17AM	PL B775 1	A.M. Sirunyan *et al.*	(CMS Collab.)
SIRUNYAN	17AV	JHEP 1711 047	A.M. Sirunyan *et al.*	(CMS Collab.)
SIRUNYAN	17CN	PR D96 072004	A.M. Sirunyan *et al.*	(CMS Collab.)
AABOUD	16I	PR D94 052002	M. Aaboud *et al.*	(ATLAS Collab.)
AABOUD	16K	PRL 117 111802	M. Aaboud *et al.*	(ATLAS Collab.)
AABOUD	16X	JHEP 1611 112	M. Aaboud *et al.*	(ATLAS Collab.)
AAD	16	PL B753 69	G. Aad *et al.*	(ATLAS Collab.)
AAD	16AC	PR D93 092005	G. Aad *et al.*	(ATLAS Collab.)
AAD	16AF	JHEP 1601 172	G. Aad *et al.*	(ATLAS Collab.)
AAD	16AL	JHEP 1605 160	G. Aad *et al.*	(ATLAS Collab.)
AAD	16AN	JHEP 1608 045	G. Aad *et al.*	(ATLAS and CMS Collabs.)
AAD	16AO	JHEP 1608 104	G. Aad *et al.*	(ATLAS Collab.)
AAD	16BL	EPJ C76 658	G. Aad *et al.*	(ATLAS Collab.)
AAD	16K	EPJ C76 6	G. Aad *et al.*	(ATLAS Collab.)
KHACHATRY...	16AB	PL B759 672	V. Khachatryan *et al.*	(CMS Collab.)
KHACHATRY...	16AR	JHEP 1604 005	V. Khachatryan *et al.*	(CMS Collab.)
KHACHATRY...	16AU	JHEP 1606 177	V. Khachatryan *et al.*	(CMS Collab.)
KHACHATRY...	16B	PL B753 341	V. Khachatryan *et al.*	(CMS Collab.)
KHACHATRY...	16BA	JHEP 1609 051	V. Khachatryan *et al.*	(CMS Collab.)
KHACHATRY...	16BQ	PR D94 052012	V. Khachatryan *et al.*	(CMS Collab.)
KHACHATRY...	16CD	PL B763 472	V. Khachatryan *et al.*	(CMS Collab.)
KHACHATRY...	16G	EPJ C76 13	V. Khachatryan *et al.*	(CMS Collab.)
AAD	15	PL B740 222	G. Aad *et al.*	(ATLAS Collab.)
AAD	15AA	PR D92 012006	G. Aad *et al.*	(ATLAS Collab.)
AAD	15AH	JHEP 1504 117	G. Aad *et al.*	(ATLAS Collab.)
AAD	15AQ	JHEP 1508 137	G. Aad *et al.*	(ATLAS Collab.)
AAD	15AX	EPJ C75 231	G. Aad *et al.*	(ATLAS Collab.)
AAD	15B	PRL 114 191803	G. Aad *et al.*	(ATLAS and CMS Collabs.)
AAD	15BC	EPJ C75 349	G. Aad *et al.*	(ATLAS Collab.)
AAD	15BD	EPJ C75 337	G. Aad *et al.*	(ATLAS Collab.)
AAD	15BE	EPJ C75 335	G. Aad *et al.*	(ATLAS Collab.)

AAD	15CE	PR D92 092004	G. Aad *et al.*	(ATLAS Collab.)
AAD	15CI	EPJ C75 476	G. Aad *et al.*	(ATLAS Collab.)
Also		EPJ C76 152 (errat.)	G. Aad *et al.*	(ATLAS Collab.)
AAD	15CX	JHEP 1511 206	G. Aad *et al.*	(ATLAS Collab.)
AAD	15F	PR D91 012006	G. Aad *et al.*	(ATLAS Collab.)
AAD	15G	JHEP 1501 069	G. Aad *et al.*	(ATLAS Collab.)
AAD	15I	PRL 114 121801	G. Aad *et al.*	(ATLAS Collab.)
AAD	15P	PRL 115 091801	G. Aad *et al.*	(ATLAS Collab.)
AAD	15T	PL B749 519	G. Aad *et al.*	(ATLAS Collab.)
AALTONEN	15	PRL 114 151802	T. Aaltonen *et al.*	(CDF and D0 Collabs.)
AALTONEN	15B	PRL 114 141802	T. Aaltonen *et al.*	(CDF Collab.)
KHACHATRY...	15AM	EPJ C75 212	V. Khachatryan *et al.*	(CMS Collab.)
KHACHATRY...	15AN	EPJ C75 251	V. Khachatryan *et al.*	(CMS Collab.)
KHACHATRY...	15BA	PR D92 072010	V. Khachatryan *et al.*	(CMS Collab.)
KHACHATRY...	15H	PL B744 184	V. Khachatryan *et al.*	(CMS Collab.)
KHACHATRY...	15Q	PL B749 337	V. Khachatryan *et al.*	(CMS Collab.)
KHACHATRY...	15Y	PR D92 012004	V. Khachatryan *et al.*	(CMS Collab.)
KHACHATRY...	15Z	PR D92 032008	V. Khachatryan *et al.*	(CMS Collab.)
AAD	14AR	PL B738 234	G. Aad *et al.*	(ATLAS Collab.)
AAD	14AS	PL B738 68	G. Aad *et al.*	(ATLAS Collab.)
AAD	14BC	PR D90 112015	G. Aad *et al.*	(ATLAS Collab.)
AAD	14BJ	JHEP 1409 112	G. Aad *et al.*	(ATLAS Collab.)
AAD	14J	PL B732 8	G. Aad *et al.*	(ATLAS Collab.)
AAD	14O	PRL 112 201802	G. Aad *et al.*	(ATLAS Collab.)
AAD	14W	PR D90 052004	G. Aad *et al.*	(ATLAS Collab.)
ABAZOV	14F	PRL 113 161802	V.M. Abazov *et al.*	(D0 Collab.)
CHATRCHYAN	14AA	PR D89 092007	S. Chatrchyan *et al.*	(CMS Collab.)
CHATRCHYAN	14AI	PR D89 012003	S. Chatrchyan *et al.*	(CMS Collab.)
CHATRCHYAN	14AJ	NATP 10 557	S. Chatrchyan *et al.*	(CMS Collab.)
CHATRCHYAN	14B	EPJ C74 2980	S. Chatrchyan *et al.*	(CMS Collab.)
CHATRCHYAN	14G	JHEP 1401 096	S. Chatrchyan *et al.*	(CMS Collab.)
CHATRCHYAN	14K	JHEP 1405 104	S. Chatrchyan *et al.*	(CMS Collab.)
KHACHATRY...	14D	PL B736 64	V. Khachatryan *et al.*	(CMS Collab.)
KHACHATRY...	14H	JHEP 1409 087	V. Khachartryan *et al.*	(CMS Collab.)
KHACHATRY...	14P	EPJ C74 3076	V. Khachatryan *et al.*	(CMS Collab.)
AAD	13AJ	PL B726 120	G. Aad *et al.*	(ATLAS Collab.)
AAD	13AK	PL B726 88	G. Aad *et al.*	(ATLAS Collab.)
Also		PL B734 406 (errat.)	G. Aad *et al.*	(ATLAS Collab.)
AALTONEN	13L	PR D88 052013	T. Aaltonen *et al.*	(CDF Collab.)
AALTONEN	13M	PR D88 052014	T. Aaltonen *et al.*	(CDF and D0 Collabs.)
ABAZOV	13L	PR D88 052011	V.M. Abazov *et al.*	(D0 Collab.)
CHATRCHYAN	13BK	PL B726 587	S. Chatrchyan *et al.*	(CMS Collab.)
CHATRCHYAN	13J	PRL 110 081803	S. Chatrchyan *et al.*	(CMS Collab.)
CHATRCHYAN	13X	JHEP 1305 145	S. Chatrchyan *et al.*	(CMS Collab.)
CHATRCHYAN	13Y	JHEP 1306 081	S. Chatrchyan *et al.*	(CMS Collab.)
HEINEMEYER	13A	arXiv:1307.1347	S. Heinemeyer *et al.*	(LHC Higgs CS Working Group)
AAD	12AI	PL B716 1	G. Aad *et al.*	(ATLAS Collab.)
AAD	12DA	SCI 338 1576	G. Aad *et al.*	(ATLAS Collab.)
AALTONEN	12Q	PRL 109 111803	T. Aaltonen *et al.*	(CDF Collab.)
AALTONEN	12R	PRL 109 111804	T. Aaltonen *et al.*	(CDF Collab.)
AALTONEN	12S	PRL 109 111805	T. Aaltonen *et al.*	(CDF Collab.)
AALTONEN	12T	PRL 109 071804	T. Aaltonen *et al.*	(CDF and D0 Collabs.)
ABAZOV	12K	PL B716 285	V.M. Abazov *et al.*	(D0 Collab.)
ABAZOV	12O	PRL 109 121803	V.M. Abazov *et al.*	(D0 Collab.)
ABAZOV	12P	PRL 109 121804	V.M. Abazov *et al.*	(D0 Collab.)
CHATRCHYAN	12BY	SCI 338 1569	S. Chatrchyan *et al.*	(CMS Collab.)
CHATRCHYAN	12N	PL B716 30	S. Chatrchyan *et al.*	(CMS Collab.)
DITTMAIER	12	arXiv:1201.3084	S. Dittmaier *et al.*	(LHC Higgs CS Working Group)
DITTMAIER	11	arXiv:1101.0593	S. Dittmaier *et al.*	(LHC Higgs CS Working Group)